

The SUBCELLULAR LOCALIZATION AND TARGETING  
PATHWAY OF HYALURONIDASE 1

BY

NEHAL PATEL

A Thesis Submitted to the Faculty of Graduate Studies in  
Partial Fulfillment of the Requirements for the Degree of

MASTER OF SCIENCE

Faculty of Medicine  
Department of Biochemistry and Medical Genetics  
University of Manitoba  
Winnipeg, Manitoba, Canada

Copyright © January 2006 by Nehal Patel

# ABSTRACT

Hyaluronidases are endoglycosidases that catabolize hyaluronan, an abundant component of the extracellular matrix surrounding vertebrate cells. We characterized one of the hyaluronidases, HYAL1, an enzyme deficient in the lysosomal storage disorder Mucopolysaccharidosis IX. HYAL1 stably expressed in BHK cells resulted in several intracellular forms, but only one secreted form. Secretion was not increased by weak bases, and no phosphate was incorporated in metabolic labeling, suggesting this enzyme is not targeted to the lysosome by the mannose 6-phosphate dependent pathway. Further analysis revealed the various forms of HYAL1 differ only in glycosylation, and are all active at pH 3.8. The forms migrated in a Percol density gradient similarly to an endosomal marker, and with partial overlap with the lysosomal marker LPG120 (Lamp1).

# ACKNOWLEDGEMENTS

I would like to express my sincere gratitude to Dr. Barbara Triggs-Raine for her guidance, generous support, and kind help throughout the graduate program. The M.Sc. program would not have been as comfortable as it was without Barb and I really appreciate her helping me gain knowledge in this area of science and directing my scientific career on to the right path. I would also like to thank my co-supervisor Dr. Steven Pind, for his guidance, support, and helpful suggestions throughout the program.

I extend my appreciation to my committee members, Dr. Wilkins and Dr. Arthur for their valuable comments and suggestions. I would also like to acknowledge my lab co-workers, Dr. Richard Hemming, Dianna Martin, and Vasantha Atmuri, who made this research experience both more comfortable and more enjoyable. I sincerely appreciate their help and gratefully thank these people. In addition, the departmental office staff (especially Ms. Tuntun Sarkar) helped me a lot and so I like to thank them as well.

Last but not the least, I would like to thank my parents and Trushar for providing me with support and courage to finish this program smoothly and successfully.

# **DEDICATION**

To Mom, Dad and Trushar

# TABLE OF CONTENTS

<b>ABSTRACT</b>	i
<b>ACKNOWLEDGEMENTS</b>	ii
<b>DEDICATION</b>	iii
<b>TABLE OF CONTENTS</b>	iv
<b>LIST OF TABLES</b>	ix
<b>LIST OF FIGURES</b>	x
<b>LIST OF ABBREVIATIONS</b>	xii
<b>1. INTRODUCTION</b>	1
1.1 Hyaluronan-A unique glycosaminoglycan (GAG)	2
1.2 Distribution of HA	5
1.3 Functions of HA	5
1.4 Metabolism of HA	7
1.4.1 Synthesis of HA	7
1.4.2 Degradation of HA	9
1.5 Hyaluronidases overview	11
1.5.1 Hyaluronidase 1 (HYAL1)	13
1.5.2 Other members of the hyaluronidase family	14
1.6 Mucopolysaccharidoses (MPS) IX	15
1.6.1 MPS IX and Hyaluronidase 1	16
1.6.2 Lysosomal storage disorders	18
1.6.3 Mannose-6-phosphate (M6P) dependant lysosomal enzymes targeting	19

1.7 Objectives and rationale of the study	21
<b>2. MATERIALS AND METHODS</b>	<b>23</b>
2.1 Generation of the HYAL1 expression construct	24
2.1.1 pIRESneo vector	24
2.1.2. Polymerase Chain Reaction (PCR) amplification of DNA	24
2.1.3 Agarose gel electrophoresis	25
2.1.4 Quantitative analysis of DNA	26
2.1.4.1 Determination of DNA concentration by spectrophotometric analysis	26
2.1.4.2 Estimation of DNA concentration using DNA MASS™ ladder	26
2.1.5 Restriction enzyme digestion	27
2.1.6 Phenol-chloroform extraction of DNA	27
2.1.7 Bacterial medium and agar preparation	28
2.1.8 Plasmid DNA preparation	28
2.1.8.1 Small scale plasmid DNA isolation	28
2.1.8.2 Large scale plasmid DNA isolation	29
2.1.9 Ligation of plasmid and insert DNA	29
2.1.10 Transformation into competent <i>E.coli</i> cells	30
2.1.11 Preparation of 50% glycerol stock	30
2.2 Mammalian cell culture	30

2.2.1 Mammalian cell lines	30
2.2.2 Maintenance and passage of mammalian cells	31
2.2.3 Freezing and thawing of mammalian cells	31
2.3 Transfection of BHK cells	32
2.4 Preparation of cell lysates and cleared medium	33
2.5 Determination of protein concentration	33
2.6 Sodium Dodecyl Sulfate-Polyacrylamide gel electrophoresis (SDS-PAGE)	34
2.6.1 Sample preparation	34
2.6.2 Protein separation by SDS-PAGE	34
2.7 Western blot analysis	35
2.7.1 Transfer to nitrocellulose membrane	35
2.7.2 Detection of proteins using antibodies	36
2.8 Zymography	37
2.8.1 Gel electrophoresis	37
2.8.2 In gel activity assay	37
2.9 Density gradient centrifugation	38
2.9.1 Preparation of cell extract	38
2.9.2 Percoll gradient centrifugation of the cell extracts	38
2.9.3 Preparation of samples for analysis	39
2.10 Metabolic labeling of BHK_HYAL1 or BHK_pIRESneo cells	39
2.10.1 Pulse labeling	39
2.10.2 Chase	40

2.10.3 Treatment of [ $S^{35}$ ]-labeled HYAL1 protein	
with glycosidases	40
2.10.4 Pulse-chase analysis of HYAL1 in the presence	
of tunicamycin	41
2.10.5 Pulse-chase analysis of HYAL1 in the presence	
of brefeldin A (BFA)	41
2.10.6 Pulse-Chase analysis of HYAL1 in the presence of	
deoxynojirimycin (DNM)	41
2.10.7 Pulse-chase analysis of HYAL1 in the presence	
of weak bases	42
2.11 Immunoprecipitation of labeled HYAL1.	42
2.11.1 Immunoprecipitation from cell lysates	42
2.11.2 Immunoprecipitation from cleared medium	43
2.11.3 Recovering antigen after immunoprecipitation	43
2.12 Fluorography	44
2.13 Triton-X 114 extraction of cell lysates and cleared medium.	44
2.14 Purification of monoclonal antibodies	44
2.14.1 Culturing hybridoma cells	44
2.14.2 Purification of monoclonal antibodies	
from cleared medium	45
<b>3. RESULTS</b>	47
3.1 The <i>HYALI</i> cDNA expression construct	48

3.2 Analysis of HYAL1 expression in transiently transfected BHK cells	49
3.3 Analysis of HYAL1 stably expressed in BHK cells	55
3.4 Detection of the HYAL1 protein in density gradient fractions	64
3.5 Pulse-chase analysis of HYAL1 stably expressed in BHK cells	67
3.6 Analysis of carbohydrate modification of [S <sup>35</sup> ]-labeled HYAL1	75
3.7 Processing of [S <sup>35</sup> ]-labeled HYAL1 in the presence of tunicamycin	80
3.8 Processing of [S <sup>35</sup> ]-labeled HYAL1 in the presence of deoxynojirimycin (DNM)	84
3.9 Processing of [S <sup>35</sup> ]-labeled HYAL1 in the presence of brefeldin A (BFA)	86
3.10 Analyzing the effect of ammonium chloride and chloroquine on the secretion of [S <sup>35</sup> ]-labeled HYAL1	87
3.11 Labeling of HYAL1 with [P <sup>32</sup> ]-orthophosphate	94
3.12 Analysis of hydrophobic properties of HYAL1 by detergent phase separation	97
<b>4. DISCUSSION</b>	100
<b>5. FUTURE DIRECTIONS</b>	110
<b>6. REFERENCES</b>	112

# LIST OF TABLES

Table-1 Functions of HA oligosaccharides	8
Table-2 Types of MPS	17

# LIST OF FIGURES

Fig-1. Structure of basic disaccharide unit of HA	3
Fig-2. Hypothetical model for HA degradation	12
Fig-3. Restriction map for the pIRES_HYAL1 construct	50
Fig-4. Restriction enzyme digests to confirm the correct insertion of the <i>HYAL1</i> cDNA	51
Fig-5. Analysis of HYAL1 expression from pIRES_HYAL1	53
Fig-6. Analysis of HYAL1 expression and secretion from transiently transfected BHK cells	54
Fig-7. Screening of neomycin resistant colonies for HYAL1 expression	56
Fig-8. Analysis of HYAL1 stably expressed in BHK cells	58
Fig-9. Analysis of HYAL1 activity by zymography	59
Fig-10. Analysis of HYAL1 carbohydrate processing by glycosidase treatment	62
Fig-11. Analysis of HYAL1 under reducing and non-reducing conditions	63
Fig-12. Analysis of HYAL1 subcellular localization by density gradient centrifugation	65
Fig-13. Analysis of HYAL1 activity in the density gradient fractions by zymography	66
Fig-14. Optimization of pulse-labeling time	68
Fig-15. Metabolic labeling of HYAL1	70
Fig-16. Immunoprecipitation of HYAL1 from medium	71
Fig-17. Pulse-chase labeling of HYAL1	73

Fig-18. The [ $S^{35}$ ]-labeled HYAL1 is stable in medium	74
Fig-19. Pulse-chase labeling of HYAL1 followed by PNGase F treatment	76
Fig-20a. Pulse-chase labeling of HYAL1 followed by Endo H treatment	78
Fig-20b. Pulse-Chase labeling of HYAL1 followed by glycosidase treatment	79
Fig-21. Pulse-chase labeling of HYAL1 in the presence of tunicamycin	83
Fig-22. Pulse-chase labeling of HYAL1 in the presence of deoxynojirimycin (DNM)	85
Fig-23. Pulse-chase labeling of HYAL1 in the presence of brefeldin A (BFA)	89
Fig-24. Immunoprecipitation of [ $S^{35}$ ]-labeled HYAL1 from the cleared medium of 10 mM $NH_4Cl$ treated cells	92
Fig-25. Immunoprecipitation of [ $S^{35}$ ]-labeled HYAL1 from the cleared medium of 150 mM chloroquine treated cells	93
Fig-26. Pulse labeling of BHK_HYAL1 and BHK_pIRESneo with [ $P^{32}$ ]-phosphate	96
Fig-27. Phase separation of HYAL1	98
Fig-28. Analysis of HYAL1 activity in the fractions obtained by phase separation	99

# ABBREVIATIONS

$\alpha$ -HRP	Anti-Horse radish peroxidase
®	Registered sign
°C	Degree Celsius
$\mu$ Ci	Micro Curie
$\mu$ g	Microgram
$\mu$ l	Microlitre
bp	Basepair
cDNA	Complementary DNA
Ci	Curie
cm	Centimetre
CO <sub>2</sub>	Carbon dioxide
dATP	2'- Deoxyadenosine 5'-triphosphate
dCTP	2'- Deoxycytidine 5'-triphosphate
dGTP	2'- Deoxyguanosine 5'-triphosphate
dTTP	2'- Deoxythymidine 5'-triphosphate
DNA	Deoxyribonucleic acid
dNTP	2'- Deoxyribonucleoside 5'-triphosphate
EST	Expressed sequence tag
g	Gram
GAG	Glycosaminoglycan
GalNAc	N-acetylgalactosamine
Glc	Glucose

GlcNAc	N-acetylglucosamine
GPI	Glycosylphosphatidyl inositol
HA	Hyaluronan
HAS1	Hyaluronan synthase 1
HAS2	Hyaluronan synthase 2
HAS3	Hyaluronan synthase 3
HYAL1	Hyaluronidase 1
HYAL2	Hyaluronidase 2
HYAL3	Hyaluronidase 3
HYAL4	Hyaluronidase 4
IgG	Immunoglobulin G
IL1	Interleukin 1
kb	Kilobase
kDa	Kilodalton
kg	Kilogram
mg	Milligram
MGEA5	Meningioma expressed antigen 5
ml	Millilitre
mm	Millimetre
mM	Millimolar
MPS IX	Mucopolysaccharidosis IX
mRNA	Messenger ribonucleic acid
ng	Nanogram

nm	Nanometre
NMR	Nuclear Magnetic Resonance
NP-40	Nonidet – P40
OD	Optical density
RHAMM	Receptor for HA mediated motility
rpm	Revolutions per minute
SPAM1	Sperm adhesion molecule 1
Taq	DNA dependent DNA polymerase from <i>Thermus aquaticus</i>
TEMED	N,N,N'N' - tetramethylethylenediamene
TNF- $\alpha$	Tumor necrosis factor - alpha
Tris	Tris (hydroxymethyl) aminomethane
V	Volts
V/V	Volume/volume ratio
X g	Times gravity

# **INTRODUCTION**

Hyaluronidases are endoglycosidases required for the breakdown of hyaluronan (HA), a large glycosaminoglycan present in the extracellular matrix surrounding vertebrate cells. HA plays a fundamental role in many biological processes involving cell proliferation, migration and differentiation, indicating that the hyaluronidases are likely to be important in many processes of health and disease. One hyaluronidase, *HYAL1*, has already been associated with a lysosomal storage disorder, mucopolysaccharidosis IX (MPS IX). The initial characterization of *HYAL1* suggested it was an atypical lysosomal enzyme. Further characterization of *HYAL1* will provide more information about where and how it functions.

### **1.1 Hyaluronan -A unique glycosaminoglycan (GAG)**

GAGs are long polysaccharides made up of repeating disaccharide units that may be sulfated. Several GAGs are known and form a GAG family that includes heparan sulfate, dermatan sulfate, keratan sulfate, chondroitin sulfate, heparan and HA. GAGs are important structural components of connective tissues (Kjellen and Lindahl 1991). HA is a simple carbohydrate with unusual characteristics and is present in the extracellular matrix surrounding most animal tissues (Knudson and Knudson 1993). HA was first isolated from bovine vitreous humor and described by Karl Meyer and his co-workers (Meyer and Palmer 1934) as “hyaluronic acid” named from hyaloid (vitreous) and uronic acid. The basic unit of HA is a disaccharide motif (Figure 1) consisting of D-glucuronic acid and D-N- acetylglucosamine linked together through alternating  $\beta$ -1, 4 and  $\beta$ -1,3 glycosidic bonds (Weissman and Meyer 1954).

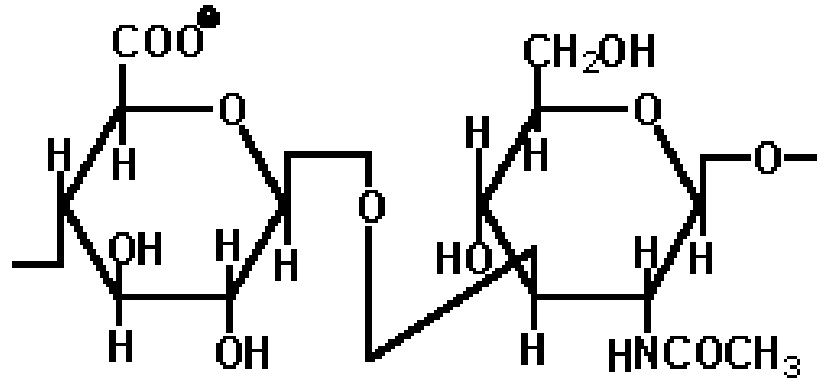


**Figure 1. Structure of the basic disaccharide unit of HA.** D-glucuronic acid and N-acetyl glucosamine are linked by  $\beta$ -1, 4 and  $\beta$ -1, 3 glycosidic bonds. Modified from “Molecular Cell Biology” text book (Lodish et al. 2005).

HA has several features, summarized below, that are distinct from other GAG family members (Fraser, Laurent, and Laurent 1997; Laurent 1998; Laurent, Laurent, and Fraser 1996; McDonald and Hascall 2002). It is the only GAG that is not attached to a core protein, and unlike most of the other GAGs, it is not sulfated. The synthesis of HA is carried out at the inner side of the plasma membrane by HA synthases rather than in the endoplasmic reticulum and Golgi apparatus, where all other GAGs are synthesized. The enormous size of HA, ranging from  $10^5$  to  $10^7$  daltons (Da) is another factor that makes it unique among the GAGs.

The structure of HA in aqueous solution was demonstrated by Nuclear Magnetic Resonance (NMR) and computer studies (Scott 1989). These studies showed the presence of hydrogen bonds between adjacent sugar units, and hydrophobic patches created by clusters of CH groups, throughout the structure of HA. Based on computer simulation, this secondary structure of HA was suggested to be stabilized by water (Scott et al. 1991). The hydrogen bonds present in HA impart stiffness, while the hydrophobic patches permit association with other HA chains and account for its capability to interact with cell membranes and other lipid structures (Scott 1989). Consequently, the stiffened HA assumes an expanded random coil structure and occupies a very large area. At concentrations above 1 mg/ml, the individual HA molecules overlap with each other and form entangled molecular networks through steric interactions and self-association between and within individual molecules.

In the ECM, HA exists either in its free form, or is bound specifically to other matrix macromolecules or cell surface receptors (Turley and Roth 1980). HA interacts with these molecules in a very similar manner as it interacts with itself. Several such HA

binding proteins have now been identified and grouped under a family termed “hyaladherins” (Toole 1990). In some cases, this interaction is stabilized by a small glycoprotein referred to as the link protein (Day 2001; Hardingham 1998).

## **1.2 Distribution of HA**

HA is an abundant GAG in the ECM of most animal tissues with its highest concentration found in loose connective tissues such as the umbilical cord, synovial fluid, skin and vitreous body. A considerable amount of HA is present in the lung, kidney, brain and muscles, but very little is found in liver, and the lowest concentration is in blood serum (Laurent and Laurent 1981). Studies in rat showed that more than half of the total HA (56%) was found in the skin, about one quarter (27%) in the skeleton and supporting tissues, 8% in muscles and 1% in the intestines and stomach. The rest of the HA (about 9%) was evenly distributed in the remaining organs (Reed, Lilja, and Laurent 1989).

HA was thought to be only an ECM component until its presence in the cytoplasm and nuclei was reported (Furukawa and Terayama 1977; Furukawa and Terayama 1979; Margolis et al. 1976). Since then, several reports supporting the intracellular localization of HA have been published (Collis et al. 1998; Evanko and Wight 1999; Tammi et al. 2001).

## **1.3 Functions of HA**

Several functions have been associated with HA; some are structural functions, and others are related to the cell signaling through cell surface receptors.

The structural functions of HA and its interaction with other matrix

macromolecules can be accounted for by its mechanical properties. HA plays an important role in structure and assembly of cartilage and other tissues, where it stabilizes the ECM by forming aggregates with proteoglycans (Knudson 1993). In the ECM, large numbers of hyaladherins bind specifically to each HA chain; some of the aggregates may also bind to HA chains linked to a cell surface receptor. The aggregates formed have a molecular mass of several hundred million daltons and attract water by osmosis. This fills the intercellular space, provides structural rigidity and a hydrated environment that facilitates migration and proliferation of cells (Fraser, Laurent, and Laurent 1997). The HA interaction with its surface receptor is also important in modulating cell-to-cell adhesion and cell aggregation (Knudson and Knudson 1993).

In solution, HA forms an entangled network that regulates the distribution and transport of macromolecules such as proteins to the tissues. At higher concentrations, such networks exhibit a visco-elastic property that cushions impact in the synovial fluid, acts as a lubricant between tissues and filters solutes through the ECM. The carboxyl groups on the glucuronic acid residues are fully ionized at the extracellular pH, which binds huge amounts of water (1000-fold of its own weight) (Laurent 1970) and maintains a turgor pressure.

HA directly influences cell behavior by signaling through the HA receptors such as CD44, and RHAMM present on the surface of the cells. The interaction of HA with its cell surface receptor initiates signaling pathways that promote cell movement, proliferation, or differentiation. The small fragments of HA, but not high molecular mass HA, are potent stimulators of angiogenesis and inflammatory responses, suggesting the importance of HA polymer size in cellular events (Asari 2005). The biological functions

of different HA fragments are summarized in Table 1. The cellular proliferation and migration events during processes such as embryogenesis (Toole 1991; Toole 2001), wound healing (Longaker et al. 1991; Weigel, Fuller, and LeBoeuf 1986), inflammation (de la Motte et al. 2003; Majors et al. 2003; Noble 2002) and cancer development (Toole 2002; Toole and Hascall 2002) are correlated with HA-mediated cell surface signaling.

The presence of HA in the cytoplasm and nucleus, along with the identification of intracellular HA-binding proteins, suggests that its action is not limited to within the ECM or at the cell surface. Several possible roles are assigned to intracellular HA including cell expansion and hypertrophy in chondrocytes, acting as a scaffold molecule in signaling events, and cell cycle control (Evanko and Thomas 2001).

## **1.4 Metabolism of HA**

### **1.4.1 Synthesis of HA**

HA is synthesized at the cytoplasmic side of the plasma membrane as a free polymer by the addition of sugar residues to the reducing end of the polysaccharide, and the growing chain is extruded through the membrane to the outside of the cells into the ECM (Spicer and McDonald 1998a). In humans and mice, three HA synthases, HAS1, HAS2, and HAS3, have been identified as internal cell membrane glycosyltransferases with several transmembrane domains (Spicer and McDonald 1998b; Weigel, Hascall, and Tammi 1997). The HA synthases are encoded by related but distinct genes, *HAS1*, *HAS2*, and *HAS3*, located on different chromosomes. They share 50-71% amino acid sequence identity (Spicer and McDonald 1998b).

**Table 1- Functions of HA oligosaccharides** (Modified from <http://www.glycoforum.gr.jp/science/hyaluronan/HA12a/HA12aE.html>)

HA (Molecular weight)	Functions
~ 10 <sup>7</sup> Da	Space filling High viscoelasticity Anti-inflammatory (McBride and Bard 1979) Anti-angiogenic (Feinberg and Beebe 1983) Immunosuppressive (Delmage et al. 1986)
20 kDa	Angiogenic (West et al. 1985) Inflammatory (Noble 2002) Stimulate cytokines synthesis (Noble 2002) Induce matrix metalloproteases (MMPs) transcription (Fieber et al. 2004) Stimulate endothelial recognition of injury (Taylor et al. 2004)
6 – 20 kDa	Angiogenic (Termeer et al. 2000) Inflammatory (Termeer et al. 2000) Immuno-stimulatory (Termeer, Sleeman, and Simon 2003)
800 Da	Induce heat shock proteins (Xu et al. 2002) Anti-apoptotic (Xu et al. 2002)

Expression of any single mammalian HAS in mammalian cell lines can lead to the biosynthesis of HA, suggesting that each functions independently as a synthase (Spicer and McDonald 1998b). However, the enzymatic properties and expression patterns of each HAS are different, indicating that each HAS protein may play a specific role in HA biosynthesis (Itano et al. 1999b; Weigel, Hascall, and Tammi 1997). HAS1 is the least active enzyme and synthesizes high molecular weight HA (~2 X 10<sup>6</sup> Da). HAS2, expressed widely throughout embryonic development, is significantly more active than HAS1 and generates high molecular weight HA (~2 X 10<sup>6</sup> Da). The most active of the three HAS enzymes, HAS3, is expressed late in embryonic development and in many adult tissues; it synthesizes short HA chains (~2 X 10<sup>5</sup> Da).

The functional relationship of the HAS proteins was assessed by generation of a knock out mouse for each HAS gene (Camenisch et al. 2000; Spicer and McDonald 1998b). Mice deficient in HAS2 activity were not obtained because the mutation was found to be lethal during embryonic development. These embryos had multiple developmental defects, including yolk sac and cardiac defects with no formation of cardiac jelly or cardiac cushion, and contain virtually no HA, suggesting that HAS2 is required for HA biosynthesis during normal embryonic development. Mice deficient in HAS1 and HAS3 activity were viable and fertile supporting the central role of HAS2 during normal embryonic development. Overproduction of HA by expression of HAS genes generates transgenic mice with increased tumor metastasis and proliferation of transformed cells, supporting the role of HA in tumorigenesis (Itano et al. 1999a; Kosaki, Watanabe, and Yamaguchi 1999). HA biosynthesis has been shown to increase during cell proliferation and migration and it decreases at high cell densities when cell proliferation is low (Huey, Moiin, and Stern 1990).

#### **1.4.2 Degradation of HA**

The synthesis of HA is balanced by catabolism, thereby maintaining a relatively constant concentration in the tissue under normal conditions. Turn over rates of HA vary between different tissues. The daily turn over of HA in an adult man is estimated to be one third of the total body HA (~ 15 g/70 kg of total weight) (Fraser and Laurent 1989; Laurent and Fraser 1991; Stern 2004c).

Metabolic studies in rat, rabbit and human, using radiolabeled HA have shown that HA turns over with a half-life of approximately 24 hours, which is relatively rapid

for an ECM molecule (Fraser and Laurent 1989). A substantial amount of HA (20-25%) is degraded locally within the tissues (Laurent and Fraser 1992). The remaining HA enters the lymphatic system and is transported to the local lymph nodes. The majority of HA is degraded in the lymph nodes but some manages to escape into the blood circulation. The HA in the blood has a half-life of a few minutes and the majority (85-90 %) of it is removed by the liver endothelial cells. A minor amount of circulating HA is metabolized by the kidney (10 %) (Laurent and Fraser 1986) and spleen (2-5 %) (Laurent and Fraser 1991); very little HA is excreted in the urine (Weigel, Hascall, and Tammi 1997).

Internalization of HA by cell surface receptors for its catabolism is now evident (Hua, Knudson, and Knudson 1993). Several HA-binding cell surface receptors such as CD44 (Culty, Nguyen, and Underhill 1992), Lymphatic Vessel Endothelial HA Receptor-1 (LYVE-1) (Banerji et al. 1999), and HA Receptor for Endocytosis (HARE) (Zhou et al. 2000) are now identified (Todd, Camenisch, and McDonald 2000). The HA taken up by endocytosis is thought to be transported to the lysosomes that contain hyaluronidase, and two exoglycosidases,  $\beta$ -glucuronidase and  $\beta$ -N-acetyl glucosaminidase, that are required for HA degradation. Hyaluronidases cleave HA internally to generate oligosaccharides, which in turn are further degraded by  $\beta$ -glucuronidase and  $\beta$ -N-acetyl glucosaminidase (Roden et al. 1989). The contribution of the two exoglycosidases was demonstrated by accumulation of small HA fragments in fibroblasts from a patient with I-cell disease (section 1.6.2) (Stern 2004b), as both of these enzymes are affected by this disease. However, HYAL1 is not elevated in the serum of the I-cell patients (Natowicz and Wang 1996).

A model for HA catabolism is proposed, emphasizing the importance of two of the hyaluronidases, HYAL1 and HYAL2, in HA degradation (Stern 2004a). According to this model, GPI-anchored HYAL2 at the plasma membrane interacts with the HA receptor CD44 and degrades HA to give 20-kDa fragments. These fragments are then delivered to lysosomes by receptor-mediated endocytosis to be further degraded by HYAL1,  $\beta$ -glucuronidase, and  $\beta$ -N-acetyl glucosaminidase (Figure 2). The interaction of HYAL2 with CD44 and the  $\text{Na}^+$ - $\text{H}^+$  exchanger, creates an acidic environment that facilitates HA degradation (Bourguignon et al. 2004), supporting the role of HYAL2 in this model.

### **1.5 Hyaluronidase overview**

The hyaluronidase activity was initially identified as a “spreading factor” from mammalian testis extracts (Claude and Duran-Reynals 1934). In 1940, Karl Meyer introduced the term “hyaluronidase”, as it degrades HA (Chain and Duthie 1940). In humans, six hyaluronidase genes (*HYAL1*, *HYAL2*, *HYAL3*, *HYAL4*, *SPAM1*, and *PHYAL1*) have now been identified that form one large family (Csoka, Scherer, and Stern 1999). They share 40% identity with each other and are clustered in groups of three on two separate chromosomes; *HYAL2*, *HYAL1*, and *HYAL3* are on human chromosome 3p21.3, and *HYAL4*, *SPAM1*, and *HYALP1* are on human chromosome 7q31.3 (Csoka, Scherer, and Stern 1999). *HYAL1*, *HYAL2* and *HYAL3* were initially identified as candidates for a lung cancer tumor suppressor as *LUCA1*, *LUCA2* and *LUCA3*, respectively, in the 3p21 region (Wei et al. 1996). All of these genes have unique tissue-specific expression profiles with *HYAL2* having the broadest expression pattern and

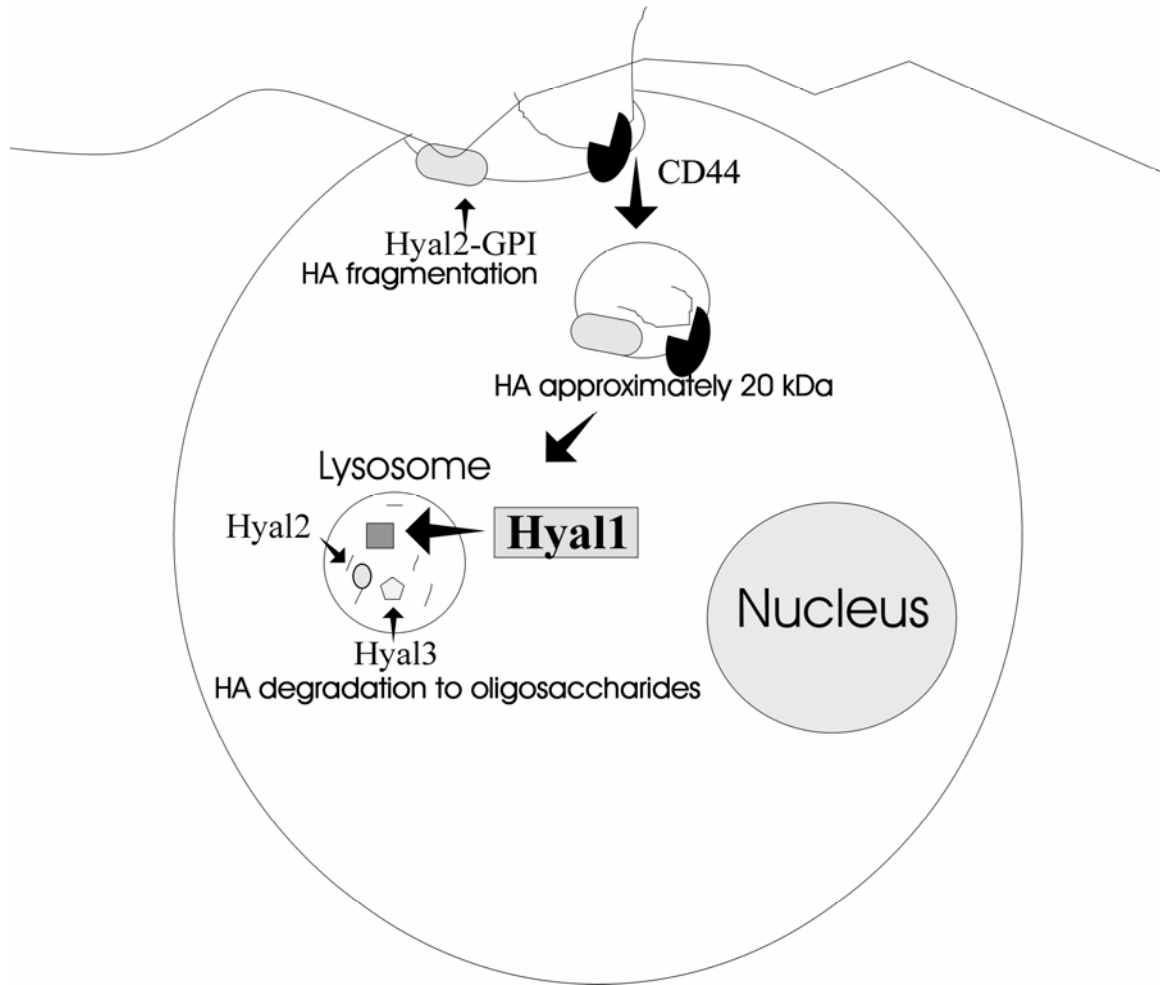


**Figure 2. Hypothetical model for HA degradation.** Diagram of the model for HA degradation that shows the possible role of HYAL1, HYAL2 and HYAL3 in HA degradation along with the help of cell surface receptor CD44 and two exoglycosidases in the lysosomes (not shown). Modified by Martin, D. from the original diagram (<http://www.glycoforum.gr.jp/science/hyaluronan/HA15a/HA15aE.html#IV>).

*SPAMI* the narrowest. The characterization of the individual gene products is still in its infancy. In humans, *pHYALI* is a pseudogene that does not encode any protein product.

### **1.5.1 Hyaluronidase 1 (HYAL1)**

*HYALI* was reported to encode a 57 kDa acid-active hyaluronidase, HYAL1, that was purified from human plasma as a detergent soluble protein (Frost et al. 1997). The 57 kDa form of HYAL1 is also found in urine, with an additional active form of 45 kDa. This 45 kDa form in urine results from the endo-proteolytic cleavage of about 99 amino acids at the C-terminus of plasma HYAL1 and forms a second smaller polypeptide of 25 kDa. The resulting two polypeptides from the 57 kDa form are assumed to be linked by a disulfide bond (Csoka et al. 1997).

*HYALI* is expressed in several human tissues, with the highest expression in liver followed by kidney, spleen and heart. It is also expressed in lung and placenta at very low levels (Csoka, Frost, and Stern 2001). In humans, two transcripts at 2.4 and 3.0 kb are detected, that result from alternative splicing of the *HYALI* 5' untranslated region (Csoka, Scherer, and Stern 1999). The expression profile of *HYALI* in mice tissues is similar to that of human, however, higher numbers of transcripts are detected (Shuttleworth et al. 2002).

*HYALI* is located at a candidate tumor suppressor gene locus (Wei et al. 1996). The regulation of hyaluronidase activity by tumor cells can provide them with a HA rich matrix for their proliferation and migration. *HYALI* deletion is reported in lung tumors (Lerman and Minna 2000), as well as in oral, head, and neck tumors (Frost et al. 2000). *HYALI* is also reported to be regulated at the transcriptional level in a number of cancer

cell lines (Frost et al. 2000). In such cases, a larger transcript of *HYAL1* mRNA is detected with a large 5' untranslated region, indicating the presence of a retained intron. On the other hand, the possible role of *HYAL1* as an oncogene is also reported. The levels of *HYAL1* are shown to correlate with prostate (Lokeshwar et al. 2001; Posey et al. 2003) and bladder (Hautmann et al. 2001; Lokeshwar et al. 2000; Lokeshwar et al. 2002) tumor progression.

### **1.5.2 Other members of the hyaluronidase family**

*HYAL2* encodes a 60 kDa acid-active hyaluronidase, *HYAL2*, that is detected in most tissues. It was originally identified as a lysosomal enzyme that degrades high molecular weight HA to fragments of approximately 20 kDa (Lepperdinger, Strobl, and Kreil 1998). The GPI-anchored form, at the outer membrane of the cells, was detected subsequently (Rai et al. 2001). The over-expression of *HYAL2* in murine cells, promotes tumor formation and invasion (Novak et al. 1999). *HYAL2* also functions as a cell surface receptor for Jaagsiekte retrovirus that causes lung cancer in sheep (Rai et al. 2001).

*HYAL3* encodes a 53 kDa acid active hyaluronidase, *HYAL3* (Hemming et al, manuscript in preparation), that is detected in a broad range of tissues at low levels (Csoka, Scherer, and Stern 1999; Shuttleworth et al. 2002). The highest expression levels in humans were detected in testis and bone marrow (Csoka, Scherer, and Stern 1999). Expression studies of *HYAL3* mRNA in chondrocytes showed that IL-1 and TNF- $\alpha$  increase its levels whereas retinoic acid decreases them (Flannery, Little, and Caterson 1998). The regulation of *HYAL3* by these inflammatory cytokines suggests that it may

play a role in regulated catabolism of HA.

*SPAMI* encodes a 64 kDa neutrally active hyaluronidase, PH-20, that is attached to the plasma and acrosomal membrane by a GPI-anchor (Gmachl et al. 1993). It is specifically expressed in the sperm and facilitates the penetration of the sperm through the cumulus mass surrounding the ovum, which is necessary for fertilization. The GPI-anchored protein is processed to generate a 53 kDa acid-active soluble protein composed of two fragments linked by disulfide bonds (Cherr et al. 1996; Sabeur et al. 1997; Seaton, Hall, and Jones 2000). Recently it has been detected in other tissues such as epididymis, seminal vesicles, prostate (Deng, He, and Martin-DeLeon 2000), female reproductive tract (Zhang and Martin-DeLeon 2003), placental and fetal tissues (Csoka, Scherer, and Stern 1999), and breast tissues (Beech, Madan, and Deng 2002).

*HYAL4* is expressed in placenta and skeletal muscle, and predicted to encode a 54 kDa HYAL4 protein (Csoka, Scherer, and Stern 1999). It is reported to have absolute chondroitinase activity (Stern 2003). No further data is available on HYAL4.

*PHYALI* is a pseudogene containing deletion mutations that cause two premature terminations, and therefore it is not translated into active enzyme in humans (Csoka, Scherer, and Stern 1999).

An additional enzyme, MGEA5, has been proposed as a seventh hyaluronidase (Heckel et al. 1998). It is located on human chromosome 10q24.1. It encodes 76 and 103 kDa cytosolic proteins reported to have hyaluronidase and N-acetylglucosaminidase activity (Comtesse, Maldener, and Meese 2001).

## **1.6 Mucopolysaccharidosis (MPS) IX**

### **1.6.1 MPS IX and HYAL 1**

The MPS disorders are a subset of lysosomal storage disorders (section 1.6.2) caused by a deficiency of lysosomal enzymes needed to degrade GAGs (mucopolysaccharides). The undegraded or partially degraded GAGs are stored in lysosomes and/or excreted in urine (Byers et al. 1998). MPSs are rare diseases that with the exception of MPS II, which is X-linked, are transmitted in an autosomal recessive manner. To date, 11 enzyme deficiencies are known that give rise to eight distinct MPS's (Table 2). The severity of MPS varies from mild to very severe; common clinical features include a chronic and progressive course, multisystem involvement, organomegaly, dysostosis multiplex, and abnormal faces. Mental retardation is observed only in the severe types of MPS I (Hurler syndrome), MPS II and all types of MPS III. Other symptoms specific to that disorder may develop.

A relatively recent addition to this family of disorders is MPS IX, caused by a deficiency of the plasma hyaluronidase enzyme (Natowicz et al. 1996). The broad distribution and abundance of HA in humans suggested that a genetic deficiency of hyaluronidase would be incompatible with life. However, the 14-year-old patient that was described had a relatively mild clinical phenotype (OMIM # 601492) that included mild short stature, peri-articular masses, bone erosions of the hip joints, submucosal cleft palate, a flattened nasal bridge and accumulation of HA in the lysosomes of the macrophages and fibroblasts. The mild clinical features provided the first clue that multiple hyaluronidases might exist.

**Table 2 - Types of MPS** (Modified from

<http://www.glycoforum.gr.jp/science/word/glycopathology/GDA05E.html>)

<b>MPS Type</b>	<b>Syndrome Name</b>	<b>Deficiency</b>	<b>Substrate Accumulation</b>
MPS type I-H/S	Hurler syndrome, Scheie syndrome	$\alpha$ -L-iduronidase	Dermatan sulfate, Heparan sulfate
MPS type II	Hunter syndrome, mild form	L-sulfofuronate sulfatase	Dermatan sulfate, Heparan sulfate
MPS type III-A	Sanfilippo syndrome type A	Heparan sulfate sulfamidase	Heparan sulfate
MPS type III-B	Sanfilippo syndrome type B	<i>N</i> -acetyl- $\alpha$ -D-glucosaminidase	Heparan sulfate
MPS type III-C	Sanfilippo syndrome type C	Acetyl-coenzyme A (CoA): $\alpha$ -glucosamide <i>N</i> -acetyltransferase	Heparan sulfate
MPS type III-D	Sanfilippo syndrome type D	<i>N</i> -acetyl- $\alpha$ -D-glucosamine-6-sulfatase	Heparan sulfate
MPS type IV-A	Morquio syndrome, classic form	<i>N</i> -acetylgalactosamine-6-sulfatase (gal-6-sulfatase)	Keratan sulfate, Chondroitin-6-sulfate
MPS type IV-B	Morquio like syndrome	$\beta$ -galactosidase	Keratan sulfate
MPS type VI	Maroteaux-Lamy syndrome	<i>N</i> -acetylgalactosamine-4-sulfatase (arylsulfatase B)	Dermatan sulfate
MPS type VII	Sly syndrome	$\beta$ -glucuronidase	Dermatan sulfate, Heparan sulfate, Chondroitin-6-sulfate
MPS type IX	N/A	Hyaluronidase 1	Hyaluronan

To determine the molecular basis of MPS IX, two candidate genes with similarity to the sperm protein, *HYAL1* and *HYAL2*, were analyzed. Two mutations in the *HYAL1* alleles of the patient were identified, a 1412G-A mutation that results in substitution of a nonconservative Lys for Glu at position 268 (a putative active site) and a complex intragenic rearrangement with a 37-bp deletion starting at nucleotide 1361 and a 14-bp insertion that causes a premature termination codon (Triggs-Raine et al. 1999). The authors further suggested that the existence of three hyaluronidases in the same region and the different expression profiles of *HYAL1*, *HYAL2* and *HYAL3* in human tissues, might explain the mild phenotype in the *HYAL1* deficient patient.

### **1.6.2 Lysosomal storage disorders**

The lysosomal enzymes can collectively degrade most of the naturally occurring endogenous or exogenous macromolecules, making lysosomes the main cellular centre for catabolism in eukaryotes. However, genetic abnormalities in a lysosomal enzyme, its transport, or its processing, can disrupt lysosomal function. In such cases, partially digested molecules or the substrate (in case of a transporter defect) such as sphingolipids, glycogen, mucopolysaccharides or glycoproteins accumulate progressively within lysosomes leading to a lysosomal storage disorder (Winchester, Vellodi, and Young 2000). Over 40 different lysosomal storage disorders have been described in humans, with an overall occurrence estimated to be approximately 1 in 8000 live births (Meikle et al. 1999). The clinical symptoms of different lysosomal storage disorders depend on the type of affected protein, the nature of the substrate, and the cells in which the substrate is accumulated. The molecular basis of the majority of lysosomal storage disorders are

known (Neufeld and Muenzer 2001).

### **1.6.3 Mannose-6-phosphate (M6P) dependant targeting of lysosomal enzymes**

Many lysosomal enzymes are synthesized in the rough ER (RER) and targeted to the lysosomes with the aid of several enzymes and a carbohydrate recognition signal on the enzymes (Hickman and Neufeld 1972; Kaplan, Adachi, and Sly 1997; Kornfeld 1992; Reitman and Kornfeld 1981). The initial step of synthesis on the membrane-bound polysome in the RER is common between lysosomal enzymes, and other proteins such as secretory and plasma membrane proteins. All three classes of enzyme contain a hydrophobic N-terminal signal peptide that facilitates the translocation of the nascent protein across the RER membrane into the lumen of this organelle. The lysosomal enzymes, as well as most of the secretory and plasma proteins, undergo cotranslational glycosylation of selected asparagine (Asn) residues within the Asn-X-Ser/Thr sequence, where X can be any amino acids except Pro or Asp. The glycosylation step involves the transfer of a large preformed oligosaccharide (three glucose, nine mannose and two N-acetylglucosamine residues) from a lipid-linked intermediate to the growing polypeptide, catalyzed by a membrane-bound oligosaccharyl transferase. The signal sequence is then cleaved and the initial processing of the Asn-linked oligosaccharide begins in the ER. The three terminal glucose residues are removed by glucosidase I and II with subsequent removal of a single mannose residue by a  $\alpha$ -1, 2-mannosidase from the oligosaccharide.

The proteins then move to the Golgi apparatus by vesicular transport where they are further modified by a variety of posttranslational modifications and sorted from one another for targeting to their final destination. The oligosaccharides on the secretory and

plasma proteins are sometimes processed to contain sialic acid containing complex-type units. Although some of the oligosaccharides on lysosomal enzymes undergo similar processing, some are specifically and uniquely modified to contain a terminal mannose-6-phosphate. This modification occurs through the sequential action of two enzymes. First, phosphotransferase transfers the N-acetylglucosamine 1-phosphate to the sixth position of mannose on a high-mannose oligosaccharide. The second, N-acetylglucosaminidase, then removes the N-acetylglucosamine residue to expose the mannose-6-phosphate (M6P). The phosphorylation of the mannose residue is a key process in sorting several lysosomal enzymes as it serves as an essential component of a recognition marker that leads to high-affinity binding to M6P receptors in the trans Golgi. The lysosomal enzyme-M6P receptor complex then exits the Golgi via a coated vesicle and is delivered to a prelysosomal compartment (endosomes) where the ligand is dissociated. Another key factor in the transport is variation of the pH in different compartments; the receptor binds ligand at nearly neutral pH in the Golgi and discharges it at acidic pH in the endosome, thereby assuring proper transport of the enzymes. The enzymes are packed into the lysosomes while the receptor recycles back to the Golgi. A small amount of the lysosomal enzymes are secreted and eventually recaptured by surface bound M6P receptors to be delivered to the lysosomes (Kornfeld 1987; Kornfeld 1990).

The lysosomal enzymes are processed further by proteolytic cleavage that appears to be initiated in prelysosomal compartments and is completed after their arrival in lysosomes. The biological significance of this processing is not very clear, but it might activate or stabilize the enzymes, inhibit their retrograde transfer to the Golgi or may even provide signals for a M6P-independent pathway (Kornfeld 1987).

The clues to elucidate this M6P receptor dependant pathway for lysosomal enzymes came from studies of patients with a lysosomal storage disorder called Inclusion cell (I-cell) disease (Hickman and Neufeld 1972). It is an autosomal recessive disorder that occurs due to a defect in the phosphotransferase that phosphorylates the mannose residues on lysosomal enzymes. The lysosomal enzymes are not recognized by the M6P receptor in the absence of the M6P recognition marker and therefore not targeted to the lysosomes but instead are carried to the cell surface and secreted. This was characterized by an elevated level of many lysosomal enzymes in the patient's plasma. However, some enzymes (e.g. acid phosphatase,  $\alpha$ -glucosidase, glucocerebrosidase) were present normally in patients fibroblast. Several cell types from the patient such as hepatocytes, Kupffer cells, and leukocytes also contain nearly normal levels of lysosomal enzymes even though the phosphotransferase activity was absent in these cells (Ginsel and Fransen 1991; Kornfeld 1986). This strongly suggests that alternative mechanism(s) for lysosomal targeting must be present.

### **1.7 Objectives and rationale of the study**

In order to more fully understand the function of HYAL1, it is necessary to know its subcellular localization(s). Mutations in HYAL1 led to lysosomal storage of HA, indicating that HYAL1 has a lysosomal localization (Natowicz et al. 1996; Triggs-Raine et al. 1999). The acidic pH optimum of HYAL1 also suggests that it is a lysosomal enzyme. However, there is also evidence for a membrane localization; it partitions to a detergent phase and was reported to be unstable in the absence of detergents (Frost et al. 1997). Further, its activity is higher in many mouse tissues when detergent is included in

the extraction buffer (Natowicz M. personal communication ), perhaps similar to the hyaluronidases PH-20 and Hyal2 that have membrane anchors (Gmachl et al. 1993; Rai et al. 2001). Bioinformatic analysis of HYAL1 amino acid sequence did not reveal any obvious membrane-spanning domain, making it likely that membrane localization may be due to a lipid molecule. This may be a modified GPI anchor or another lipid molecule, as phospholipase C (which removes some GPI anchors), did not release HYAL1 from cells (Ray, R. personal communication).

In addition to the possibility of a membrane localization, there is existing evidence that HYAL1 may not be targeted to the lysosomes by the classical M6PR-dependent pathway. HYAL1 activity is not elevated in the serum of patients with I-cell disease (Natowicz and Wang 1996), an inborn error of metabolism that prevents the addition of the mannose 6-phosphate lysosomal targeting signal and thus results in elevated serum levels of some lysosomal enzymes.

Based on the evidence above, we hypothesized that HYAL1 is a lysosomal enzyme that is targeted to the lysosomes by a novel pathway that may include a transient membrane localization. The characterization of alternate lysosomal targeting routes is important as it may allow new strategies for the targeting of therapeutic enzymes to be developed for lysosomal storage disorders. I will also provide new knowledge about where and how HYAL1 functions.

The overall objectives of this study were to examine the subcellular localization and targeting route of HYAL1.

# **MATERIALS AND METHODS**

## **2.1 Generation of the HYAL1 expression construct**

To overcome the problem of low endogenous HYAL1 expression in the cell lines examined by our laboratory, the minimal HYAL1 coding sequence was cloned into pIRESneo to generate pIRES\_HYAL1.

### **2.1.1 pIRESneo vector**

The pIRESneo (described originally as pCIN4, GenBank Accession # U89673) mammalian expression vector (CLONTECH Laboratories Inc-USA), was chosen because the gene of interest is expressed as a co-transcript with the selectable marker for neomycin resistance. The expression cassette of pIRESneo contains the human cytomegalovirus (CMV) major immediate early promoter/enhancer followed by a multiple cloning site (MCS). The encephalomyocarditis virus (ECMV) internal ribosome entry site (IRES) that is downstream of the MCS permits the translation of a second open reading frame, neomycin phosphotransferase (NP II). The polyadenylation signal of the bovine growth hormone ends the cassette. When a cDNA is cloned into the MCS, both the cDNA and the NP II selection marker are transcribed from the CMV promoter; thus, culturing cells in a high concentration of antibiotic should select cells expressing a high level of the gene of interest. The presence of an ampicillin resistance gene allows the selection of this vector in *E.coli*.

### **2.1.2 Polymerase Chain Reaction (PCR) amplification of DNA**

The full-length human HYAL1 coding sequence (Genbank Accession # U96078) was amplified by PCR from the EST clone AA223264. The cDNA (0.2 to 0.5 µg) was

mixed with 80  $\mu$ l of double distilled water, 10  $\mu$ l of 10 X PCR Buffer (100 mM Tris-HCl pH 8.3, 500 mM KCl, 15 mM MgCl<sub>2</sub>), 2  $\mu$ l each of 10 mM dNTPs (10 mM dATP, 10 mM dCTP, 10 mM dTTP, 10 mM dGTP), 1  $\mu$ l (0.1  $\mu$ g) sense primer WPG 380, 1  $\mu$ l (0.1  $\mu$ g) anti-sense primer WPG 381 and 0.5 units Taq DNA Polymerase<sup>TM</sup> (Invitrogen). The primers WPG 380 5'GCGGAATTCTGCCATGCAGCCCACCTGCT3' and WPG 381 5'GCGGATCCAATCACCATGCTCTTCCGC3' were designed to introduce an EcoRI restriction enzyme site at the 5' end and a BamHI restriction enzyme site at the 3' end of the coding sequence. The reactions were overlaid with approximately 50  $\mu$ l of mineral oil and the PCR amplification was performed in a Cetus DNA Thermal Cycler (Perkin Elmer). The reactions were incubated at 94°C for 2 minutes and the amplification was carried out using 32 cycles with the following program setting: a denaturation step for 30 seconds at 94°C, an annealing step for 1 minute at 59°C and an extension step for 1 minute at 72°C.

The amplified cDNA fragments were restriction enzyme digested (section 2.1.5) and separated on an agarose gel (section 2.1.3). The *HYALI* fragments were purified from the gel using a QIAquick Gel Extraction Kit (Qiagen), following the manufacturer's instructions.

### **2.1.3 Agarose gel electrophoresis**

DNA samples were prepared for electrophoresis by adding 6 X Sample Buffer (0.25% bromophenol blue [Sigma], 0.25% xylene cyanol [Sigma], 30% glycerol [Sigma]) to a final concentration of 1 X, and the mixture was separated by electrophoresis. The DNA fragments were routinely analyzed by separation on 1% agarose gels prepared in 1

X TAE Buffer (40 mM Tris, 40 mM acetate, 1 mM ethylene diamine tetra acetic acid [EDTA]) containing 0.5 µg/ml ethidium bromide. Electrophoresis was performed using 1 X TAE Buffer as running buffer at 110 V. The separated DNA fragments were visualized using an ultraviolet transilluminator and photographed by a Polaroid MP-4 Land Camera. The sizes of the DNA fragments were determined by comparison with the 1 Kb DNA ladder (Gibco/BRL).

#### **2.1.4 Quantitative analysis of DNA**

##### **2.1.4.1 Determination of DNA concentration by spectrophotometric analysis**

The DNA concentration of plasmid was determined by measuring the absorbance (A) of the sample at a wavelength of 260 nm through a one cm light path. The concentration was calculated based on the formula (below) where the absorbance of 1 corresponds to 50 µg/ml of DNA (Sambrook, Fritsch, and Maniatis 1989).

$$[\text{DNA } (\mu\text{g/ml})] = (A_{260 \text{ nm}}) \times (50 \mu\text{g/ml}) \times (\text{dilution factor})$$

##### **2.1.4.2 Estimation of DNA concentration using DNA MASS™ Ladder**

DNA MASS™ Ladder (4 µl, Gibco/BRL) and experimental samples were loaded on a 1% agarose gel containing 0.5 µg/ml ethidium bromide and separated by electrophoresis (section 2.1.3). After separation, the DNA MASS Ladder™ yields bands containing 200, 120, 80, 40, 20, and 10 ng of DNA respectively. The fluorescent intensity of the sample of interest was compared by eye to that of the ladder, and the DNA concentration in the sample was estimated based on the closest match.

### **2.1.5 Restriction enzyme digestion**

The restriction enzyme digestions of plasmid DNA or PCR-products were done using one or two restriction enzymes at a time. The enzyme digests were set up by adding 1  $\mu$ l of restriction enzyme (10–20 units), 2  $\mu$ l of 10 X restriction enzyme buffer (as recommended by the enzyme manufacturer) to a DNA sample (1-5  $\mu$ g) and double distilled water up to a final volume of 20  $\mu$ l. In the case of double digests, the DNA was restriction enzyme digested with one restriction enzyme followed by the second restriction enzyme. The reactions were incubated for 1 to 2 hours at the temperature specific for the restriction enzymes. To prevent self-ligation of linearized plasmid DNA, 1  $\mu$ l of Calf Intestinal Alkaline phosphatase (CIAP, NEB) was added to the digested fragments and incubated at 37°C for 1 hour, when necessary. The digested DNA products were purified by phenol: chloroform extraction followed by ethanol precipitation (section 2.1.6), dissolved in sterile distilled water, and analyzed by agarose gel electrophoresis. (section 2.1.3)

### **2.1.6 Phenol-chloroform extraction of DNA**

Phenol-chloroform extraction, followed by ethanol precipitation, was performed to purify and concentrate DNA, as described in “Current Protocols in Molecular Biology” (Moore and Dowhan 2002). Briefly, the DNA samples were mixed with an equal volume of a phenol: chloroform: isoamyl alcohol mixture (25:24:1) in a 1.5 ml Eppendorf tube. The mixture was vortexed vigorously for 10 seconds and the phases were separated by centrifugation at 16000 x g in an Eppendorf centrifuge 5415D. The aqueous phase was transferred to a new tube and the organic phase was re-extracted by repeating the above

procedure. The aqueous phases were pooled, and mixed with an equal volume of chloroform: isoamyl alcohol (24:1), followed by centrifugation to separate the phases as described earlier. The aqueous phase was collected and mixed with 2.5 volumes of ice-cold 95% ethanol. After incubation at -20°C for 15 minutes, the DNA was pelleted by centrifugation at maximum speed in an Eppendorf centrifuge 5415D for 20 minutes. The DNA pellet was washed in cold 70% ethanol and pelleted by centrifugation as described above. The pellet was air-dried and resuspended in sterile double distilled water.

### **2.1.7 Bacterial medium and agar preparation**

Luria Bertani (LB) broth and agar were prepared from pre-made mixes (Invitrogen) as recommended by the manufacturer. Ampicillin (100 µg/ml) was added as a supplement when required.

### **2.1.8 Plasmid DNA preparation**

#### **2.1.8.1 Small scale plasmid DNA isolation**

Small quantities of plasmid DNA (5 – 20 µg) were prepared using the alkaline lysis method (Birnboim 1983). Briefly, a single plasmid-bearing colony was inoculated into 5 ml of sterile LB Broth containing 100 µg/ml ampicillin (LBA broth), and incubated overnight at 37°C with constant shaking. From this, 1.5 ml of culture was used for plasmid isolation and the remainder was retained to use as a starter culture for large-scale plasmid production. Cells were pelleted from the 1.5 ml of culture by centrifugation at 16000 x g in an Eppendorf 5415D centrifuge for 20 seconds. The supernatant was

discarded, the pellet was lysed, and the plasmid DNA was isolated as described (Moore and Dowhan 1991).

#### **2.1.8.2 Large scale plasmid DNA isolation**

Two flasks, each containing 250 ml of LBA broth, were inoculated with 0.5 ml of starter culture (section 2.1.8.1) and incubated overnight at 37°C with shaking. The bacterial cells containing plasmid DNA were pelleted by centrifugation at 5000 x g for 15 minutes. The plasmid DNA was isolated from the bacterial cell pellet using a Qiagen Maxi Prep Kit (Qiagen) and following the manufacturer's protocol. The concentration of purified plasmid DNA was measured by spectrophotometric analysis (section 2.1.4.1).

#### **2.1.9 Ligation of plasmid and insert DNA**

The 1.3 kb *HYAL1* insert, restriction enzyme digested with BamHI and EcoRI, was cloned into the MCS of the BamHI/EcoRI digested pIRESneo plasmid, to generate the pIRES\_HYAL1 construct. The ligation reaction consisted of ~ 280 ng of insert DNA, ~ 150 ng of vector DNA, 5 µl of 10 X ligase Buffer (New England Biolabs NEB), 1 µl of T4 DNA ligase (400 units/µl, NEB) and sterile double distilled water to make up a final volume of 50 µl. The ligation mixture was incubated at 14°C for 4 hours. The ligation products were transformed into electrocompetent bacterial cells as described in 2.1.10 below.

#### **2.1.10 Transformation into competent *E.coli* cells**

Plasmid DNA and ligation products were introduced into competent bacterial

cells by electroporation, following the conditions and protocol provided by the manufacturer of the ELECTRO CELL MANIPULATOR 600 (BTX). Immediately after electroporation, 960  $\mu$ l of warmed SOC Medium (2% Bacto Tryptone, 0.5% Bacto Yeast Extract, 0.05% NaCl, 2.5 mM KCl, 20 mM glucose [added after autoclaving], pH 7.0) was added, mixed gently and transferred to a sterile microcentrifuge tube. The cells were incubated at 37°C for 1 hour with shaking. After incubation, 50  $\mu$ l and 100  $\mu$ l of the mixture, was evenly spread on a LBA plate (section 2.1.7) and incubated overnight at 37 °C.

#### **2.1.11 Preparation of 50% glycerol stock**

Equal volumes of 100% glycerol, and bacterial culture that had grown overnight, were mixed and stored at -20°C. The culture was recovered by streaking on LBA plates.

## **2.2 Mammalian cell culture**

### **2.2.1 Mammalian cell lines**

BHK-21 is a Syrian hamster kidney cell line that was obtained from the American Type Culture Collection (Rockville, MD). It was originally derived as clone 13 (C-13) by Stoker and McPherson from a primary culture of 1-day old hamster kidney tissue (Stoker and Macpherson 1964). The BHK\_HYAL1 and BHK\_pIRESneo lines were derived by stable transfection of BHK-21 cells with pIRES\_HYAL1 and pIRESneo respectively (section 2.3).

### **2.2.2 Maintenance and passage of mammalian cells**

BHK-21 cells were maintained on tissue culture flasks or plates containing Complete Medium (Minimum Essential Medium-alpha [ $\alpha$ -MEM, Gibco/BRL], 100 units/ml Penicillin/100  $\mu$ g/ml Streptomycin [Gibco/BRL], 2 mM glutamine [Gibco/BRL], 10% Fetal bovine serum [FBS, Gibco/BRL]) at 37°C with 5 % CO<sub>2</sub>. Cells were subcultured when they reached about 85 % confluence. Briefly, the conditioned medium was aspirated and the cell monolayer was rinsed with 2 ml of pre-warmed trypsin-EDTA (Gibco/BRL) solution. The cells were harvested by incubating the flask with 2-3 ml of pre-warmed trypsin-EDTA at 37°C for 2-3 minutes and the trypsinized cells were diluted with 5 ml of warm Complete Medium. The suspended cells (1-2 ml) were added to a new flask (T25) containing 8 ml of Complete Medium and incubated as described above. The BHK\_HYAL1 and BHK\_pIRESneo cells were maintained as described above but in the presence of 200  $\mu$ g/ml Geneticin® (Sigma).

### **2.2.3 Freezing and thawing of mammalian cells**

For long-term storage, cells grown to ~ 80% of confluence in tissue culture plates (150 mm X 20 mm) or a tissue culture flask (T75) were detached with trypsin (section 2.2.2). The trypsinized cells were diluted into 8 ml of warm Complete Medium, and pelleted at 500 x g for 5 minutes. The conditioned medium was aspirated; the cells were resuspended in 2 ml of cold Freezing Medium (Gibco/BRL), transferred to a cold prelabeled cryovial, and stored at -80°C overnight. The cryovials were transferred to liquid nitrogen for long-term storage.

Cells stored in liquid nitrogen were thawed at 37°C. As soon as the vial contents

thawed, one ml of warm Complete Medium was mixed with the cell suspension, and then transferred to a 15 ml conical tube containing 10 ml of warm Complete Medium. The cells were pelleted by centrifugation at 500 x g for 5 minutes. The conditioned medium was discarded and the cells were resuspended in 10 ml of warm Complete Medium. The cell suspension was transferred to a tissue culture flask (T25) or plate and incubated overnight at 37°C with 5 % CO<sub>2</sub>.

### **2.3 Transfection of BHK cells**

BHK cells to be transfected were grown to 90-95% of confluence in Complete Medium (section 2.2.2). One hour prior to transfection, the medium was replaced. The BHK cells were transfected using Lipofectamine™ 2000 solution following the manufacturer's instructions with some modification. Briefly, the Lipofectamine™ 2000 and DNA sample to be transfected were diluted with 500 µl of α-MEM Medium (Gibco/BRL) in separate tubes, incubated for 5 minutes at room temperature and combined together; one tube was prepared for each transfection. The transfection mixture was mixed well, and added to the cells. For transient transfection, the plates were incubated for 24 hours at 37°C with 5% CO<sub>2</sub> before cell lysates were prepared as described in section 2.4.

For stable transfection, 24 hours post transfection, cells (transfected with pIRES-HYAL1 or pIRES-Neo) were passaged (1:10 dilution) into fresh Complete Medium. One day later, the Complete Medium was replaced with medium containing 1mg/ml of Geneticin® (Selection Medium) and the plates were incubated for 18 days. Colonies were picked and subcultured in 12-well plates containing Selection Medium. All further

experiments were carried out in Maintenance Medium (Complete Medium with 200 µg/ml Geneticin®).

#### **2.4 Preparation of cell lysates and conditioned medium**

Cells grown in a 100 mm X 20 mm or 60 mm X 20 mm tissue culture dishes were placed on ice. The conditioned medium was collected and stored at 4°C, and the cell monolayer was washed 3 times with ice-cold phosphate buffered saline (PBS: 137 mM NaCl, 4.3 mM Na<sub>2</sub>HPO<sub>4</sub>, 2.7 mM KCl, 1.47 mM KH<sub>2</sub>PO<sub>4</sub>, pH 7.3). The cells were scraped into 0.5-1 ml Lysis Buffer (5 mM Tris-HCl pH 7.4, 150 mM NaCl, 10% glycerol, 1% Triton X-100, 1 X Protease Inhibitor [PI] Cocktail [Sigma]) and then transferred to a 1.5 ml Eppendorf tube. The tube was incubated on ice for 20 minutes with intermittent vortexing. To remove unbroken cells and membrane debris, the sample was subjected to centrifugation at maximum speed for 15 minutes in an IEC MICROMAX centrifuge at 4°C. The supernatant from the cell lysate was transferred to a new tube. The protein concentration of the cell lysate was measured (section 2.5) and the remainder of the sample was stored at -20°C. In the case of metabolic labeling, the cells grown to confluence were labeled first and then lysed in the same way described above.

The conditioned medium was subjected to centrifugation, as described above, to remove dead or floating cells. The conditioned medium was stored directly at -20°C.

#### **2.5 Determination of protein concentration**

Protein concentrations were determined with a BioRad assay kit, based on the method of (Bradford 1976) and following the manufacturer's protocol. Protein samples

diluted with 800  $\mu$ l of distilled water were mixed with 200  $\mu$ l of BioRad reagent and incubated for 5 minutes. The absorbance (O.D) was measured at 595 nm. Gamma globulin (5  $\mu$ g/ml, 10  $\mu$ g/ml, and 15  $\mu$ g/ml) was diluted in 800  $\mu$ l of distilled water, and used to generate a standard curve. Lysis Buffer was added to the blank (prepared to set the absorbance at zero) and gamma globulin samples at a concentration equivalent to that in the experimental samples. The protein concentration in the samples was determined by comparison to the standard curve.

## **2.6 Sodium Dodecyl Sulfate-Polyacrylamide Gel Electrophoresis (SDS- PAGE)**

### **2.6.1 Sample preparation**

Cell lysate or conditioned medium was mixed with 4 X Sample Loading Buffer (SLB: 8% SDS, 40% glycerol, 250 mM Tris-HCl, pH 6.8, 100 mM Dithiothreitol [DTT], 0.01% Bromophenol blue) to get a final concentration of 1 X SLB. The samples were vortexed, then denatured by heating for 5 minutes in a boiling water bath. In some cases, samples were prepared as described above in 4 X SLB, but without DTT. The samples were diluted to equalize their volume (if required), using 1 X SLB (with or without DTT) prior to SDS-PAGE.

#### **2.6.1.2 Protein separation by SDS-PAGE**

Proteins were separated by 7.5 %, 10 % or 12 % SDS-PAGE (the ratio of water to acrylamide was changed according to the percentage of resolving gel required) based on the method of Laemmli (Laemmli 1970). The resolving gel (10 % acrylamide:

bisacrylamide solution, 37 mM Tris-HCl pH 8.8, 0.1 % SDS, 0.1 % ammonium persulfate [APS], 5  $\mu$ l TEMED) was cast in a Mini-Protean vertical gel casting apparatus (BioRad) using 0.75 mm, 1.0 mm or 1.5 mm spacers and allowed to polymerize for 1 hour. The stacking gel (4% acrylamide: bisacrylamide solution, 125 mM Tris-HCl pH 6.8, 0.1% SDS, 0.1% APS, 5  $\mu$ l TEMED) was prepared and cast immediately on the top of the resolving gel. A comb (10 well or 15 well) was inserted into the gel, avoiding any air bubbles, and the gel was allowed to polymerize for 30 minutes. Protein samples and prestained protein marker (Amersham Biosciences) prepared in 1 X SLB were then loaded into the wells and separated by electrophoresis at 150 V (constant voltage). The gels were run in 1 X Running Buffer (25 mM Tris, 192 mM glycine, 0.1% SDS) for approximately 70 minutes at room temperature. Subsequent processing of the gel depended on the application.

## **2.7 Western blot analysis**

### **2.7.1 Transfer to nitrocellulose membrane**

Proteins separated by SDS-PAGE, were transferred to a nitrocellulose membrane as described by Towbin *et al* (Towbin, Staechelin, and Gordon 1979). A transfer sponge (2 piece), Whatman paper (4 piece) and a piece of nitrocellulose membrane (cut to the size of gel), were prewet in 1 X Western Transfer Buffer (25 mM Tris, 190 mM glycine, 20% methanol). A sandwich clamp was arranged in the following order bottom to top, transfer sponge, two pieces of Whatman paper, a SDS-PAGE gel, a piece of nitrocellulose membrane, two pieces of Whatman paper and a transfer sponge. The

sandwich clamp was then assembled into the Mini Trans-Blot Cell apparatus (BioRad). The apparatus was filled with ice cold 1 X Western Transfer Buffer and the transfer was carried out at 100 V (constant voltage) for 90 minutes at 4°C.

### **2.7.2 Detection of proteins using antibodies**

The nitrocellulose membrane (section 2.7.1) was rinsed with distilled water and stained with Ponceau S (0.2% [Sigma] in 5% acetic acid,) to verify proper transfer. The stain was washed off using Tween-Tris Buffered Saline (TTBS: 25 mM Tris, 150 mM NaCl, 0.05% [V/V] Tween-20 [Fisher] pH 7.4). The membrane was blocked with TTBS containing 5% Skim milk powder for 1 hour and incubated overnight at 4°C with anti-HYAL1 antibodies (1:1000) diluted in TTBS containing 5% skim milk powder and 0.02% sodium azide. The next day, the blot was washed three times for 10 minutes each with 1 X TTBS. The sheep anti-mouse antibodies conjugated to Horse Radish Peroxidase (Jackson Immuno Research) were diluted 7500 fold in TTBS containing 5 % skim milk powder and incubated with the membrane for 1 hour at room temperature. The blot was subsequently washed three times with TTBS for 10 minutes each and rinsed with distilled water. The proteins were detected with the aid of an ECL Plus kit (Amersham Biosciences) and following the manufacturer's instructions. The membrane was blotted with KimWipes to remove excess solution, wrapped in plastic wrap, and exposed to BioMax-Light film (Kodak) for 3 to 10 minutes, as required.

## **2.8 Zymography**

### **2.8.1 Gel electrophoresis**

Cell lysates and conditioned medium samples were prepared (section 2.4); except the Sample Loading Buffer was prepared without DTT and samples were incubated with 1 X SLB at 37°C for 5 minutes instead of heating in a boiling water bath. The samples were separated by 7% SDS-PAGE (section 2.6) with some modification. Briefly, 0.18 mg/ml of hyaluronic acid (Sigma) from human umbilical cord was incorporated into the 7% SDS-PAGE gel (0.75 mm thickness), and samples were separated in a cold room at 20 mA constant current for approximately 1 hour.

### **2.8.2 In gel activity assay**

SDS gels were incubated in a 3% Triton X-100 solution for 2 hours (several changes of detergent) to remove SDS. The gels were subsequently equilibrated with Assay Buffer (100 mM formate, 150 mM NaCl, 0.1% Triton X-100, pH 3.8) for 30 minutes, followed by overnight incubation in the same buffer at 37°C. The next day, the gels were equilibrated with 20 mM Tris-HCl solution pH 8.0 for 30 minutes at 37°C, then treated with 0.2 µg/ml of protease (Sigma, Catalogue number P-5147) dissolved in 20 mM Tris-HCl for 4 hours 37°C. The gels were rinsed with distilled water, equilibrated in Fix solution (30 % methanol, 10 % acetic acid) for 30 minutes, and stained with 2 % Alcian Blue solution by shaking it overnight at room temperature. The gels were destained using Fix solution and counter stained with 0.1 % Coomassie Blue stain.

## **2.9 Density gradient centrifugation**

### **2.9.1 Preparation of cell extract**

Five 150 X 20 mm culture plates of 90-95% confluent cells ( $\sim 3 \times 10^6$  cells) (BHK\_HYAL1) grown overnight in Maintenance Medium (section 2.2.2) were placed on ice. The conditioned medium was aspirated, and the cells were washed three times with 1 X PBS (section 2.4) and once with 1 X SHE Buffer (0.25 M sucrose, 20 mM 4-[2-hydroxyethyl]-1-piperazineethanesulfonic acid [HEPES] pH 7.4, 2 mM EDTA, 1X PI cocktail). Each plate of cells was scraped into 2 ml of 1 X SHE Buffer and transferred to a 15 ml conical tube. The cells were collected by centrifugation at 500 x g for five minutes and resuspended at a 3:1 ratio (V/V) of 1 X SHE Buffer containing 1 X PI cocktail to cells ( $\sim 1$  ml in total). The cell suspension was gently passed through a 25 Gauge needle seven to eight times, and the resulting extract was centrifuged at 1000 x g for 10 minutes to remove the nuclei and cell debris. The volume of the post-nuclear supernatant was adjusted to 0.5 ml with 1 X SHE Buffer, if required, and subjected to gradient centrifugation. All manipulations were done on ice.

### **2.9.2 Percol gradient centrifugation of the cell extracts**

The post-nuclear supernatant was gently layered on top of pre-chilled 25 % Percol solution prepared by dilution of 90 % Percol solution (90 % Percol [SIGMA], 10 % 2.5 M sucrose solution, 0.2 % 1 M HEPES pH 7.4) with 1 X SHE Buffer. The subcellular organelles were separated, based on their density by centrifugation at 36,000 x g for 45 minutes at 4°C in a BECKMAN L80 ultracentrifuge. After centrifugation, the tube was carefully assembled into an automated Density Gradient Fractionator (model 183, Instrument Specialties Company) and samples were collected from the top of the gradient

by pumping the Buffered Sucrose solution (60% sucrose, 20 mM HEPES pH 7.4, 0.01% Bromophenol Blue [SIGMA]) through the bottom of the tube. Fractions of 15 drops were collected from the top in prelabeled 1.5 ml Eppendorf tubes (~24-26 fractions in total) and kept on ice.

### **2.9.3 Preparation of samples for analysis**

To all the fractions, 10% Triton X-100 was added to give a final concentration of 0.1%. The tubes were incubated on ice for 30 minutes to facilitate lysis. Aliquots (150  $\mu$ l) from each fraction were mixed with 50  $\mu$ l of 4 X SLB (section 2.6.1), and boiled for 5 minutes, the rest of the samples were stored at -20°C. After boiling, the Percol was removed by centrifugation for 10 minutes at room temperature at maximum speed in an Eppendorf 5415D Centrifuge. The supernatants were transferred to new tubes for subsequent analysis.

## **2.10 Metabolic labeling of BHK\_HYAL1 or BHK\_pIRESneo cells**

### **2.10.1 Pulse labeling**

BHK\_HYAL1 and BHK\_pIRESneo cells were grown to confluence on 60 mm X 20 mm culture plates. The pulse labeling was performed as described in Current Protocols in Protein Science (Coligan et al. 1995a). Prior to labeling with [<sup>35</sup>S]-labeled met/cys (Pro-mix L-[<sup>35</sup>S] *in vitro* cell labeling mix, Amersham Biosciences), the cell monolayer were rinsed 3 times with Starvation Medium (D-MEM, 1X glutamine [GIBCO/BRL], 100 units/ml Penicillin/100  $\mu$ g/ml Streptomycin, 200  $\mu$ g/ml Geneticin®,

without methionine and cysteine) and incubated with 1 ml per plate of the same medium for 30 minutes. The cells were metabolically labeled by replacing Starvation Medium with 1 ml of Labeling Medium containing 14  $\mu$ l (200  $\mu$ Ci) of [ $^{35}$ S]-labeled met/cys and incubated for various time intervals.

Prior to labeling with [ $^{32}$ P]-orthophosphate (Perkin Elmer), the cell monolayer was rinsed three times with Starvation Medium ( $\alpha$ -MEM, 1 X glutamine, 100 units/ml Penicillin/100  $\mu$ g/ml Streptomycin, 200  $\mu$ g/ml Geneticin®, without sodium phosphate) and incubated for 30 minutes in 1 ml of the same medium to deplete the intracellular phosphate. The cells were then labeled for different time points in 1 ml of Labeling Medium containing 5  $\mu$ l (500  $\mu$ Ci) of [ $^{32}$ P]-labeled phosphate.

### **2.10.2 Chase**

The pulse labeling with [ $^{35}$ S]-labeled met/cys was terminated by washing the cell monolayer three times with 3 ml of Starvation Medium containing an excess amount of cold (non radioactive) methionine and cysteine (Chase Medium). The cells were then incubated with 1 ml of Chase Medium for various time intervals (chase points), before processing.

### **2.10.3 Treatment of [ $^{35}$ S]-labeled HYAL1 with glycosidases**

BHK\_HYAL1 and BHK\_pIRESneo cells grown to confluence in a 60 mm X 20 mm culture plate were pulse-labeled for 10 minutes, followed by chase, and HYAL1 protein was immunoprecipitated as described in 2.11. The immunoprecipitated protein was digested overnight at 37°C with either 10 units of Peptide N glycosidase F (PNGase

F from NEB) at pH 7.4 or 10 units of endoglycosidase H (Endo H from NEB) at pH 5.5 as described earlier (Sambrook, Fritsch, and Maniatis 1989).

#### **2.10.4 Pulse-chase analysis of HYAL1 in the presence of tunicamycin**

BHK\_HYAL1 and BHK\_pIRESneo cells, grown to confluence in 60 mm X 20 mm culture plates, were treated for 2 hours with 10 µg/ml of tunicamycin, an inhibitor of N-linked protein glycosylation, prior to pulse-chase analysis as described in Current Protocols in Protein Sciences (Coligan et al. 1995b). The cells were then starved for 30 minutes, pulse labeled with [<sup>35</sup>S]-labeled met/cys for 10 minutes and chased for 3 hours in the presence of 10 µg/ml of tunicamycin (Duksin and Bornstein 1977).

#### **2.10.5 Pulse-chase analysis of HYAL1 in the presence of brefeldin A (BFA)**

BHK\_HYAL1 and BHK\_pIRESneo cells, grown to confluence in 60 mm X 20 mm culture plates, were treated for 3 hours with 20 µg/ml of BFA, an inhibitor of protein transport from endoplasmic reticulum to Golgi, prior to pulse-chase analysis. The cells were then starved for 30 minutes, pulse labeled with [<sup>35</sup>S]-labeled met/cys for 10 minutes and chased for 3 hours in presence of 20 µg/ml BFA as described in Current Protocols in Protein Science (Coligan et al. 1995b)

#### **2.10.6 Pulse-Chase analysis of HYAL1 in the presence of deoxynojirimycin (DNM)**

BHK\_HYAL1 and BHK\_pIRESneo cells, grown to confluence in 60 mm X 20 mm culture plates, were starved for 1 hour followed by pulse labeling with [<sup>35</sup>S]-labeled met/cys for 10 minutes and chase analysis for 30 minutes in the presence of 3 mM DNM

as described in “Current Protocols in Protein Science” chapter-12 volume 2 (Coligan et al. 1995b). DNM inhibits glucosidase I and glucosidase II preventing the modification of oligosaccharides attached to the newly synthesized proteins in the ER.

### **2.10.7 Pulse-chase analysis of HYAL1 in the presence of weak bases**

Starvation Medium supplemented with ammonium chloride (10 mM) or chloroquine (150 mM) was used to prepare Labeling Medium and Chase Medium. Cells grown to confluence (BHK\_HYAL1 and BHK\_pIRESneo) in a 60 mm X 20 mm culture plate were starved for 30 minutes, followed by 10 minutes pulse labeling with [<sup>35</sup>S]-labeled met/cys, and the HYAL1 protein was chased for 5 hour, 6 hour and 7-hour time points in the presence of 10 mM ammonium chloride or 150 mM chloroquine. The conditioned medium was collected and processed further as described in 2.11.2.

## **2.11 Immunoprecipitation of labeled HYAL1**

### **2.11.1 Immunoprecipitation from cell lysates**

To immunoprecipitate the labeled proteins, the cells were washed with 1 X PBS and lysed as described in section 2.4. The cell lysates, after centrifugation, were transferred to 1.5 ml screw cap tubes (Starstedt) and rotated in a cold room for 1 hour, with 75 µl of a 50% slurry of Protein G beads (Amersham Biosciences) prepared in 1 X PBS, to preclear the lysates. The beads were pelleted by a 30-second centrifugation at 16000 x g using an IEC MICROMAX centrifuge; the precleared lysates were incubated subsequently with a fresh 75 µl aliquot of Protein G beads slurry, and 5 µl of antibodies,

overnight at 4°C, on a rotator.

### **2.11.2 Immunoprecipitation from conditioned medium**

The conditioned medium was collected and cleared as described in 2.4. The medium extracts were prepared by adding 0.5% SDS and heating in a boiling water bath for 1 minute. A slurry of Protein G beads (75 µl) and 5 µl of antibodies (anti-Hyal1 antibodies or anti-β-hex antibodies) were added to the medium extracts and rotated overnight at 4°C.

### **2.11.3 Recovering antigen after immunoprecipitation**

The complex of beads attached to antigen-antibodies was pelleted by centrifugation at maximum speed for one minute in an IEC MICROMAX centrifuge at room temperature and the supernatants were stored at -20°C. The beads were washed three times with cold wash Buffer (5 mM Tris-HCl pH 7.4, 150 mM NaCl, 1% Triton X-100) and twice with cold PBS to get rid of any loosely bound protein contaminants. The beads were boiled in 2 X SLB with 100 mM DTT for 5 minutes to release the antigen-antibody complexes, beads were pelleted by centrifugation, and the supernatant containing the antigen and antibodies was transferred to a new tube. The boiling process with 2 X SLB was repeated to ensure complete recovery of the antigen-antibody complexes. The supernatants obtained after the boiling processes were pooled together and subjected to SDS-PAGE (described in 2.6) followed by fluorography (described in 2.12).

## **2.12 Fluorography**

After immunoprecipitation, the labeled proteins were separated by SDS-PAGE and the gel was subjected to fluorography. The gel was rinsed with distilled water, fixed for an hour by changing the fixing solution (30 % methanol, 10 % acetic acid) every 20 minutes, and stained for 30 minutes with 0.1 % Coomassie Blue stain. The gel was subsequently washed three times with distilled water for 10 minutes and incubated with 1 M salicylic acid for 1 hour. The gel was dried and exposed to X-Omat-AR film (Kodak) for the required length of time at -80°C.

## **2.13 Triton-X 114 extraction of cell lysates and conditioned medium**

The BHK\_HYAL1 and BHK\_pIRESneo cells were grown to 90% confluence in 100 mm X 20 mm culture plates. The cell lysates and conditioned medium were prepared as described in 2.4 and subjected to phase partitioning using a Mem-PER kit and following the protocol and conditions provided by the manufacturer (Pierce Biotech).

## **2.14 Purification of monoclonal antibodies**

### **2.14.1 Culturing hybridoma cells**

An aliquot of hybridoma cells producing monoclonal antibodies against HYAL1 were thawed (section 2.2.3) in RPMI Medium (Rosewell Park Memorial Institute [RPMI] Medium, 100 units/ml Penicillin/100 µg/ml Streptomycin, 2 mM glutamine). The flask was incubated at 37°C with 5% CO<sub>2</sub> until the cells were confluent. The cells were passaged as mentioned in 2.2 with minor modification. Briefly, the cells in suspension

culture, along with the conditioned medium, were added directly to a new T75 tissue culture flask containing fresh Culture Medium. The cells were incubated at 37°C with 5% CO<sub>2</sub> for a week without further passage to get maximum secretion of antibodies from the cells. The cells were removed by centrifugation at 5000 g for 20 minutes at 4°C, the supernatant was supplemented with 0.02% sodium azide solution and filter sterilized using a 0.2 µM membrane filter.

#### **2.14.2 Purification of monoclonal antibodies from conditioned medium**

The monoclonal antibody from conditioned medium was purified using a Hitrap Protein G HP column (Amersham Biosciences) according to the manufacturer's instructions. The purification unit, comprised of a static Pump P3, Absorbance/fluorescence monitor and Dual Beam Optical unit, Type-4, was assembled as per instruction provided by the manufacturer (Pharmacia Fine Chemicals). The pump tubing were sterilized by running 70% ethanol through the system followed by washing with Binding Buffer. The Hitrap Protein G HP column was connected to the unit by removing the top and bottom cap, without allowing air into the column, and equilibrated by running approximately 30 ml of the Binding Buffer (140 mM NaCl, 8 mM NaH<sub>2</sub>PO<sub>4</sub>, 2 mM KH<sub>2</sub>PO<sub>4</sub>, 10 mM KCl, pH 7.4) through it. The flow rate was maintained at 2 ml/minute throughout the purification procedure. The conditioned medium, diluted with equal an volume of 2 X Binding Buffer containing 0.02% sodium azide, was then filled into the top reservoir and pumped through the column. The conditioned medium was recycled overnight through the column. Next day the conditioned medium was removed and the column was washed with approximately 50 ml of Washing Buffer (140 mM

NaCl, 8 mM NaH<sub>2</sub>PO<sub>4</sub>, 2 mM KH<sub>2</sub>PO<sub>4</sub>, 10 mM KCl, pH 7.4). The antibodies were removed from the column using Elution Buffer (100 mM glycine-HCl, pH 2.7) and the fractions containing the antibodies were identified by their O.D at 280 nm. The eluted antibodies were neutralized immediately with 1 M Tris-HCl pH 8.0 and stored on ice. The whole purification process was performed in a cold room. The column was washed 3 times with approximately 30 ml of Washing Buffer and stored in 20% ethanol at 4°C.

The protein concentration of the eluted sample was determined using the BioRad assay (section 2.5). The eluted sample was concentrated using an Amicon® Ultra-15 centrifugal filter device (Millipore) according to the instructions provided. Briefly, the filter unit was pre-rinsed using cold 1 X PBS (recipe in section 2.4.) and 15 ml of sample was concentrated at a time. The samples were concentrated by centrifugation at 4000 x g for approximately 20 minutes in a swinging bucket rotor (Centra® CL2, IEC). The retentate was diluted with 14 ml of 1 X PBS and concentrated using a centrifugal filter as described above. The same process was repeated twice to further concentrate the antibodies and to replace the Elution Buffer with PBS. The total protein concentration of the final retentate sample was estimated using the BioRad assay Kit (section 2.5) and SDS-PAGE analysis (2 µl of concentrated antibody sample and 5 µg Gamma globulin as standard). The concentrated antibodies were supplemented with 0.02% sodium azide solution and stored at -20°C in aliquots. The anti-Hyal1 antibodies (1D10 and 4F9) were checked qualitatively by western blot analysis (described in 2.7) on BHK-HYAL1 and BHK-pIRESneo cell lysates.

# **RESULTS**

### 3.1 The *HYAL1* cDNA expression construct

To study the subcellular localization and processing of HYAL1, cells expressing readily detectable levels of HYAL1 protein are required. In previous experiments performed in this laboratory, the endogenous levels of HYAL1 in cell lines that were examined were found to be too low to permit these studies. It was therefore essential to generate a cell line expressing easily detectable levels of HYAL1 protein. Members of the laboratory generated a HYAL1 expression construct with a C-terminal His-tag. Unfortunately, the protein expressed with the His-tag was not secreted (Shuttleworth et al., unpublished data). A second attempt to express HYAL1, without a His-tag, resulted in low levels of HYAL1 expression; this was thought to be due to the presence of the 5' or 3' non-coding sequence flanking the HYAL1 coding sequence. To avoid the same problems, we decided to generate a construct containing the minimal coding region without any protein-tag.

As a first step, the full-length *HYAL1* cDNA was amplified by PCR with forward and reverse primers WPG 380 and WPG 381 (section 2.1.2). The amplified product was digested with BamHI, followed by EcoRI, and separated by agarose gel electrophoresis (section 2.1.3). The 1.3 Kb BamHI/EcoRI digested insert was isolated and the concentration was estimated by comparison to the Low MASS™ DNA Ladder (section 2.1.4.2). The pIRESneo plasmid was prepared by digestion with BamHI and EcoRI (section 2.1.5), purification with phenol: chloroform (section 2.1.6), and quantitated by spectrophotometry (section 2.1.4.1).

The expression vector (Figure 3) was generated by ligating the EcoRI/BamHI digested pIRESneo vector and 1.3 Kb EcoRI/BamHI digested HYAL1 insert, for 4 hours

(section 2.1.9). The ligated product was electroporated into competent *E.coli* cells and ampicillin resistant bacterial colonies were selected (section 2.1.9). Plasmid DNA from 16 colonies was isolated (section 2.1.6) and tested for the presence of the *HYAL1* insert by restriction enzyme digestion with BglII (Figure 4A). The *HYAL1* insert introduces a third BglII restriction enzyme site, producing 0.6 kb, 1.78 kb, and 4.12 kb DNA fragments if the *HYAL1* cDNA is inserted in the proper orientation. Four potential clones identified by BglII digestion (marked by an asterisk in Figure 4A), were subsequently confirmed by restriction enzyme digestion using SacII which yields 2 fragments (1.2 kb and 5.05 kb) (Figure 4B). SacII has a single restriction site in the pIRESneo vector but the *HYAL1* insert introduces a second restriction site. One clone (number 1) was sent for sequencing at “The Centre for Applied Genomics” in Toronto and the *HYAL1* cDNA was confirmed to have the same sequence as that in Genbank accession # U96078 and was named pIRES\_HYAL1. All four clones with *HYAL1* in the correct orientation were stored in 50% glycerol at -20°C (section 2.1.11.2) but only clone # 1 was used in subsequent studies.

### **3.2 Analysis of *HYAL1* expression in transiently transfected BHK cells**

To determine if the newly constructed *HYAL1* expression construct (pIRES\_HYAL1) expressed *HYAL1*, the construct was transiently transfected into BHK cells (section 2.3). The pIRESneo vector was transfected into BHK cells in a similar manner for control purposes. The BHK cells were transfected with 1:2.2 and 1:3 ratios of DNA to Lipofectamine™ 2000 and using differing amounts of DNA. The levels of *HYAL1* protein expressed using different DNA to Lipofectamine™ 2000 ratios, and

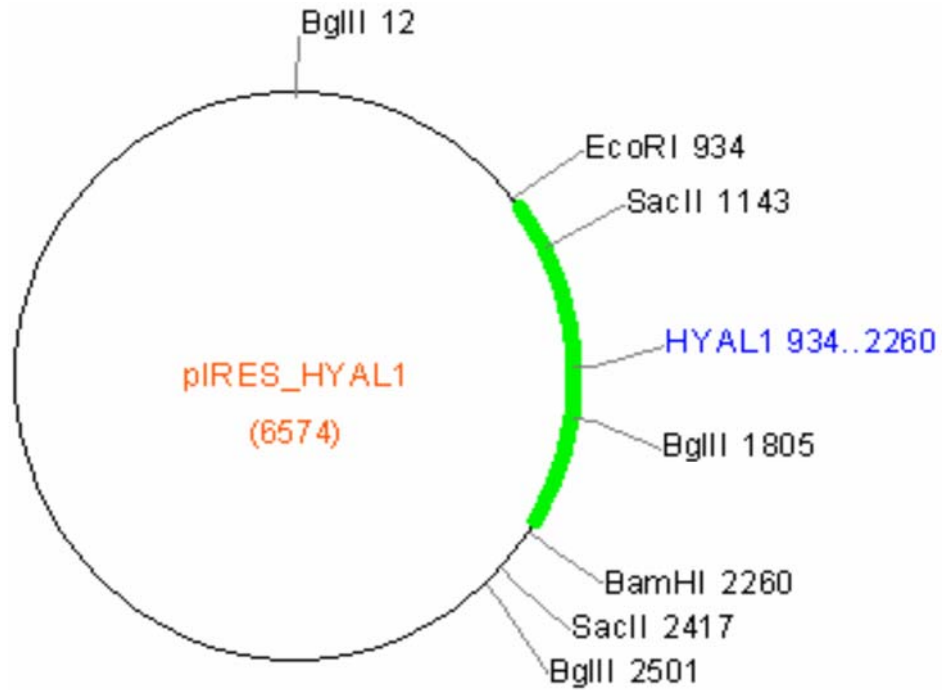
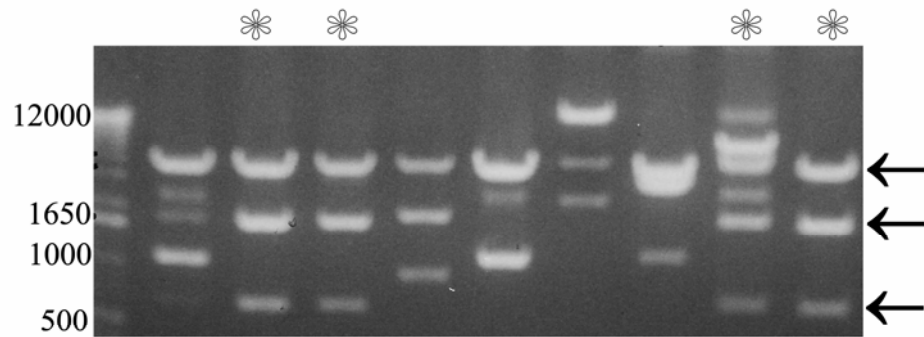


**Fig-3. Restriction map for the pIRES\_HYAL1 construct.** The *HYAL1* cDNA (green colored part in diagram) was inserted at the MCS of the vector at EcoRI and BamHI sites. The positions of the restriction sites are mentioned along with each enzyme. (This diagram was created using GenamicsExpression software).

A) BglII digestion



B) SacII digestion

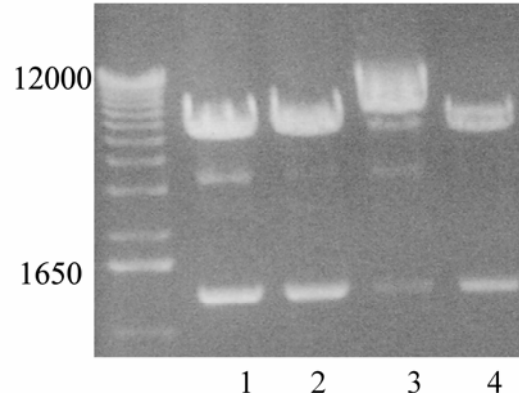


**Fig-4. Restriction enzyme digests to confirm the correct insertion of the *HYALI* cDNA.** Plasmid DNA was screened by restriction enzyme digestion for the presence of the *HYALI* insert in the correct orientation. A) Initial screening of the isolated DNA with BglII. B) Putative positives from BglII screening were confirmed by SacII digestion. The asterisks in panel A indicate the potential *HYALI* clones, while the arrows show the digestion products. The size and position of the DNA Ladder is shown on the left.

concentrations of DNA are shown in Figure 5. The highest levels of HYAL1 were detected when 6 or 7  $\mu\text{g}$  of the HYAL1 cDNA construct was transfected using a 1:3 ratio of DNA to Lipofectamine<sup>TM</sup> 2000 (Figure 5, lanes 6 and 8). Three bands were detected with molecular weights of approximately 43, 50, and 52 kDa in pIRES\_HYAL1 transfected cell lysates, and were absent in empty vector transfected cell lysates. A DNA concentration of 7  $\mu\text{g}$  and a 1:3 ratio of DNA to Lipofectamine<sup>TM</sup> 2000 was chosen for subsequent experiments.

Once suitable conditions for the expression of HYAL1 were identified, we wanted to determine if the HYAL1 protein was adequate for analysis and if the protein appeared properly processed; both pIRESneo and pIRES\_HYAL1 (7  $\mu\text{g}$ ) were transfected into BHK cells, and cell lysates and conditioned medium were analyzed for HYAL1 expression by western blot analysis (Figure 6). The HYAL1 protein was readily detected in cell lysates (Figure 6, lanes 2 and 3) and conditioned medium (lanes 5 and 6) of pIRESneo\_HYAL1 transfected BHK cells, but was absent in vector transfected BHK cell lysates (lane 1) and conditioned medium (lane 4).

Multiple forms of HYAL1 with molecular masses of approximately 43 kDa, 50 kDa and 52 kDa were detected in cell lysates of pIRESneo\_HYAL1 transfected cells (lanes 2 and 3) while only one form of HYAL1, at approximately 51 kDa, was detected in conditioned medium (lane 5 and 6). An “X” marks a cross-reacting band that was present in the control lane (vector transfected cells) on most western blots.

These results confirmed that the pIRES\_HYAL1 expression construct is able to express a level of HYAL1 that is readily detectable by western blot. Further, it is secreted, suggesting that it is processed normally.

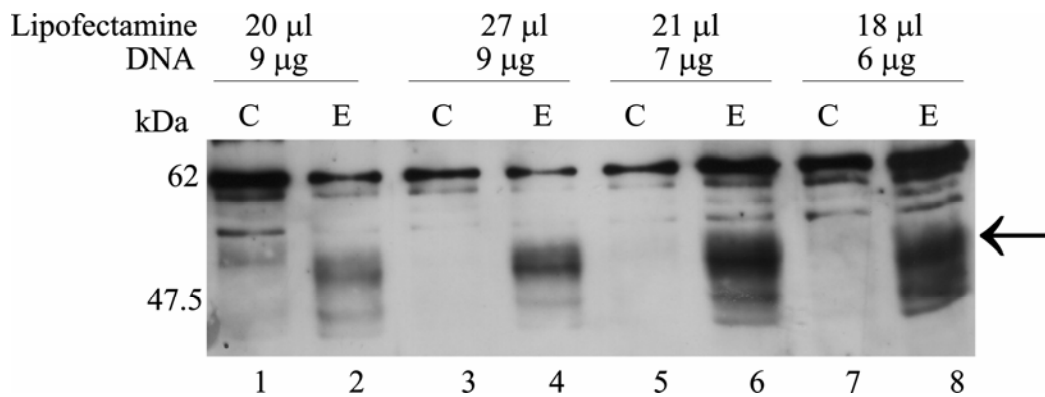


**Fig-5. Analysis of HYAL1 expression from pIRES\_HYAL1.** Different concentrations of the pIRES\_HYAL1 expression construct (E), or a control vector, pIRESneo (C), were mixed at a 1:2.2 or 1:3 ratio with Lipofectamine solution and transiently transfected into the BHK cells. The pIRES\_HYAL1 and pIRESneo transfected BHK cells were harvested at 24 hour post transfection, and the resulting cell lysates (30  $\mu$ g of total protein) were separated by 10% SDS-PAGE. Western blot analysis was performed with anti-HYAL1 antibodies (1D10) at a 1:1000 dilution. An arrow indicates the major HYAL1 band. The size and position of the molecular mass markers is shown on the left.

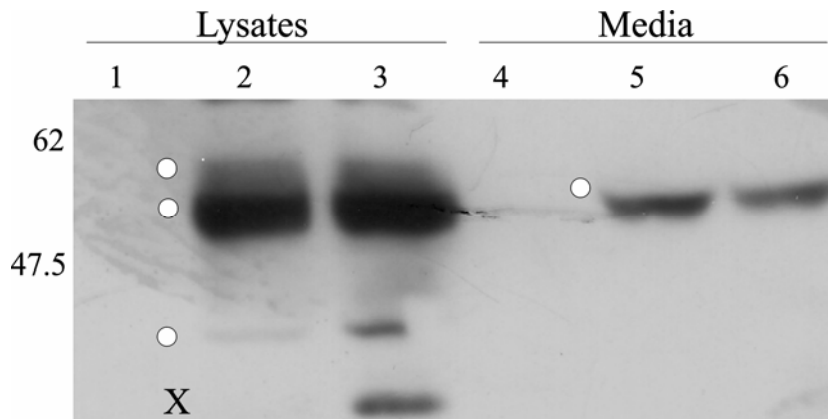


**Fig-6. Analysis of HYAL1 expression and secretion from transiently transfected BHK cells.** BHK cells were transiently transfected with pIRES\_HYAL1 or the control vector, pIRESneo. Cell lysates (30  $\mu$ g of total protein), as well as conditioned medium (30  $\mu$ l), were separated by 10% SDS-PAGE followed by western blot analysis using anti-HYAL1 (1D10) antibodies. Lanes: 1, 4 (control); 2, 3, 5, 6 (pIRES\_HYAL1). White dots show the different bands of HYAL1 protein recognized by anti-HYAL1 antibodies in the lysates (1-3) and conditioned medium (4-6). The size and position of the molecular mass markers is shown on the left. X indicates a cross-reacting band.

### 3.3 Analysis of HYAL1 stably expressed in BHK cells

It is difficult to use transiently transfected cells for metabolic labeling, as by the time cells are maximally expressing, it may not be possible to do treatments of 4-10 hours without excessive cell death. To avoid this problem, pIRES\_HYAL1 and pIRESneo were stably transfected into the BHK cells (section 2.3) to generate BHK\_HYAL1 and BHK\_pIRESneo, respectively. Thirty-one colonies resistant to neomycin were picked 15-18 days post-transfection and screened for HYAL1 expression by western blot analysis (section 2.7). Figure 7 shows protein detected from ten colonies, along with one control (C) colony. Out of 31 colonies screened, 12 colonies were found to be positive for HYAL1 expression, and stored in aliquots in liquid nitrogen. One of the colonies with the highest level of HYAL1 expression, number 31 (marked by asterisk in figure 7) was selected for use in all subsequent experiments. The pIRESneo vector alone was transfected in a similar manner and the colonies were picked to be used as controls.

Once a stable cell line had been selected, we wanted to determine if the HYAL1 forms expressed were similar to that in transiently transfected cells. The BHK\_HYAL1 and BHK\_pIRESneo cell lysates and conditioned medium samples were separated by 10% SDS-PAGE (section 2.6) and analyzed by western blot (section 2.7). The cell lysates from BHK\_HYAL1 cells (Figure 8, lane 1) showed forms of HYAL1 similar in mass to those detected after transient transfection (43, 50 and 52 kDa). Similarly, as in the transient transfection, only one band was present in conditioned medium (lane 2) at approximately 52 kDa. No HYAL1 bands were detected in vector transfected cell lysates (lane 3) or conditioned medium (lane 4) as expected.

To determine if the various forms of HYAL1 protein expressed by BHK\_HYAL1

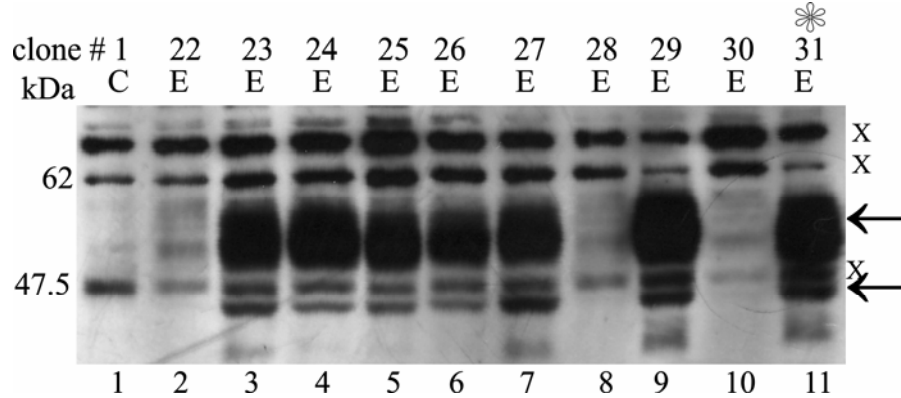


**Fig-7. Screening of neomycin resistant colonies for HYAL1 expression.** BHK cells were stably transfected with the human HYAL1 expression construct (pIRES\_HYAL1) or a control vector (pIRESneo). Cell lysate (30  $\mu$ g of total protein) from each neomycin resistant colony was separated by 7.5% SDS-PAGE and analyzed for HYAL1 expression by western blot using anti-HYAL1 antibody (1D10). Arrows show the different bands of HYAL1 protein recognized by anti-HYAL1 antibodies in the lysates from BHK\_HYAL1 transfected cells (E) that are absent in vector transfected cells lysates (C). X indicates cross-reacting bands.

were active, in-gel enzyme activity assays (zymography, section 2.8) were performed on cell lysates and conditioned medium samples of BHK\_HYAL1 and BHK\_pIRESneo. As seen by the clearing of the gel (Figure 9), BHK\_HYAL1 cells (lanes 2, and 4) show activity towards HA, while no activity was detected in BHK\_pIRESneo cells (lanes 1, and 3). All three forms of HYAL1 detected in BHK\_HYAL1 cell lysates (lane 2) and the secreted HYAL1 protein from conditioned medium (lane 4) were found to be active at pH 3.8.

Western blot analysis of HYAL1 from BHK\_HYAL1 cell lysates revealed multiple forms of HYAL1, with a single form present in the medium. However, the relationship between those multiple forms within cells and the secreted form was not clear at this point. To examine the contribution of N-glycosylation to any of these forms of HYAL1, and the type of carbohydrate structure present, the BHK\_HYAL1 and BHK\_pIRESneo lysates and conditioned medium were treated with common glycosidases; Peptide N Glycosidase F (PNGase F) removes both high mannose and complex oligosaccharide chains whereas Endoglycosidase H (Endo H) removes high mannose and hybrid oligosaccharide chains. The HYAL1 protein from cell lysates (Figure 10, lanes 1, and 2) and conditioned medium (lanes 3, and 4) of BHK\_HYAL1 cells, migrated as one strong band at approximately 43 kDa upon PNGase F treatment (lanes 5, 6, 7, and 8 respectively). The presence of bands at 50 kDa and 45 kDa (lanes 5 and 6) might represent undigested or partially digested forms of HYAL1. This result indicates that the different bands found in the cell lysates can be accounted for by differences in carbohydrate modification. The HYAL1 protein from cell lysates of BHK\_HYAL1 cells was sensitive to Endo H treatment (lanes 9, and 10) and migrated at

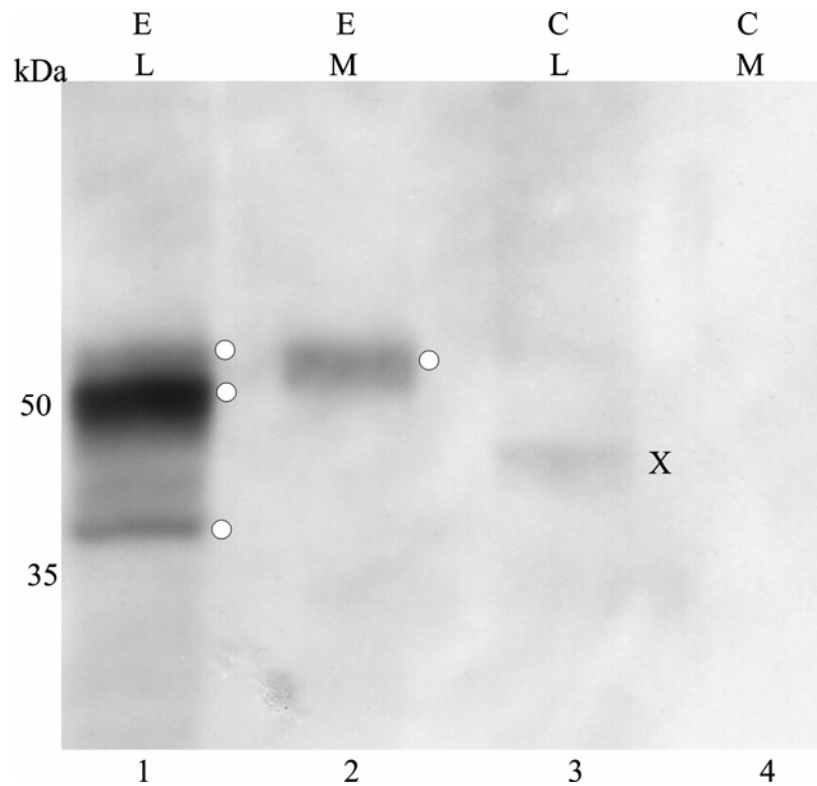


**Fig-8. Analysis of HYAL1 stably expressed in BHK cells.** Cell lysates ([L], 30  $\mu$ g of total protein) and conditioned medium ([M], 30  $\mu$ l) from BHK cells stably expressing HYAL1; BHK\_HYAL1(E) and BHK\_pIRESneo (C) were analyzed by western blot analysis using anti-HYAL1 antibodies. White dots show the different bands of HYAL1 protein recognized by anti-HYAL1 antibodies. X indicates a cross-reacting band. The size and position of the molecular mass markers is shown along the left hand side of the gel.

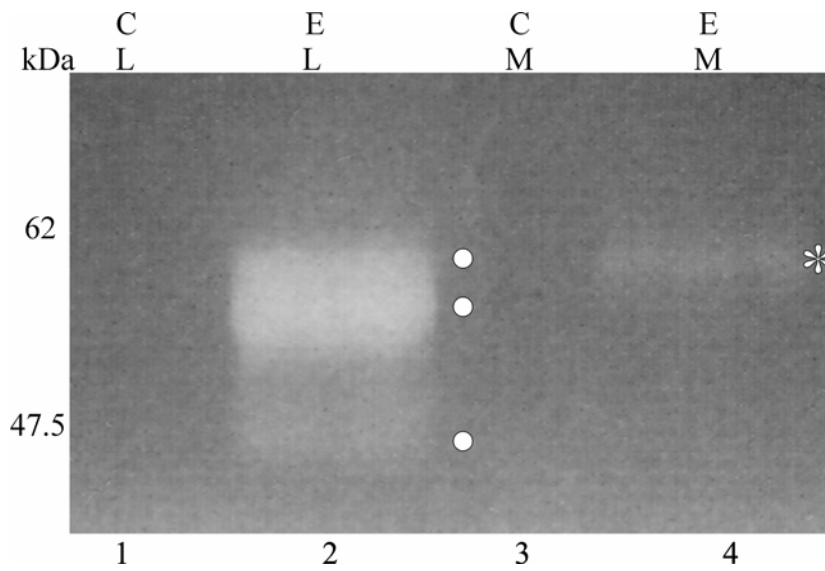


**Fig-9. Analysis of HYAL1 activity by zymography.** The enzymatic activity of cell lysates ([L], 30  $\mu$ g of total protein) and conditioned medium ([M], 30  $\mu$ l) from BHK\_HYAL1 (E) and BHK\_pIRESneo (C) cells was analyzed by zymography. The clear area marked by white dots and asterisk represents the active HYAL1 protein present in cell lysates (L), as well as from the conditioned medium (M). The position and size of the molecular mass markers is shown on the left.

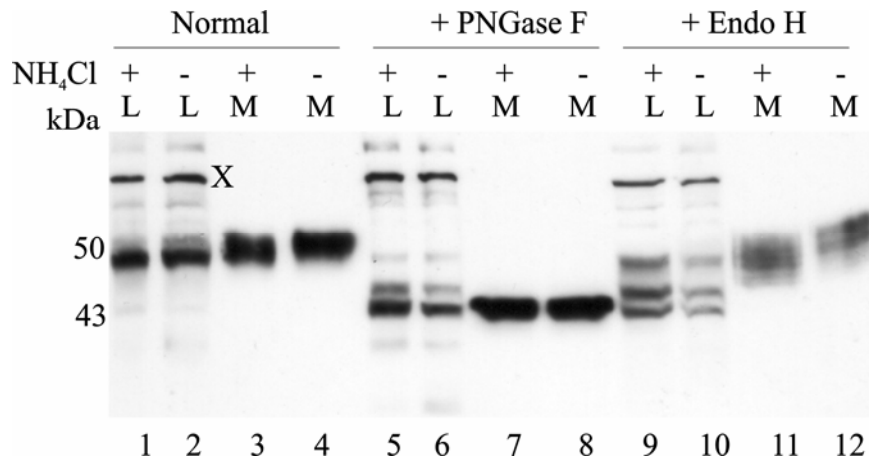


**Fig-10. Analysis of HYAL1 carbohydrate processing by glycosidase treatment.** Cell lysates (L) and conditioned medium (M) from BHK\_HYAL1 cells cultured in presence or absence of NH<sub>4</sub>Cl, were subjected to overnight treatment with PNGaseF and EndoH. Treated, as well as untreated cell lysates and conditioned medium were separated on SDS-PAGE followed by western blot analysis using anti-HYAL1 antibodies. The position and size of the molecular mass markers is shown on the left. X indicates a cross reacting band.

approximately 43 kDa suggesting high-mannose or hybrid type modification, whereas the secreted HYAL1 protein (lanes 11, and 12) was partially resistant to Endo H suggesting it has a complex type of carbohydrate. This was further confirmed during subsequent experiments (Figure 20b and 21). The undigested 50 kDa band and partially digested 45 kDa band was also present in Endo H treated cell lysates (lanes 9 and 10) as found in PNGase F treatment.

We found that HYAL1 migrated at a slightly lower position in the presence of  $\text{NH}_4\text{Cl}$  or chloroquine (Figure 24 and 25). To analyze if this is the result of a difference in some post-translational modification, we treated cell lysates as well as conditioned medium from BHK\_HYAL1 cells grown in presence or absence of  $\text{NH}_4\text{Cl}$  with PNGase F and Endo H. Upon PNGase F and Endo H treatment, the ammonium chloride treated and untreated forms migrated at the same position (Figure 10, lanes 7, and 11), suggesting the difference in electrophoretic mobility of the secreted form of HYAL1 in the presence of  $\text{NH}_4\text{Cl}$  might be due to some alteration in glycosylation of HYAL1. This experiment was only performed once.

To determine if disulfide bonds were present in HYAL1, the BHK\_HYAL1 cell lysates and conditioned medium were separated by SDS-PAGE under non-reducing conditions and compared to the HYAL1 separated under reducing conditions. As seen in Figure 11, the HYAL1 protein migrated slower, at a higher position of approximately 67 kDa in cell lysates (lane 6) and approximately 69 kDa from conditioned medium (lane 7) under non-reducing conditions. This was considerably larger than the HYAL1 separated under reducing conditions (lanes 1 and 2). These results are representative of three independent experiments. This result suggests that HYAL1 contains disulfide bonds both

inside and outside the cells. Further, bioinformatic analysis of HYAL1 using disulfide bond predicting software “DiANNA” also suggests disulfide bonds exist.

This initial HYAL1 characterization suggests that it is readily detected and processed properly in BHK\_HYAL1 cells. Multiple forms of HYAL1 proteins are detected in cell lysates, while only one form is secreted; and all of the forms are active. The various forms of HYAL1 are products of differences in N-glycosylation modification of an approximately 43 kDa core protein, as indicated by PNGaseF treatment. Endo H treatment suggested HYAL1 in cell lysates has a high-mannose or hybrid type structure, but the secreted form of HYAL1 has complex types of carbohydrate modification.

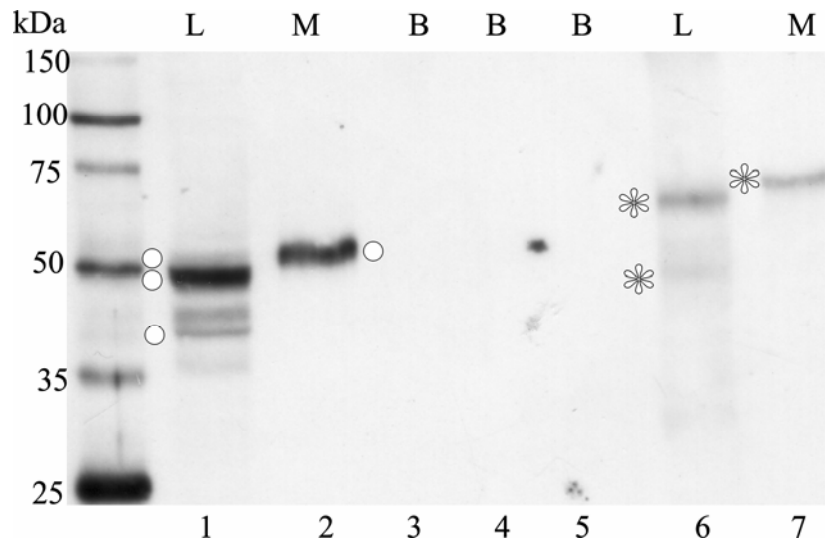


**Fig-11. Analysis of HYAL1 under reducing and non-reducing conditions.** Cell lysates (L) as well as conditioned medium (M) from BHK\_HYAL1 were prepared for 10% SDS-PAGE in reducing and non-reducing sample buffers. White dots show the HYAL1 protein under reducing conditions while asterisks indicate the non-reduced forms of HYAL1. The position and size of the molecular mass markers is shown on the left. “B” indicates blank lanes.

### 3.4 Detection of HYAL1 protein in density gradient fractions

As a first step in analyzing the subcellular localization of HYAL1, we used density gradient centrifugation. The post-nuclear supernatant from BHK\_HYAL1 cells was fractionated by Percol gradient centrifugation (section 2.9) and fractions were analyzed by western blot, using antibodies toward markers specific for particular subcellular compartments.

Upon analysis of gradient fractions, HYAL1 was found in approximately fourteen fractions, spanning a broad range of densities (Figure 12). The highest level of HYAL1 was found in fraction numbers 12 to 18. This distribution was most similar to that of the late endosomal marker Rab9 and it overlaps with the fractions (fractions 14 to 20) positive for the lysosomal marker LAMP1, (detected with anti-LAMP1 antibodies, a kind gift from Dr. Jean Gruenberg) (Figure 12). The distribution of HYAL1 also extended to the fractions that were positive for the endoplasmic reticulum (E.R.) marker calnexin (fractions 6 to 14), membrane marker caveolin (fractions 12 and 14) and the Golgi marker, GM-130 (fractions 2 to 20). These results are representative of three independent experiments.

HYAL1 activity was detected in almost all the fractions as seen in Figure 13, by zymography (section 2.8). However, the highest activity was observed in fractions 12 to 18, consistent with the western blot results.

These results suggest that all the three forms of HYAL1 were present in fractions that have similar densities to that of late endosomes and lysosomes.

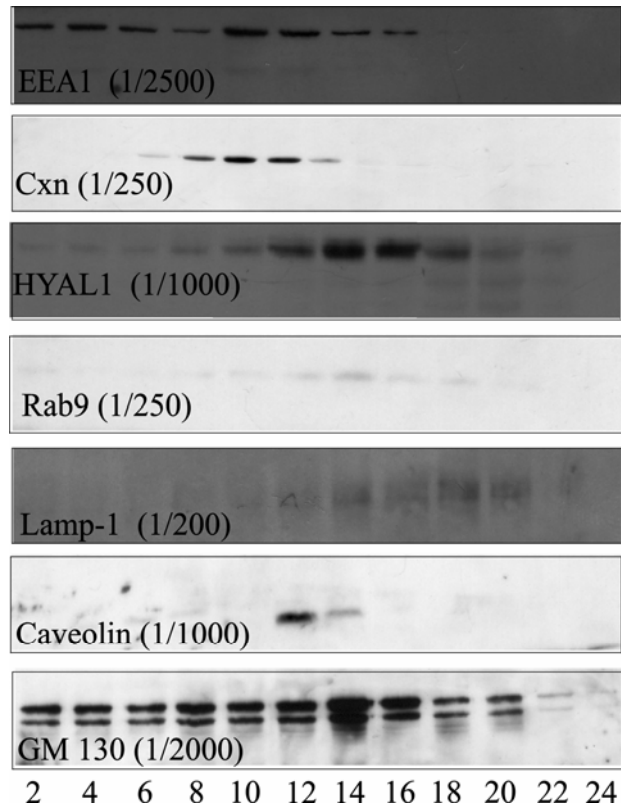


**Fig-12. Analysis of HYAL1 subcellular localization by density gradient centrifugation.** The BHK\_HYAL1 cell lysates were overlaid on 25% Percoll and the subcellular organelles were separated based on their density by centrifugation. The fractions (approximately 0.5 ml) were collected from the top of the gradient and analyzed by western blot analysis using antibodies that detected specific organelle markers. The antibodies used and their dilution factor is indicated on the lower left of each insert. The fraction numbers are indicated at the bottom of the figure. EEA1: early endosomal marker 1, Cxn: calnexin, Rab9: late endosomal marker, Lamp-1: lysosomal associated membrane protein 1, GM 130: golgi membrane 130

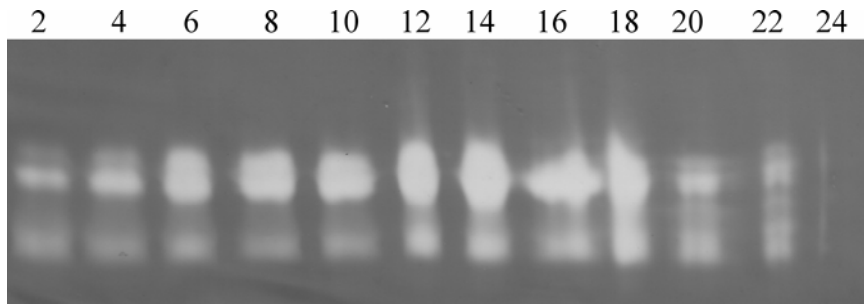


**Fig-13. Analysis of HYAL1 activity in the density gradient fractions by zymography.**

The HYAL1 activity from each fraction obtained by density gradient centrifugation was assessed by zymography. An aliquot from each fraction (8  $\mu$ l), was incubated with 4X Sample Loading Buffer, without reducing agent, for 5 minutes and separated on an HA-containing 7% SDS-Polyacrylamide gel. Activity assay was performed according to protocol (section 2.8.2). The fraction numbers are indicated at the top of the figure.

### 3.5 Pulse-chase analysis of HYAL1 stably expressed in BHK cells

To follow the processing pathway of HYAL1, metabolic labeling of BHK\_HYAL1 and BHK\_pIRESneo cells was performed and the protein was chased to detect different forms of the protein as it moved from its immature proprotein form in the endoplasmic reticulum to its mature form in its final destination.

Before proceeding with the pulse-chase analysis, optimization of the pulse labeling step was essential to determine an adequate length of time to label the cells. The BHK\_HYAL1 and BHK\_pIRESneo cells were pulse-labeled with [<sup>35</sup>S]-met/cys for varying times, ranging from 2 to 10 minutes. As seen in Figure 14, two forms of HYAL1, approximately 48 and 50 kDa in size, were detected in BHK\_HYAL1 cell lysates at all labeling time points; these bands were absent in BHK\_pIRESneo cell lysates. The pulse time of 10 minutes was found to be an appropriate length of time as the level of labeled HYAL1 detected was sufficient for pulse-chase analysis, and both forms were already present at 2 minutes of labeling.

Once the pulse labeling time was optimized, BHK\_HYAL1 and BHK\_pIRESneo cells were pulse-labeled with [<sup>35</sup>S]-met/cys for 10 minutes, then chased for 0 to 5 hours to follow the processing of HYAL1. The cell lysates and conditioned medium samples, at each chase point, were subjected to immunoprecipitation as mentioned above. As seen in the BHK\_HYAL1 cell lysates, two forms of HYAL1 were readily detected at 10 minutes of pulse labeling (Figure 15, lane 2), that are not seen in the BHK\_pIRESneo cell lysates (lane 1). A third faint band at approximately 52 kDa was noted above the two forms at 30 minutes of chase (lane 3), which became more prominent at later chase points while the

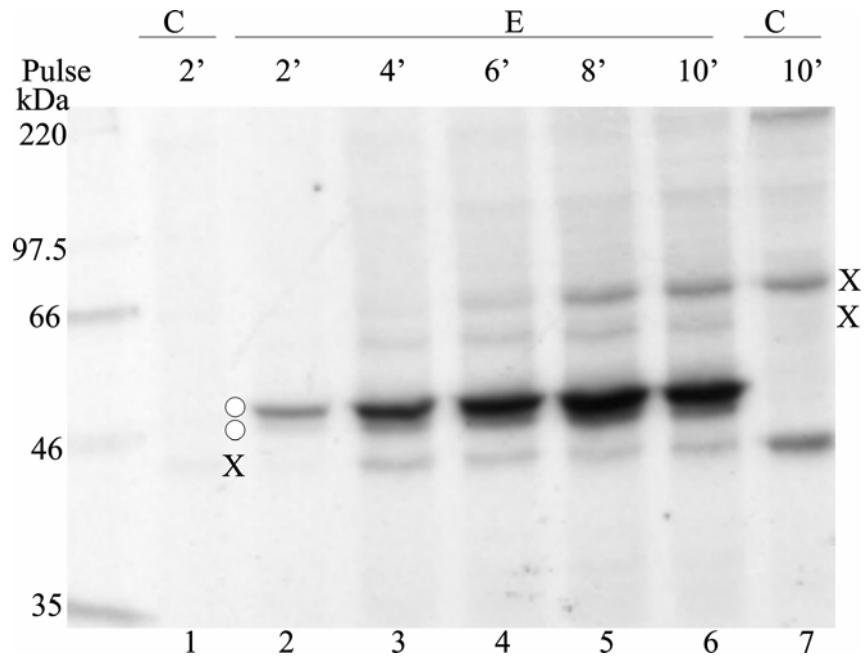


**Fig-14. Optimization of pulse-labeling time.** The pulse-labeling time was optimized by incubating BHK\_HYAL1 (E) and BHK\_pIRESneo (C) cells with 0.2 mCi [<sup>35</sup>S]-met/cys for different time points ranging from 2 to 10 minutes. Cell lysates were then subjected to immunoprecipitation using anti-HYAL1 antibodies (4F9) followed by SDS-PAGE, and fluorography. The detectable HYAL1 proteins are indicated by white dots. X indicates a cross-reacting band. The position and size of the [<sup>14</sup>C]-labeled molecular mass markers is shown on the left.

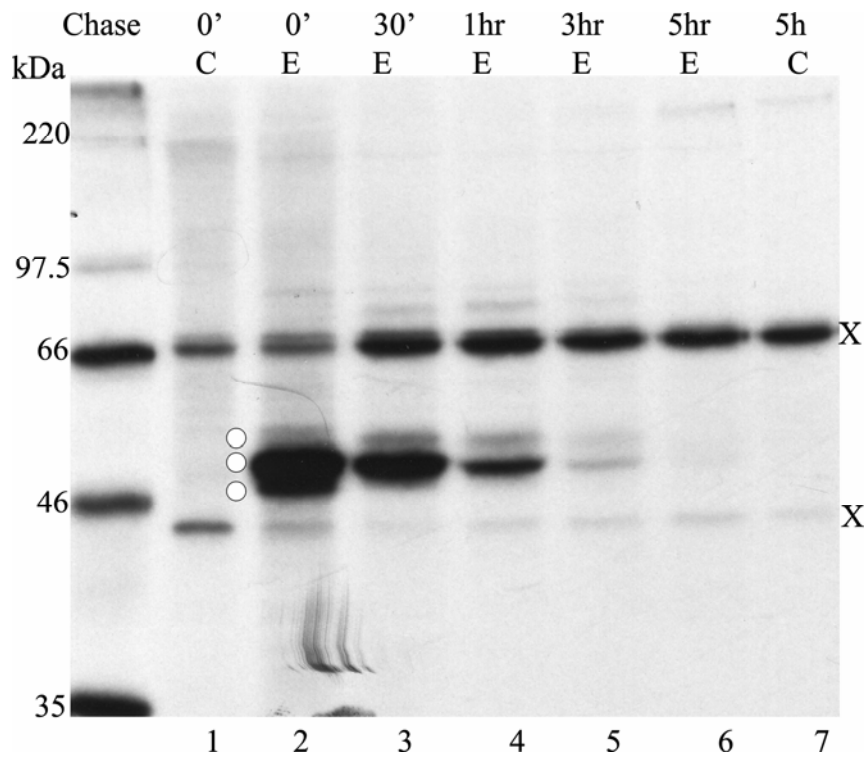


**Fig-15. Metabolic labeling of HYAL1.** The BHK\_HYAL1 (E) and BHK\_pIRESneo (C) cells were pulse labeled for 10 minutes using 0.2 mCi of [<sup>35</sup>S]-labeled met/cys followed by chase periods of 0 to 5 hours. HYAL1 protein was immunoprecipitated from cell lysates and conditioned medium (data not shown) using anti-HYAL1 antibodies. The immunoprecipitated proteins were separated by 10% SDS-PAGE and analyzed by fluorography. White dots indicate the three bands of HYAL1 protein detected. X indicates cross-reacting bands. The position and mass of the [<sup>14</sup>C]-labeled molecular mass markers are shown on the left.

lower bands at approximately 49 and 50 kDa disappeared. However, the approximately 43 kDa band seen in western blot analysis was not detected in pulse-chase analysis. The HYAL1 from BHK\_HYAL1 cells was removed from the cells by 5 hours of chase (lane 6). At this point, attempts to immunoprecipitate HYAL1 from conditioned medium were unsuccessful (data not shown) making it difficult to predict if these HYAL1 forms were secreted and/or degraded.

In order to immunoprecipitate HYAL1 from the conditioned medium of the BHK\_HYAL1 cells, several different conditions were tested for the immunoprecipitation. These included, the presence of different detergents, reducing agents (DTT) as well as denaturing conditions (SDS, boiling). The [<sup>35</sup>S]-labeled HYAL1 was successfully immunoprecipitated from conditioned medium of BHK\_HYAL1 cells only under denaturing conditions (i.e. the presence of SDS and/or boiling) as seen in Figure 16 (lanes 4,5, and 6) where HYAL1 is detected in conditioned medium from BHK\_HYAL1 but not BHK\_pIRESneo cells (lanes 1,2 and 3). The presence of SDS alone (lane 4) or just heat denaturation (lane 5) was sufficient for immunoprecipitation of HYAL1 from conditioned medium; however, the samples treated by heat denaturation in the presence of SDS, showed fewer background bands (lane 6) compared to the independent treatment with either SDS or heat denaturation.

Once the conditions for the immunoprecipitation of HYAL1 from conditioned medium were established, the pulse-chase experiment was repeated. BHK\_HYAL1 and BHK\_pIRESneo cells were pulse labeled with [<sup>35</sup>S]-met/cys for 10 minutes and chased for 0 to 5 hours. Cell lysates, as well as the conditioned medium, were subjected to immunoprecipitation followed by fluorography as described above. As observed

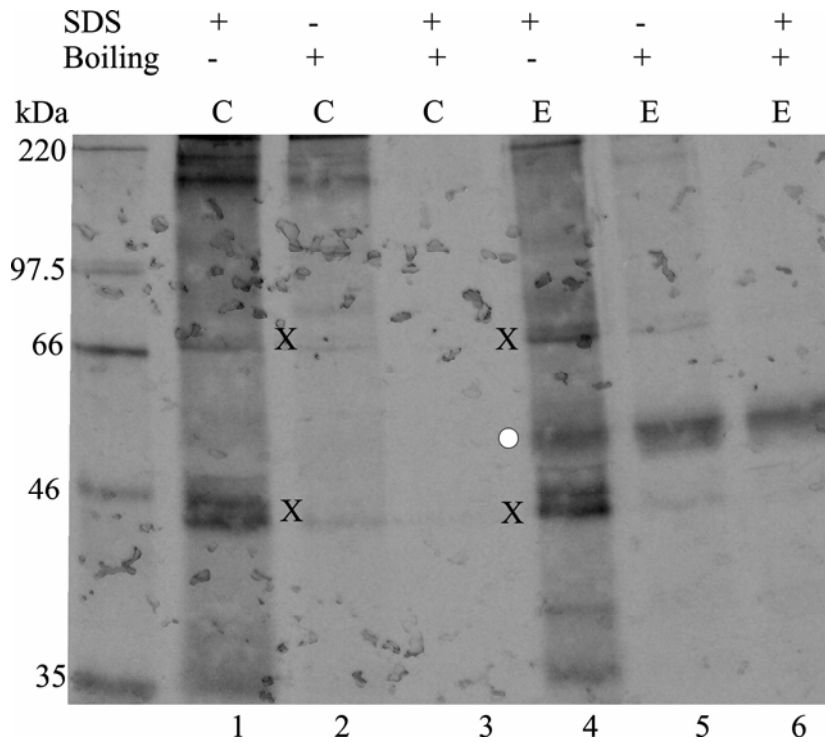


**Fig-16. Immunoprecipitation of HYAL1 from medium.** The BHK\_HYAL1 (E) and BHK\_pIRESneo (C) cells were pulse labeled for 10 minutes using 0.2 mCi of [<sup>35</sup>S]-labeled met/cys followed by 3 hours of chase. The conditioned medium from BHK\_HYAL1 and BHK\_pIRESneo cells was immunoprecipitated under protein denaturing conditions using anti-HYAL1 antibodies. The immunoprecipitated [<sup>35</sup>S]-labeled-HYAL1 was separated by 10% SDS-PAGE followed by fluorography. A white dot indicates the secreted HYAL1 protein. X indicates cross-reacting bands. The position and mass of the [<sup>14</sup>C]-labeled molecular mass markers are shown on the left.

previously, two forms of HYAL1 at approximately 49 and 50 kDa, were detected in cell lysates from BHK\_HYAL1 (Figure 17, lane 3) that were not seen in BHK\_pIRESneo cell lysates at 10 minutes of pulse labeling (lane 1). The results also showed that the lower approximately 49 kDa form, disappears during chase (lane 5), while the upper, approximately 52 kDa form, appears (lane 5). It was also noted that several forms of approximately 52 kDa were eventually detected in the medium. The relationship to the bands in the cell lysate was not obvious (lane 10). The disappearance of the middle approximately 50 kDa form, by 5 hours of chase (lane 13) suggested that it might be degraded from the cells within 5 hours, while the approximately 52 kDa HYAL1 form may be secreted into the medium. This result represents three independent experiments. The 52 kDa form in the medium was found to be stable, as it was detected even after 24 hours of chase (Figure 18, lane 10).

These results suggested that the HYAL1 protein is synthesized rapidly as it was easily detected at 2 minutes of pulse labeling (Figure 14) and had a half-life of approximately 2.5 hours within the cells (Figure 15). It was also found to be stable in media (Figure 18). Three bands were detected at 30 minutes chase; the 50 or 49 kDa form might be modified to give an approximately 52 kDa band that was secreted from the cells. The approximately 50 kDa form was degraded within the cells by 5 hours (Figure 17). The presence of two bands as early as 2 minutes after initiating labeling suggested these species might be derived from a single protein by differing numbers of carbohydrate modification. Alternatively, they might represent two different protein forms synthesized from a single transcript.

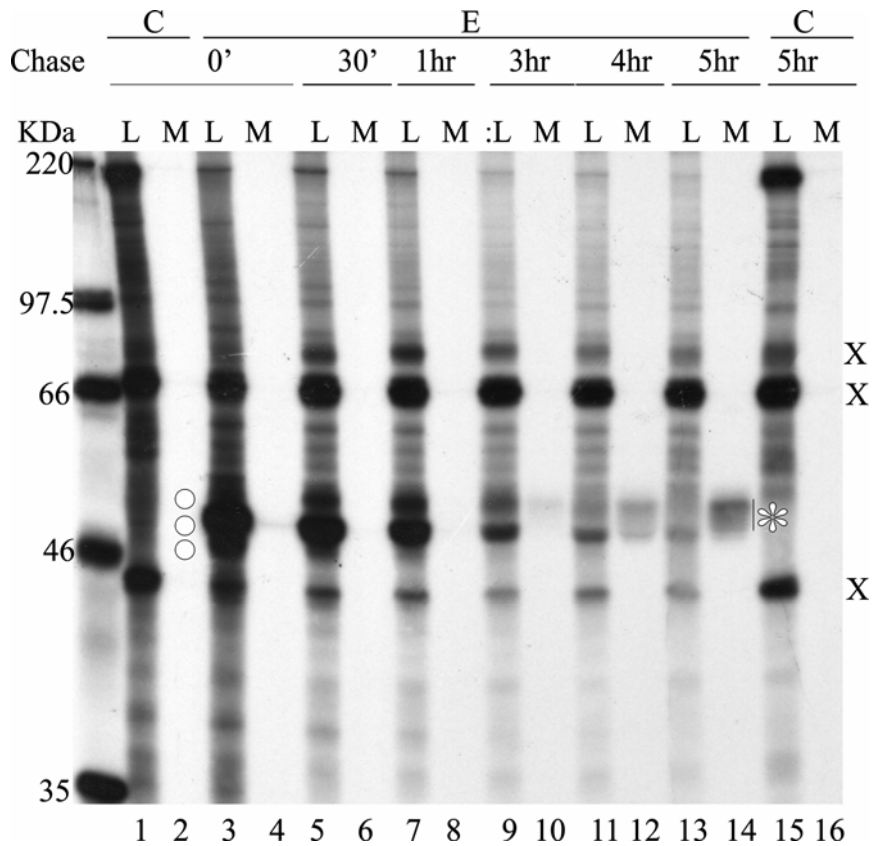


**Fig-17. Pulse-chase labeling of HYAL1.** BHK\_HYAL1 (E) and BHK\_pIRESneo (C) cells were pulse-labeled for 10 minutes using 0.2 mCi of [<sup>35</sup>S]-met/cys per sample followed by a chase period of 0 to 5 hours. Cell lysates (L) and conditioned medium (M) were immunoprecipitated using anti-HYAL1 antibodies. White dots indicate the three bands of HYAL1 protein detected in the BHK\_HYAL1 lysates, while the asterisk shows the HYAL1 protein secreted in media. X indicates cross-reacting bands. The position and mass of the [<sup>14</sup>C]-labeled molecular mass markers are shown on the left.

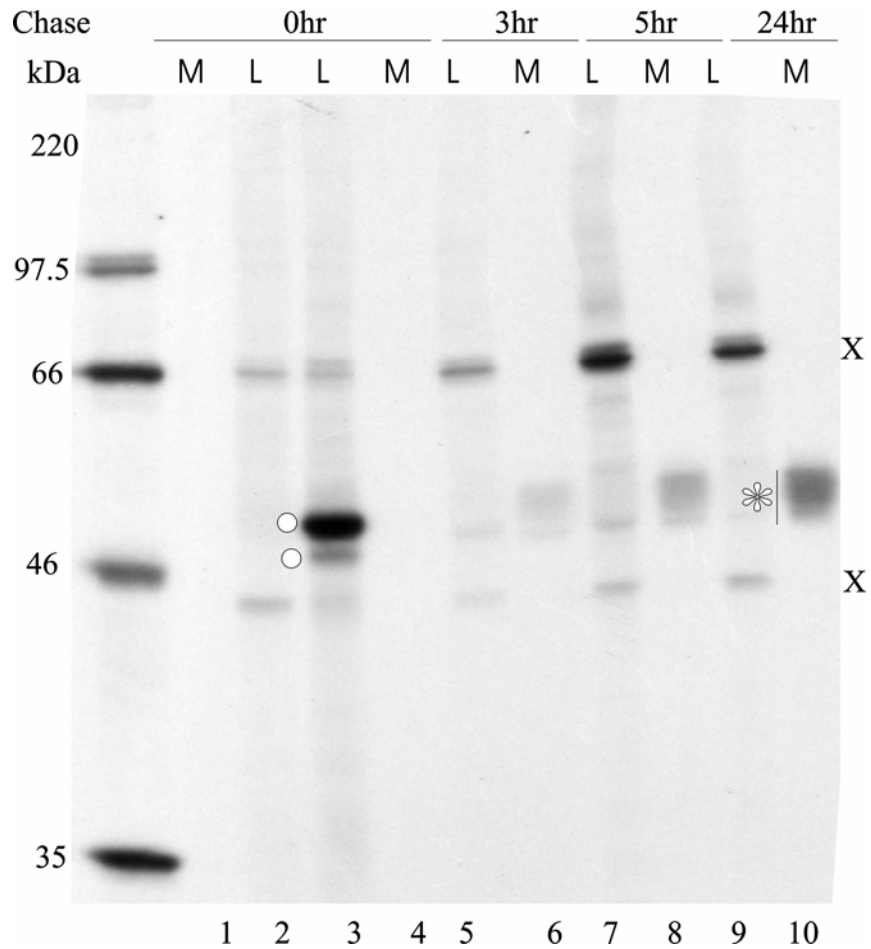
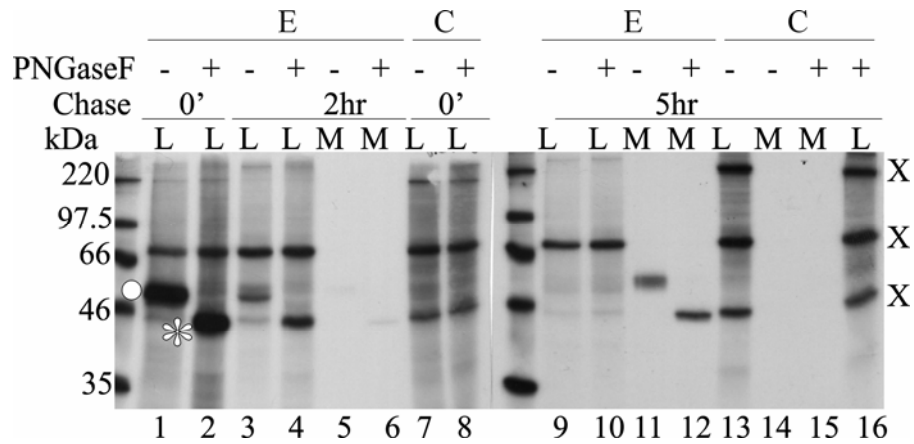


**Fig-18. The  $[^{35}\text{S}]$ -labeled HYAL1 is stable in medium.** BHK\_HYAL1 (E) and BHK\_pIRESneo (C) cells were chased for 24 hours after pulse labeling for 10 minutes using 0.2 mCi of  $[^{35}\text{S}]$ -met/cys per sample. Cell lysates (L) and conditioned medium (M) were subjected to immunoprecipitation using anti-HYAL1 antibodies. White dots show HYAL1 protein in cell lysates while an asterisk indicates the HYAL1 protein in conditioned medium. X indicates cross-reacting bands. The position and mass of the  $[^{14}\text{C}]$ -labeled molecular mass markers is shown on the left.

### 3.6 Analysis of carbohydrate modification of [<sup>35</sup>S]-labeled HYAL1

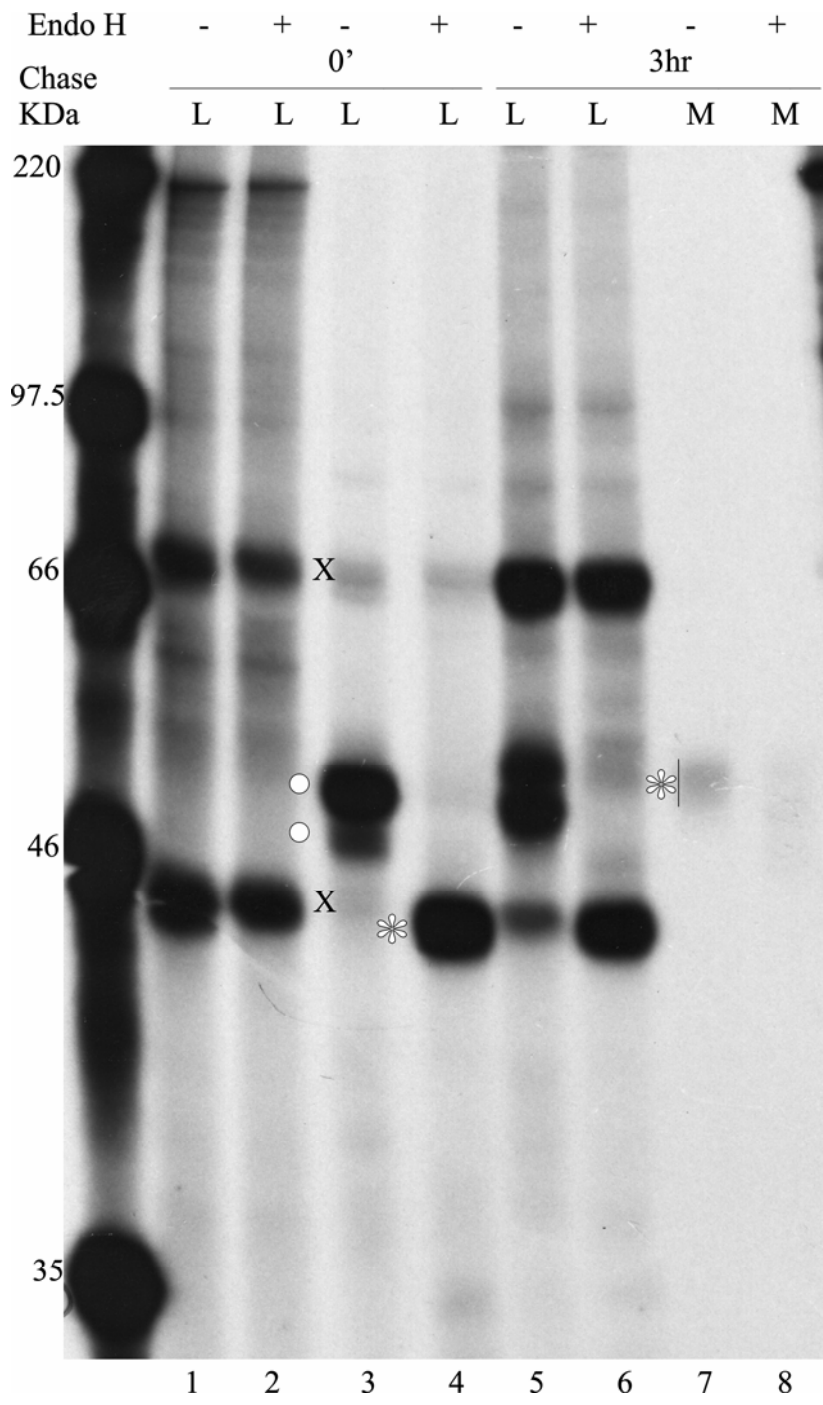
The carbohydrate processing of different forms of [<sup>35</sup>S]-labeled HYAL1 protein was analyzed by Peptide N: Glycosidase F and Endo H treatment. BHK\_HYAL1 and BHK\_pIRESneo cells were pulse labeled for 10 minutes followed by chase analysis. Cell lysates and conditioned medium from different time points were subjected to immunoprecipitation followed by PNGase F or Endo H treatment and compared to untreated samples. After PNGase F treatment, the [<sup>35</sup>S]-labeled HYAL1 migrated at approximately 43 kDa (Figure-19), as observed previously. A cross-reacting band similar in size to HYAL1 was seen in samples immunoprecipitated from BHK\_pIRESneo cells (lanes 7,8,13 and 16) but this band was not altered by PNGase F treatment. This figure represents a single experiment. This experiment was repeated twice with non-labeled BHK\_HYAL1 and BHK\_pIRESneo cell lysates as well as conditioned medium followed by western blot analysis and is described elsewhere in the thesis.

The Endo H treatment of immunoprecipitated [<sup>35</sup>S]-labeled HYAL1 protein from cell lysates of BHK\_HYAL1 cells resulted in a single band at approximately 43 kDa that was not observed in BHK\_pIRESneo cell lysates or conditioned medium (Figure 20a). The Endo H treatment had little effect on [<sup>35</sup>S]-labeled HYAL1 protein immunoprecipitated from conditioned medium (Lane 8) of BHK\_HYAL1 cells of as compared to untreated form (Lane 7), and migrated at approximately 52 kDa. The Endo H treated [<sup>35</sup>S]-labeled HYAL1 protein from conditioned medium was present at very low levels and therefore, only a faint band was detected (Figure 20a, lane 8). This was further analyzed by labeling the BHK\_HYAL1 cells, treating the immunoprecipitated



**Fig-19. Pulse-chase labeling of HYAL1 followed by PNGase F treatment.** BHK\_HYAL1 (E) and BHK\_pIRESneo (C) cells were pulse labeled for 10 minutes using 0.2 mCi of [<sup>35</sup>S]-met/cys and then chased for 0 to 5 hours. HYAL1 immunoprecipitated from cell lysates (L) or conditioned medium (M) was divided into two equal aliquots; one aliquot was treated with PNGase F. Treated and untreated samples were separated by 10% SDS-PAGE, followed by fluorography. A white dot indicates the HYAL1 protein without PNGase F treatment and the treated HYAL1 form is represented by an asterisk. X indicates the cross-reacting bands. The size and position of the [<sup>14</sup>C]-labeled molecular mass markers is shown on the left.

**Fig-20a. Pulse-Chase labeling of HYAL1 followed by Endo H treatment.** BHK\_HYAL1 (lanes 3 - 8) and BHK\_pIRESneo cells (lanes 1 - 2) were pulse labeled using 0.2 mCi of [<sup>35</sup>S]-met/cys for 10 minutes in duplicates. This was followed by a chase periods of 0 to 3 hours. Cell lysates (L) and conditioned medium (M) were subjected to immunoprecipitation using anti-HYAL1 antibodies. One set of samples was subjected to the Endo H treatment, while the other set was not treated with Endo H. The white dots represent untreated HYAL1 forms, while the treated form is indicated by an asterisk. X indicates cross-reacting bands. The position and size of the [<sup>14</sup>C]-labeled molecular mass markers is shown on the left.



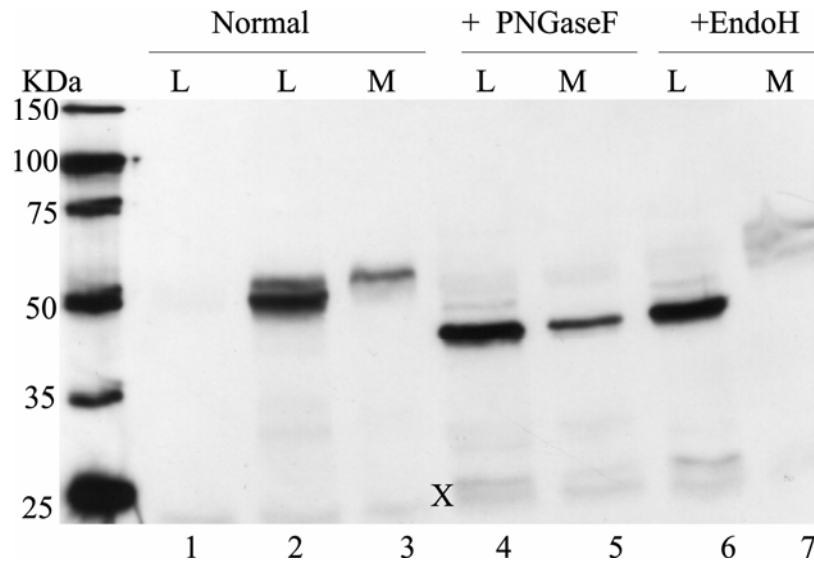


**Fig-20b. Pulse-Chase labeling of HYAL1 followed by glycosidase treatment.**

BHK\_HYAL1 (lanes 2 – 7) and BHK\_pIRESneo cells (lane 1) were pulse labeled using 0.2 mCi of [<sup>35</sup>S]-met/cys for 10 minutes followed by a 3 hour chase. Cell lysates (L) and conditioned medium (M) were subjected to immunoprecipitation using anti-HYAL1 antibodies. The immunoprecipitated samples from cell lysates as well conditioned medium were treated with either PNGase F or Endo H. One set of sample was not treated with any glycosidase. The treated as well as untreated samples were then separated on 10 % SDS followed by western blot analysis. X indicates cross-reacting bands. The position and size of the [<sup>14</sup>C]-labeled molecular mass markers is shown on the left.

[<sup>35</sup>S]-labeled HYAL1 protein with PNGase F (Figure 20b lanes 4 and 5) and Endo H (lanes 6 and 7), followed by western blot analysis instead of fluorography. The HYAL1 band was readily detected in both Endo H treated (lane 7) as well untreated (lane 3) samples. This result also confirms that the HYAL1 is partially resistant to Endo H treatment.

These results support the previous finding that the different forms of HYAL1 are N-glycosylated products of an approximately 43 kDa precursor HYAL1 protein, with HYAL1 in cell lysates containing the high mannose/hybrid type carbohydrate (sensitive to Endo H) and the secreted form containing the complex type of carbohydrate (resistant to Endo H). The two bands detected earlier (Figure 10, lanes 5, 6, 9, and 10) at 50 kDa and 45 kDa upon PNGase F treatment and Endo H treatment were not observed during these experiments, and all the forms migrated as a single band, indicating that these bands were observed due to incomplete digestion.

### **3.7 Processing of [<sup>35</sup>S]-labeled HYAL1 in the presence of tunicamycin**

To verify that both of the HYAL1 forms detected at 2 minutes of pulse were the result of differences in glycosylation and to examine its effect on HYAL1 secretion, BHK\_HYAL1 and BHK\_pIRESneo cells were pulse-labeled for 10 minutes with [<sup>35</sup>S]-met/cys followed by chase analysis (0 to 3 hours) in the presence of the N-glycosylation inhibitor, tunicamycin (10 µg/µl) that prevents the addition of N-linked oligosaccharides to newly synthesized proteins in the ER.

The tunicamycin treatment had the same effect on the migration pattern of [<sup>35</sup>S]-labeled HYAL1 from BHK\_HYAL1 cell lysates as that observed after PNGase F

treatment; HYAL1 migrated at approximately 43 kDa (Fig-21, lanes 7 and 9). As seen in Figure 21, untreated BHK\_HYAL1 cells showed the normal pattern of two HYAL1 forms in cell lysates (lanes 3 and 5), and a single band in conditioned medium (lane 6) at 10 minutes of pulse labeling. These bands were not detected in BHK\_pIRESneo cells (lanes 1,2,11 and 12). The HYAL1 band was, however, not detected in conditioned medium from tunicamycin treated BHK\_HYAL1 cells (lane 10) suggesting carbohydrate processing is required for its secretion. This result represents a single experiment. The experiment was repeated twice with non-labeled BHK\_HYAL1 and BHK\_pIRESneo cells.

The tunicamycin treatment confirms that the approximately 43 kDa form is an unglycosylated precursor form of HYAL1 that is modified co-translationally, and therefore is not detected during pulse-chase analysis. Glycosylation seems to be essential in proper processing and secretion of HYAL1. It also suggests that the two HYAL1 bands detected at 2 minutes of pulse labeling (Figure 14) only differ in their carbohydrate content as they migrated as a single band after tunicamycin treatment.

**Fig-21. Pulse-Chase labeling of HYAL1 in the presence of tunicamycin.** BHK\_HYAL1 (lanes 3-12) and BHK\_pIRESneo cells (lanes 1 and 2) were pulse labeled for 10 minutes using 0.2 mCi of [<sup>35</sup>S]-met/cys followed by a chase periods of 0 to 3 hours in the presence (+) or absence (-) of 10 µg/ml of tunicamycin. Cell lysates (L) and conditioned medium (M) were subjected to immunoprecipitation using anti-HYAL1 antibodies. White dots show different forms of HYAL1 protein present in the absence of tunicamycin and an asterisk indicates HYAL1 after tunicamycin treatment. X indicates cross-reacting bands.



### **3.8 Processing of [<sup>35</sup>S]-labeled HYAL1 in the presence of deoxynojirimycin (DNM)**

BHK\_HYAL1 and BHK\_pIRESneo were grown in the presence of 3 mM DNM, an inhibitor of glucosidases I and II, for 1 hour. This was followed by pulse-chase analysis using [<sup>35</sup>S]-met/cys, in presence of 3 mM DNM, and compared to untreated cells. The aim of this study was to determine if the two bands observed, even at short pulse labeling times, were two different species of HYAL1 or a single HYAL1 form processed rapidly to give two bands. Glucosidases I and II trim the first three glucose residues from the N-linked oligosaccharide chain and the protein is then available for export from endoplasmic reticulum. Inhibiting the glucose trimming will not allow any further processing of the N-linked oligosaccharide chain and thereby proteins accumulated in the ER will have high mannose chains. Therefore, if the HYAL1 protein was synthesized as a single form and co-translationally modified to give two forms, which may be the case given that tunicamycin treatment resulted in a single band, deoxynojirimycin treatment should result in one form of HYAL1 within the cells. If two bands are still detected after treatment then it will indicate two different species of HYAL1 are formed.

The cell lysates from treated and untreated BHK\_HYAL1 and BHK\_pIRESneo cells were subjected to immunoprecipitation followed by fluorography as described above. As seen in Figure 22, after 10 minutes of pulse labeling, the DNM treatment had no effect on the number of HYAL1 forms present in the cell lysate of BHK\_HYAL1 cells, however, these forms migrated at a higher position (lanes 5 and 6) compared to those of an untreated 10 minute pulse labeled cell lysate samples (lanes 2 and 3). This was expected because of the presence of the unmodified high mannose oligosaccharide

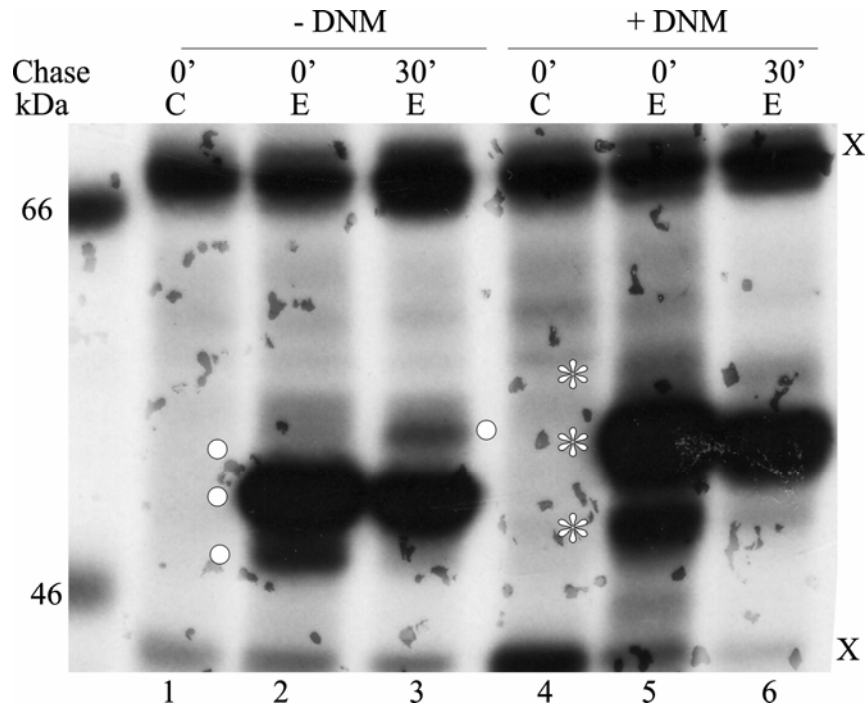


**Fig-22. Pulse-chase labeling of HYAL1 in presence of deoxynojirimycin (DNM).**

BHK\_HYAL1 (E) and BHK\_pIRESneo (C) cells were pulse labeled for 10 minutes using 0.2 mCi of [<sup>35</sup>S]-met/cys followed by a chase period of 30 minutes in the presence (+) or absence (-) of 3 mM DNM. Cell lysates (L) and conditioned medium (M) were subjected to immunoprecipitation using anti-HYAL1 antibodies. White dots show HYAL1 protein modified in the absence of DNM, while the asterisk indicates the HYAL1 protein separated after DNM treatment. X indicates a cross-reacting band. The position and size of the [<sup>14</sup>C]-labeled molecular mass markers is shown on the left.

chains that result in the presence of DNM. No HYAL1 band was detected in cell lysates of BHK\_pIRESneo cells (lanes 1 and 4). It was also noted that DNM treatment prevents the modification of both the ~ 49 and ~ 50 kDa forms, suggesting both are independent forms of HYAL1 synthesized in the ER. It is also possible that both forms of HYAL1 represent single species but the higher form at ~ 50 kDa contains one more N-linked oligosaccharide than the lower ~ 49 kDa form. The ~ 52 kDa (lane 6) form that is observed otherwise at 30 minutes of chase in untreated BHK\_HYAL1 cells (lane 3) suggests that it is derived from either the ~ 49 or the ~ 50 kDa form. This experiment was only performed once.

### **3.9 Processing of [<sup>35</sup>S]-labeled HYAL1 in the presence of brefeldin A (BFA)**

The absence of the approximately 52 kDa form in the presence of DNM suggested that it might be modified from one of the lower 50 or 49 kDa forms. To confirm this finding, the BHK\_HYAL1 and BHK\_pIRESneo cells were pulse labeled using [<sup>35</sup>S]-met/cys followed by chase analysis in presence of BFA (20 µg/µl), and compared with non-treated cells. BFA is a fungal metabolite that has multiple effects on the secretory pathway, including inhibition of trafficking from ER to the Golgi apparatus, and the fusion of the cis, medial Golgi with the ER (Misumi et al. 1986). In the case of HYAL1, BFA treatment might be expected to prevent the modification of the 50 or 49 kDa bands, and secretion of HYAL1, as its export from the ER is blocked.

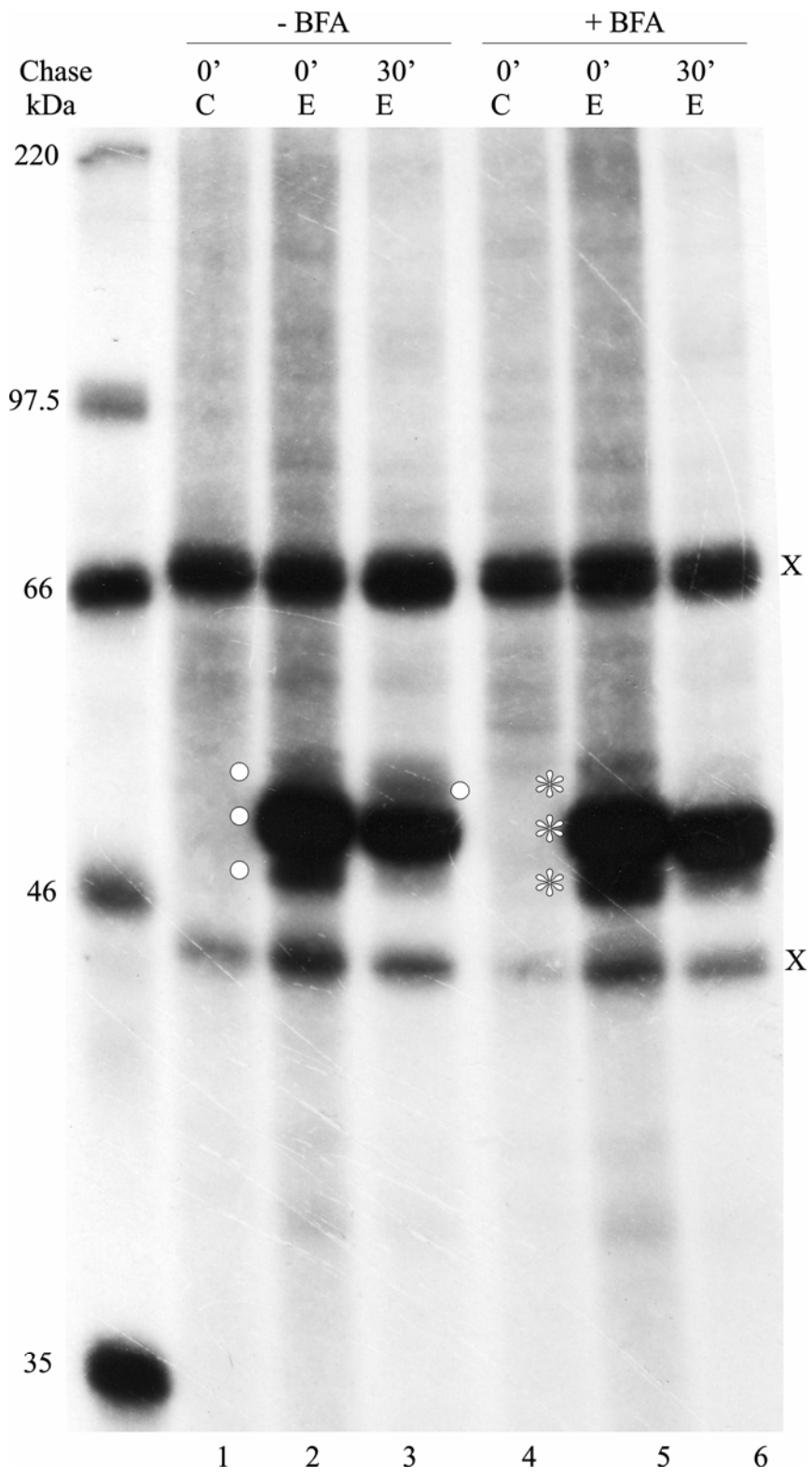
The [<sup>35</sup>S]-labeled cell lysates from untreated and BFA treated BHK\_HYAL1 and BHK\_pIRESneo were subjected to immunoprecipitation followed by fluorography as described earlier. The [<sup>35</sup>S]-labeled HYAL1 protein was detected at ~ 49 and ~ 50 kDa, in

untreated (Fig- 23, lane 2) as well as BFA treated (lane 5) BHK\_HYAL1 cell lysates, but was not seen in BHK\_pIRESneo cell lysates (lanes 1 and 4). The approximately 52 kDa band was detected at 30-minute chase (lane 3) in untreated BHK\_HYAL1 cells; however in the BFA treated BHK\_HYAL1 cells, the ~ 52 kDa band was missing (lane 6). The absence of the ~ 52 kDa band in the BFA treated cell lysates suggest that it is derived from either the ~ 49 or ~ 50 kDa forms by modification in the Golgi. This figure is representative of three independent experiments.

### **3.10 Analyzing the effect of ammonium chloride and chloroquine on the secretion of [<sup>35</sup>S] labeled HYAL1**

The targeting of many of the soluble lysosomal enzymes in higher eukaryotes is mediated by the mannose-6-phosphate (M6P) dependant pathway (section 1.6.1), where the enzymes are modified to contain a terminal M6P. The lysosomal enzymes with the mannose-6-phosphate marker then bind to the M6P receptor in the trans Golgi and are transferred to lysosomes. The lysosomal enzyme-M6P receptor complex exits the Golgi via a coated vesicle and is delivered to a prelysosomal compartment (endosomes) where the ligand is dissociated. The key factor in the transport is the variation of the pH in different compartments; the receptor binds its ligand at neutral pH in the Golgi and discharges it at acidic pH in the endosome. This ensures the proper transport of the enzymes. However, some lysosomal enzymes are not targeted by this pathway and HYAL1 was reported to be one of them (Natowicz et al. 1979; Natowicz and Wang 1996), suggesting that the intracellular transport of HYAL1 was independent of the

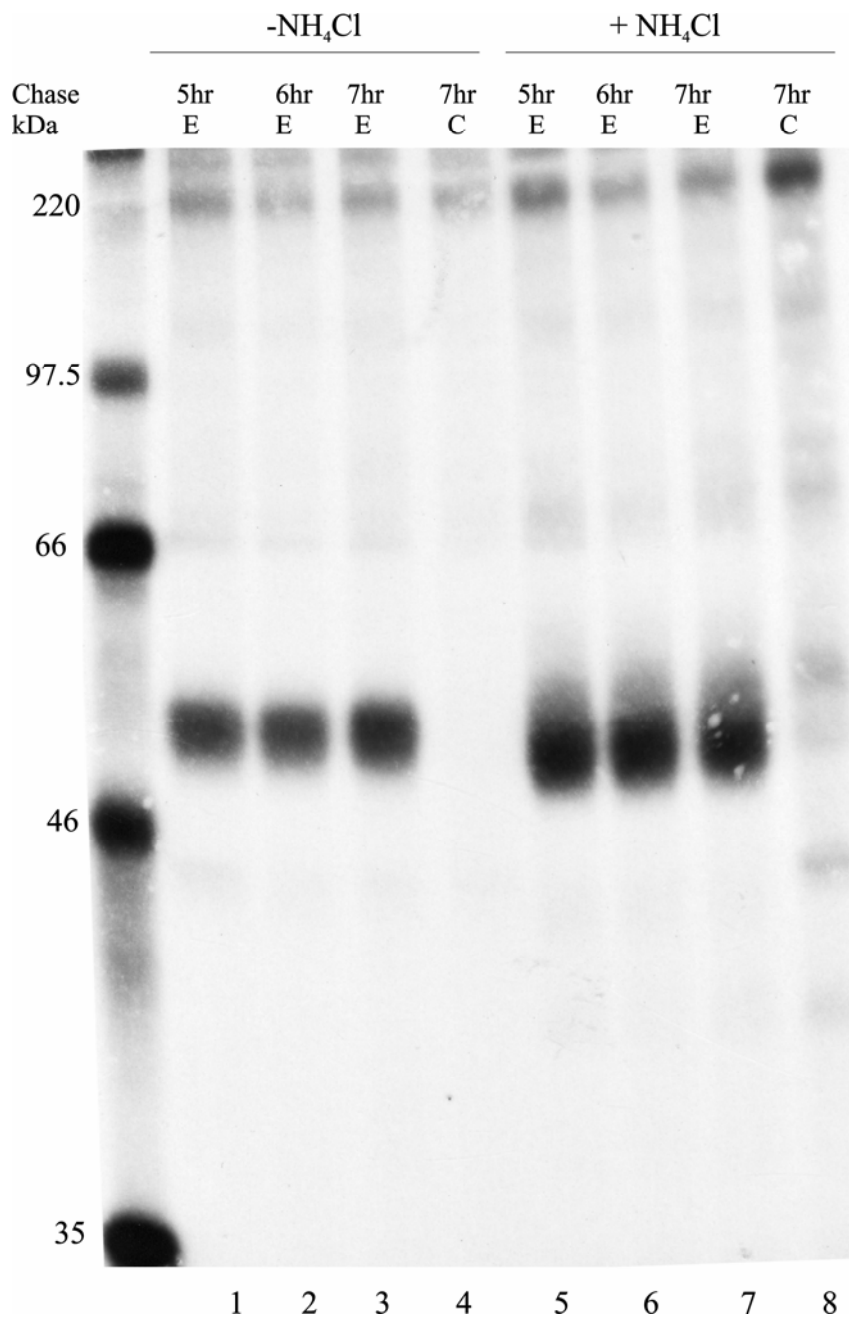
**Fig-23. Pulse-Chase labeling of HYAL1 in the presence of brefeldin A (BFA).** BHK\_HYAL1 (E) and BHK\_pIRESneo (C) cells were pulse labeled for 10 minutes using 0.2 mCi of [<sup>35</sup>S]-met/cys followed by a 30 minute chase in presence (+) or absence (-) of 10 µg/ml of BFA. Cell lysates (L) and conditioned medium (M) were subjected to immunoprecipitation using anti-HYAL1 antibodies. White dots indicate HYAL1 protein under normal conditions while the asterisk represents HYAL1 treated with BFA. X indicates a cross-reacting band. The position and size of the [<sup>14</sup>C]-labeled molecular mass markers is shown on the left.



M6P receptor pathway. To reassess this in our system, we used a simple and common approach. The intracellular pH was imbalanced thereby inducing misrouting of newly synthesized lysosomal enzymes bearing the M6P recognition marker, to the medium. Ammonium chloride (NH<sub>4</sub>Cl) or chloroquine was used to increase the pH of the endosome and lysosome during pulse-chase analysis. The BHK\_HYAL1 and BHK\_pIRESneo cells were pulse-labeled for 10 minutes using [<sup>35</sup>S]-met/cys followed by chase analysis for 5, 6, and 7 hours in the presence of 10 mM ammonium chloride or 150 mM chloroquine. The conditioned medium was collected at each chase point and subjected to immunoprecipitation followed by fluorography as described earlier.

The presence of 10 mM NH<sub>4</sub>Cl or 150 mM chloroquine had no significant effect on the level of [<sup>35</sup>S]-labeled HYAL1 that is secreted, as seen in Figure 24 and Figure 25 respectively, compared to the HYAL1 secreted by untreated BHK\_HYAL1 cells. No HYAL1 protein was detected in the conditioned medium of untreated or treated BHK\_pIRESneo cells (lanes 4 and 8 in Figure 24 and 25). Both of the figures are represents a single experiment. The ammonium chloride experiment was repeated twice and chloroquine treatment was repeated once with non-labeled cells.

**Fig-24. Immunoprecipitation of [<sup>35</sup>S]-labeled HYAL1 from the conditioned medium of 10 mM NH<sub>4</sub>Cl treated cells.** The BHK\_HYAL1 (E) and BHK\_pIRESneo (C) cells were pulse labeled for 10 minutes using 0.2 mCi of [<sup>35</sup>S]-met/cys followed by chase of 5, 6 and 7 hours in the presence (+) and absence (-) of 10 mM NH<sub>4</sub>Cl. Conditioned medium from treated as well as untreated cells were collected after 5, 6 and 7 hours of incubation and subjected to immunoprecipitation using anti-HYAL1 antibodies. The position and size of the [<sup>14</sup>C]-labeled molecular mass markers is shown on the left.



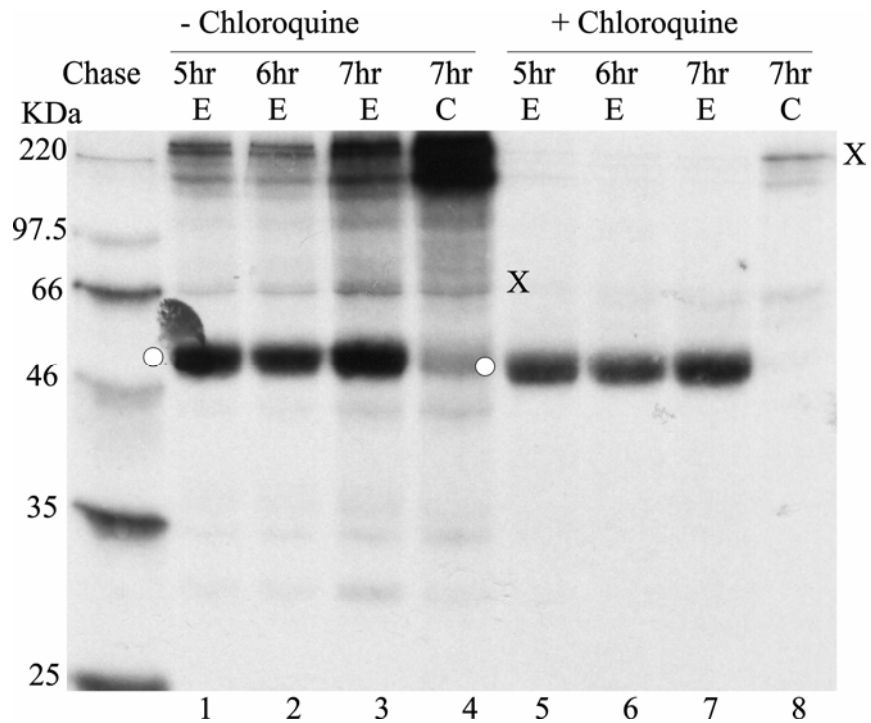


**Fig-25. Immunoprecipitation of [<sup>35</sup>S]-labeled HYAL1 from the conditioned medium of 150 mM chloroquine treated cells.** The BHK\_HYAL1 (E) and BHK\_pIRESneo (C) cells were pulse labeled for 10 minutes using 0.2 mCi of [<sup>35</sup>S]-met/cys followed by a chase of 5, 6 and 7 hours in the presence (+) and absence (-) of 150 mM chloroquine. Conditioned medium from treated as well as untreated cells were collected after 5, 6 or 7 hours of incubation and subjected to immunoprecipitation using anti-HYAL1 antibodies. White dots indicate the position of the immunoprecipitated HYAL1 protein, while X indicates cross reacting band. The position and size of the [<sup>14</sup>C]-labeled molecular mass markers is shown on the left.

The presence of 10 mM NH<sub>4</sub>Cl or 150 mM chloroquine had no significant effect on the level of [<sup>35</sup>S]-labeled HYAL1 that is secreted, as seen in Figure 24 and Figure 25 respectively, compared to the HYAL1 secreted by untreated BHK\_HYAL1 cells. No HYAL1 protein was detected in the conditioned medium of untreated or treated BHK\_pIRESneo cells (lanes 4 and 8 in Figure 24 and 25). Both of the figures represents a single experiment. The ammonium chloride experiment was repeated twice and chloroquine treatment was repeated once with non-labeled cells.

It was also noted that the [<sup>35</sup>S]-labeled HYAL1 migrated at a slightly lower position in the presence of NH<sub>4</sub>Cl or chloroquine. This is the result of a difference in some post-translational modification, as upon the PNGase F and Endo H treatment, the ammonium chloride treated and untreated forms migrated at the same position (Figure 10, lanes 7, 8, 10, and 11).

This result supports the suggestion that HYAL1 is not targeted via the M6P receptor dependent targeting pathway.

### **3.11 Labeling of HYAL1 with [<sup>32</sup>P]-orthophosphate**

The results obtained by NH<sub>4</sub>Cl and chloroquine treatment suggested that HYAL1 was not targeted via a M6P-dependant pathway. Further, when the cell lysates and conditioned medium samples from BHK\_HYAL1 cells were passed through a M6P receptor column, HYAL1 did not bind to the M6P receptor (Jadot, M. personal communication); again suggesting HYAL1 is targeted by a M6P-independent pathway. To confirm these findings, cells were labeled with inorganic phosphate and cell lysates were analyzed for the incorporation of labeled phosphate in high mannose

oligosaccharide chains to give the M6P recognition marker. The BHK\_HYAL1 and BHK\_pIRESneo cells were pulse-labeled for 30 minutes or 3 hours using 500  $\mu$ Ci of [ $^{32}$ P]-phosphate per 1 ml of phosphate free medium. The cell lysates after 30 minutes of labeling were subjected to immunoprecipitation using anti-HYAL1 antibodies. The 3-hour labeling was done to label  $\beta$ -hexosaminidase as a positive control and it was immunoprecipitated from cell lysates using anti- $\beta$ -hexosaminidase A antibodies available in the lab (Hasilik and Neufeld 1980). The immunoprecipitated samples were analyzed by 10% SDS-PAGE and fluorography.

As seen in the Figure 26 neither BHK\_pIRESneo (lane 1) nor HYAL1 expressing cell lysates (lane 2) incorporated any radioactive phosphate that could be immunoprecipitated with anti-HYAL1 antibodies. The endogenous  $\beta$ -hexosaminidase immunoprecipitated using anti  $\beta$ -hexosaminidase showed [ $^{32}$ P]-labeled bands at approximately 39 kDa, 48kDa and 67 kDa (lane 3) in contrast to the expected molecular weight of 100 kDa, 68 kDa and 37 kDa. Three independent experiments were performed, and a representative experiment is shown.

This result suggests no phosphorylation of mannose residues occurs in the case of the HYAL1 protein, again consistent with it not containing a M6P signaling molecule.

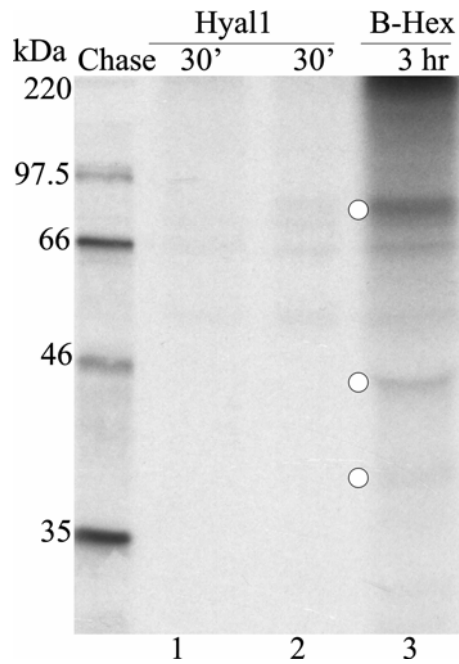


**Fig-26. Pulse labeling of BHK\_HYAL1 and BHK\_pIRESneo with [<sup>32</sup>P]-phosphate.**

The BHK\_HYAL1 and BHK\_pIRESneo cells were pulse labeled for 30 minutes and 3 hours using 500  $\mu$ Ci of [<sup>32</sup>P]-labeled orthophosphate. The cell lysates from 30 minutes of pulse were subjected to immunoprecipitation with anti-HYAL1 antibodies and the cell lysates from 3 hours of pulse were subjected to immunoprecipitation with anti-hexosaminidase antibodies. The white dots indicate the hexosaminidase protein forms recognized by anti-hexosaminidase antibodies (Hasilik and Neufeld 1980). The position and size of the [<sup>14</sup>C]-labeled molecular mass markers is shown on the left.

### **3.12 Analysis of hydrophobic properties of HYAL1 by detergent phase separation**

The HYAL1 isolated from human plasma was reported to partition to a detergent phase, suggesting it had hydrophobic properties. However, no evidence for such properties was found using bioinformatics analysis of HYAL1 amino acid sequence, and it was not released upon phospholipase C treatment, an enzyme that releases many GPI-linked membrane proteins (data not shown). To reassess the hydrophobic properties of HYAL1 expressed by BHK\_HYAL1 cells, phase separation was performed on cell lysates, as well as on conditioned medium, of BHK\_HYAL1 and BHK\_pIRESneo cells. The aqueous and detergent phases collected were separated by 10% SDS-PAGE (section 2.6) and analyzed by western blot analysis (section 2.7). As seen in Figure 27, HYAL1 was detected in the aqueous as well as the detergent phase (lanes 1, 2, 3, and 4) from BHK\_HYAL1 cells, but not in BHK\_pIRESneo cells (lanes 5, 6, 7, and 8). The equal distribution of all forms of HYAL1 in the aqueous (lanes 1 and 2) and detergent phases (lanes 3 and 4) suggested HYAL1 has both hydrophobic as well as hydrophilic properties. This figure is representative of three independent experiments.

To determine if the HYAL1 detected in the aqueous and detergent phases was active, zymography was performed on these samples. As seen in Figure 28, all the forms of HYAL1 in BHK\_HYAL1 lysates from the aqueous (lane 1) and detergent phases were active (lane 2). However, HYAL1 was less active in the detergent fraction (lanes 4 and 5) as compared to the aqueous phase (lanes 1 and 2). No activity was detected in BHK\_pIRESneo lysates (lanes 6 and 8) or conditioned medium (lanes 7 and 9). The significance of these findings is not clear at this point.

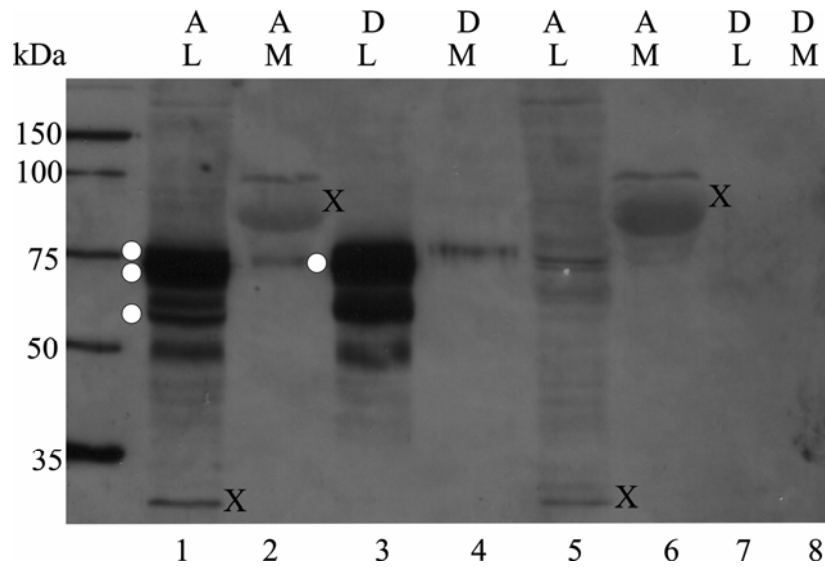


**Fig-27. Phase separation of HYAL1.** BHK\_HYAL1 and BHK\_pIRESneo cells were grown to confluence in a 100 mm X 20 mm culture plate. The cell lysates (L) as well as conditioned medium (M) were subjected to phase separation using the Mem-PER eukaryotic membrane protein extraction protein Kit (Piercenet Inc.). Western blot analysis using anti-HYAL1 antibodies was performed on the hydrophilic (A) and the detergent (D) phases. The white dots indicate HYAL1 protein recovered from the top hydrophilic fraction, as well as the bottom detergent phase. The size and position of the molecular mass markers is shown on the left.

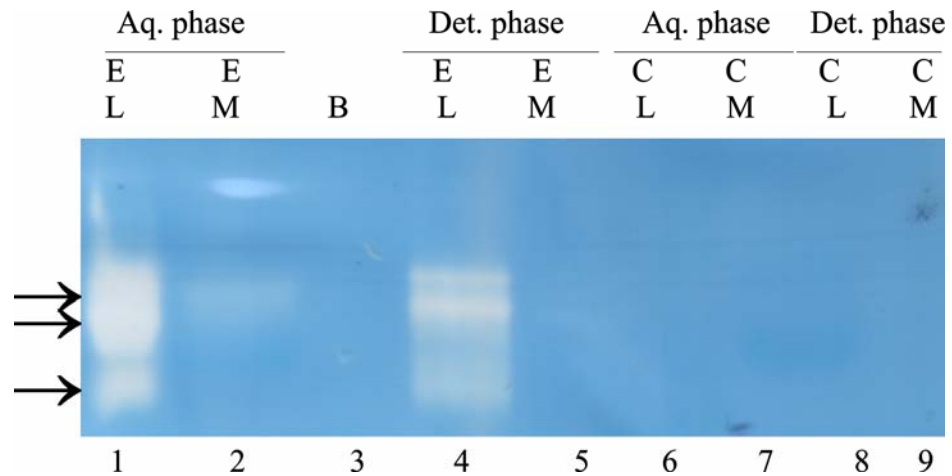


**Fig-28. Analysis of HYAL1 activity in the fractions obtained by phase separation.** BHK\_HYAL1 (E) and BHK\_pIRESneo (C) cells were subjected to phase partitioning. The HYAL1 activity from the cell lysates (L) as well as the conditioned medium (M) in both the aqueous phase and detergent phase was assessed by an in gel activity assay. The clearing of the gel is shown by arrows. The aqueous phase and detergent phase in the case of the BHK\_HYAL1 cells were separated by a blank (B).

# **DISCUSSION**

The studies presented here were initiated to shed some light on the subcellular localization of HYAL1 and its processing, with anticipation that the characterization of alternate route(s) for lysosomal targeting may allow new strategies for the targeting of therapeutic enzymes to be developed for LSD. The current therapies available for lysosomal storage disorders are either limited to non-neural LSD (enzyme replacement therapy) or to LSDs that results from protein missorting or misfolding (enzyme enhancement therapy), indicating a need for alternative therapies.

To begin to study the processing and intracellular localization of HYAL1, a cell line expressing an easily detectable amount of HYAL1 was required. However, HYAL1 was found to be expressed at very low levels in the cell lines that were examined in our laboratory, necessitating the construction of a HYAL1 expression vector. Attempts to generate a HYAL1 expression construct with a C-terminal His tag, or including a portion of the untranslated region, resulted in low levels of HYAL1 expression and/or improper processing. A vector containing only the HYAL1 coding sequence, pIRES\_HYAL1, was found to express levels of protein that were easily detected in both the cell lysate and medium (Figure 6). These results suggested that the non-coding 3' or 5' untranslated region might interfere with translation of HYAL1 as was reported previously (Csoka, Scherer, and Stern 1999).

The pIRES\_HYAL1 construct was stably transfected into the BHK cells. BHK cells were used, because they had low levels of endogenous HYAL1. BHK cells stably expressing different levels of HYAL1 were isolated and one of the lines with the highest level of HYAL1 expression (Figure 7) was selected for subsequent studies. The level of HYAL1 expression in the BHK cells was found to drop off quickly during passage of the

cells. As a result, a western blot was routinely performed at the same time as most experiments to make sure that the levels of HYAL1 expression were adequate for the experiment being performed.

Human HYAL1 expressed in stably-transfected BHK cells was found to have 3 different forms in the cell lysates (49, 50, and 52 kDa). Human HYAL1 when expressed in the breast cancer line, CAL51, showed two HYAL1 forms while only one form was detected when it was expressed in a prostate cancer line (Patel et al. 2002), suggesting that HYAL1 might be processed differently in different types of cells. Different electrophoretic forms of hyaluronidases are shown to be present in different human tissues (Fischer-Szafarz, Litynska, and Zou 2000). Our data is consistent with previous reports of the presence of different forms of hyaluronidase in different types of cells/tissue. Only one form of HYAL1 was detected in the medium (52 kDa). Previous studies have focused on the human serum or plasma enzyme, which was reported to be one form with a molecular mass of 57 kDa (Frost et al. 1997). Our studies are consistent in that a single secreted form was detected in the medium. However, the size of the secreted form of HYAL1 was smaller in our studies, probably because of differences in the glycosylation in human versus hamster cells. The difference in electrophoresis conditions or in calculating apparent molecular weight of protein is also possible.

HYAL1 isolated from human plasma was reported to have a molecular mass of 57 kDa with 8 kDa of that made up of carbohydrate (Frost et al. 1997). On the other hand, several forms of acid active hyaluronidase were detected from human somatic tissues by zymography under native conditions (Fischer-Szafarz, Litynska, and Zou 2000). Bioinformatic analysis of the HYAL1 amino acid sequence predicted a molecular mass of

48 kDa with three potential N-glycosylation sites. In our studies, the presence of multiple forms of expressed HYAL1 suggested the protein might be modified by glycosylation. This was confirmed by treatment of HYAL1 with the endoglycosidase, PNGase F. The multiple bands detected in cell lysates migrated as single form at approximately 43 kDa after PNGase F digestion (Figure 10), suggesting that all the forms were N-glycosylation products of the unglycosylated 43 kDa form.

Further analysis of the carbohydrate modifications of intracellular and secreted forms of HYAL1 was performed using endo H, an enzyme that removes only high mannose or hybrid N-linked oligosaccharides from proteins. All of the intracellular forms of HYAL1 were found to be sensitive to endo H (Figures 10), but the secreted form was found to be partially resistant to the Endo H activity (Figures 10), suggesting a complex-type of carbohydrate modification unlike that of the high mannose/hybrid modification detected in the intracellular form of HYAL1. This result agreed with the previous report of differences in the migration pattern of human serum hyaluronidase (HYAL1) upon sialidase treatment (Fischer-Szafarz, Litynska, and Zou 2000). These results were further confirmed by treating [<sup>35</sup>S] labeled HYAL1 with PNGase F and Endo H (Figure 19 and 20 respectively).

Analysis of HYAL1 that was prepared in reducing or non-reducing conditions was done by SDS-PAGE (Figure 11). The increase in the size of HYAL1 under non-reducing conditions showed that disulfide bonds were likely to be present. This finding was consistent with the presence of several cys residues and potential disulfide bonds(s) predicted by bioinformatics analysis of the HYAL1 amino acid sequence using disulfide bond predicting software (DiANNA). The importance of disulfide bonds is reported in

several lysosomal enzymes including  $\beta$ -hexosaminidase and members of the cathepsin family. Another member of the hyaluronidase family, PH20, is also reported to have disulfide bonds.

The activity of the HYAL1 expressed by BHK\_HYAL1 was demonstrated using an in-gel activity assay, zymography. All of the forms of HYAL1 in cell lysates, as well as the secreted HYAL1 form, were active at pH 3.8 (Figure 9), as previously reported (Frost et al. 1997). However, if the samples were treated with a reducing agent prior to zymography, all of the HYAL1 activity was lost. This suggests that either intrachain disulfide bond(s) in HYAL1, or interchain disulfide bond(s) with other HYAL1 subunits or other proteins, are important for its activity (data not shown).

The subcellular localization of HYAL1 was performed by fractionation of BHK\_HYAL1 lysates on a Percol gradient. The data from the Percol gradient suggested HYAL1 is located in a vesicular compartment with similar density to that of late endosomes and lysosomes (Figure 12). The HYAL1 was present in several fractions with similar density to that of late endosomal marker Rab9, some overlapping with lysosomal marker LAMP1 and ER marker calnexin. The zymogram revealed the fractions that carry active forms of HYAL1; most of the activity was seen in the fractions with similar density to that of Rab9 with some overlap with LAMP1 (Figure 13). The zymography data was consistent with the western blot results. While these results are consistent with having some enzyme localized to a compartment with a similar density to lysosomes, the majority of the enzyme was not found in this region of the gradient. It may be that a large proportion of HYAL1 exists in a pre-lysosomal compartment, as has been shown for some other lysosomal enzymes, including cathepsin H (Claus et al. 1998). It is possible

that only a small proportion of HYAL1 is in the lysosome at any time and/or that its transport to the lysosomes is regulated in some way. Given the lysosomal accumulation of HA in macrophages and fibroblast cells in the absence of HYAL1 (Natowicz et al. 1996), it seems likely that HYAL1 must exist in the lysosomes at some point in its lifespan.

Human HYAL1 was isolated from plasma by phase partitioning. It was found to partition to the Triton X-114 phase, and was found to be unstable in the absence of detergent (Frost et al. 1997). However, no data were presented about HYAL1 behavior in the aqueous phase and no comparison was reported between HYAL1 activity/stability in the presence and absence of detergent. In our case, the phase separation studies of HYAL1 from BHK\_HYAL1 cell lysates, as well as conditioned medium, resulted in an equal distribution of HYAL1 in both the aqueous phase and detergent phase (Figure 27). The activity assay, however, suggested that HYAL1 was less active in the presence of detergent compared to HYAL1 isolated in the aqueous phase (Figure 28). The significance of this distribution pattern of HYAL1 is not clear at this point. However, it provides the direct comparison between aqueous as well as detergent phases, and also suggested that HYAL1 can be isolated from the aqueous phase without the help of detergent, in contrast to what was reported previously (Frost et al. 1997).

The processing of HYAL1 was characterized by pulse-chase analysis. Two forms of [<sup>35</sup>S]-labeled HYAL1 with molecular masses of approximately 49 kDa and 50 kDa were detected (Figure 14) even at two minutes of pulse labeling, indicating significant levels of synthesis in our transfected cells. The relationship between those forms became clear upon treatment with endoglycosidases: PNGase F and Endo H. Both forms of

HYAL1 detected at 10 minutes pulse labeling in cell lysates of BHK\_HYAL1 migrated as single form with a molecular mass of 43 kDa, indicating that both forms were N-glycosylation products of the 43 kDa precursor molecule. The glycosylation pattern of HYAL1 was verified by tunicamycin treatment, an N-linked glycosylation inhibitor that prevents the addition of N-linked oligosaccharides to the newly synthesized protein in the endoplasmic reticulum. The [<sup>35</sup>S]-labeled HYAL1 migrated as a single band at 43 kDa in cell lysates upon tunicamycin treatment, supporting the previous finding. This result suggested that both forms of HYAL1 differ only in their glycosylation. However, treatment with DNM (Figure 22), an inhibitor of glucosidase I and II had no effect on the number of HYAL1 forms present in cell lysates, suggesting that, single species of HYAL1 is present but the lower form has one less N-linked oligosaccharide attached.

The chase analysis of [<sup>35</sup>S]-labeled HYAL1 showed that the protein has a half-life of about 2.5 hours within the cells, as it disappeared from the cells at the 5 hour chase point (Figure 15). On the other hand, the secreted form of HYAL1 was stable, as it was detected in the medium even after 24 hours of chase (Figure 18). This result suggested that HYAL1 is synthesized within minutes and after 3-5 hours, secreted from the cells, where it is more stable compared to the HYAL1 within the cells. The half-life of individual proteins is different and it varies from several minutes to several days. The lysosomal enzymes have relatively long half-lives, suggesting that regulation of HYAL1 expression is under specific control.

The [<sup>35</sup>S]-labeled HYAL1 was not detected from conditioned medium under conditions that were used for immunoprecipitation of HYAL1 from cell lysates. In an attempt to immunoprecipitate HYAL1 from medium, different conditions were used. The

use of detergents such as Triton X 100, NP-40 or sodium deoxycholate, or the reducing agent DTT did not result in increased immunoprecipitation from the medium. However, the addition of SDS to the medium facilitated the immunoprecipitation of HYAL1 from the medium, suggesting denaturation of HYAL1 was required for immunoprecipitation from the conditioned medium (Figure 16), for reasons that are not clear at this point. However, the possibilities of self-association or its association with other molecules cannot be ruled out. Heat denaturation of HYAL1 also facilitated its immunoprecipitation from medium, supporting the previous finding (Figure 16).

The fate of the [<sup>35</sup>S]-labeled HYAL1 from cell lysates was studied by pulse-chase analysis, when the conditions for HYAL1 immunoprecipitation from the conditioned medium were established. The 49 kDa form observed after 10 minutes of pulse labeling disappeared after 30 minutes of chase analysis, with appearance of another band at approximately 52 kDa. The 52 kDa form was then detected in medium at later time points while the 50 kDa form appeared to be degraded within the cells with a half-life of 2.5 hours (Figure 17). The DNM treatment (Figure 22) showed that the 49 kDa form that disappeared in untreated cells was still present in DNM treated cells while the third HYAL1 form of 52 kDa, that normally appeared at 30 minutes of chase, was missing. The BFA treatment had same effect on HYAL1 as that observed with DNM treatment; both forms (49 and 50 kDa) were initially modified to contain high mannose/hybrid type carbohydrates but the third form at 52 kDa was missing in treated cells (Figure 23). It is possible that both forms of HYAL1 (49 and 50 kDa) originate from a single HYAL1 species, where the higher form at 50 kDa has one more N-linked oligosaccharide chain added to it compared to the lower form (49 kDa), and a small amount of the higher form

(50 kDa) is modified post-translationally to yield the 52 kDa form. The lower form of 49 kDa on the other hand, might just be degraded without any further modification. It is possible that the lower form of 49 kDa is post translationally modified to give the 52 kDa form. On the other hand, the lower band of 49 kDa in size may not be HYAL1 but rather another protein, co-immunoprecipitated with HYAL1 using anti-HYAL1 antibodies. However, upon glycosidase treatment, both forms migrated at a single position, suggesting that both forms are HYAL1. Our data strongly supports the 43 kDa band as a precursor form of HYAL1, that is modified by N-linked glycosylation to give the different forms of HYAL1 observed by western blot and pulse-chase analysis.

Our data suggest that HYAL1 is synthesized and modified co-translationally by addition of N-linked carbohydrates in the ER, resulting in 2 bands at 50 and 52 kDa forms (Figure 22). The N-linked sugars from both of these HYAL1 forms, 50 and 52 kDa, are trimmed in ER by glucosidases I, II, and mannosidases quickly to give the two forms of HYAL1 at 49 and 50 kDa respectively. One of these forms is then modified further in the Golgi compartment(s) to the 52 kDa protein, which is secreted into the medium. The 50 kDa form, present in the cell lysates, might represent an endosomal/lysosomal form, as it is the predominant form in the cell lysates. The 50 kDa form is also present in the subcellular fractions with similar density to that of endosomes and lysosomes (Figure 12).

A M6P independent targeting route for HYAL1 was speculated based on evidence from studies of serum from an I-cell disease patient (Natowicz and Wang 1996). The ammonium chloride as well as chloroquine treatment of BHK\_HYAL1 supports this finding, as no increase in levels of secreted HYAL1 was detected in either case (Figure

24 and 25 respectively). Further, no [<sup>32</sup>P]-labeled HYAL1 bands were detected by anti-HYAL1 antibodies (Figure 26) using ortho-phosphate labelling. Finally, evidence of M6P-independent targeting also came from an experiment by our collaborators in Belgium (unpublished data, Jadot, M.), where they ran BHK\_HYAL1 cell lysates and conditioned medium through a M6P receptor column and showed no HYAL1 binding to the column. Several other lysosomal enzymes have been reported to be targeted via a M6P independent pathway, including lysosomal acid phosphatase (Tanaka et al. 1990), which is reported to be targeted to the lysosomes via the cell surface (Braun, Waheed, and Von Figura 1989). The absence of a M6P moiety along with the hydrophobic as well hydrophilic behavior of HYAL1, suggest that HYAL1 might have a transient membrane association at some point in its biogenesis.

Taken together, my data suggests that HYAL1 exists as multiple forms; all forms differ from each other only in their glycosylation. HYAL1 is secreted in substantial quantity. HYAL1 is present in a vesicular fraction similar in density to endosomes and it is not targeted by a M6P dependent pathway.

# FUTURE DIRECTIONS

Currently, two different strategies are available, enzyme replacement therapy (ERT) and enzyme enhancement therapy (EET) for treatment of lysosomal storage disorders. The ERT is based on the M6P receptor mediated targeting of lysosomal enzyme, which is not useful for lysosomal storage disorders with neurological involvement. Our data confirmed a M6P independent pathway for HYAL1. The metabolic labeling studies and density gradient studies suggested vesicular transport of HYAL1. Characterizing the nature of such vesicles and the mechanism of transport of HYAL1 can provide with details that might be useful in designing new enzyme targeting strategies for lysosomal storage disorders.

The subcellular localization studies of HYAL1 by density gradient centrifugation suggested an endosomal/lysosomal localization. To confirm these findings, further studies using a direct approach, such as immunofluorescence staining, is necessary. Intracellular distribution of HYAL1, and other organelle markers can be examined by fixing the BHK\_HYAL1 cells and incubating them with specific antibodies. Co-localization of HYAL1 with other organelle marker can provide direct evidence of HYAL1 localization.

The presence of two forms of HYAL1 during pulse labeling suggests either two species of HYAL1 are present or the same species of HYAL1 with different numbers of N-linked oligosaccharides. Sequencing of both forms can provide further details about their relationship. Further characterization of the secreted form of HYAL1 is also

required; the data presented here suggests possible self-association or association with other molecule (s).

# REFERENCES

1. Asari, A. Novel functions of hyaluronan oligosaccharides.  
<http://www.glycoforum.gr.jp/science/hyaluronan/HA12a/HA12aE.html> . 2-24-2005.  
Ref Type: Electronic Citation
2. Banerji S et al (1999) LYVE-1, a new homologue of the CD44 glycoprotein, is a lymph-specific receptor for hyaluronan. *J.Cell Biol.* 144 (4):789-801.
3. Beech FJ, Madan AK, and Deng N (2002) Expression of PH-20 in normal and neoplastic breast tissue. *J.Surg.Res.* 103:203-207.
4. Birnboim HC (1983) A rapid alkaline extraction method for the isolation of plasmid DNA. *Meth.Enzymol.* 100:243-255.
5. Bourguignon LY et al (2004) CD44 Interaction with Na<sup>+</sup>-H<sup>+</sup> Exchanger (NHE1) Creates Acidic Microenvironments Leading to Hyaluronidase-2 and Cathepsin B Activation and Breast Tumor Cell Invasion. *J.Biol.Chem.* 279 (26):26991-27007.
6. Bradford MM (1976) A rapid and sensitive method for the quantitation of microgram quantities of protein utilizing the principle of protein-dye binding. *Anal.Biochem.* 72:248-254.
7. Braun M, Waheed A, and Von Figura K (1989) Lysosomal acid phosphatase is transported to lysosomes via the cell surface. *EMBO J.* 8:3633-3640.
8. Byers S et al (1998) Glycosaminoglycan accumulation and excretion in the mucopolysaccharidoses: characterization and basis of a diagnostic test for MPS. *Mol.Genet.Metab* 65 (4):282-290.
9. Camenisch TD et al (2000) Disruption of hyaluronan synthase-2 abrogates normal cardiac morphogenesis and hyaluronan-mediated transformation of epithelium to mesenchyme. *J.Clin.Invest* 106 (3):349-360.
10. Chain E and Duthie ES (1940) Identity of hyaluronidase and spreading factor. *Br.J.Expl.Path.* 21:324-338.
11. Cherr GN et al (1996) The PH-20 protein in cynomologus macaque spermatozoa: identification of two different forms exhibiting hyaluronidase activity. *Dev.Biol.* 175:142-153.
12. Claude A and Duran-Reynals F (1934) On the existence of a factor increasing tissue permeability in organs other than testicle. *J.Exp.Med.* 60 (4):457-462.
13. Claus V et al (1998) Lysosomal enzyme trafficking between phagosomes,

- endosomes, and lysosomes in J774 macrophages. Enrichment of cathepsin H in early endosomes. *J Biol.Chem.* 273 (16):9842-9851.
14. Coligan JE, Dunn BM, Ploegh HL, Speicher DW, Wingfield PT (1995a) Detection and Assay Methods. In: Coligan JE et al (eds) Current Protocols In Protein Science.
  15. Coligan JE, Dunn BM, Ploegh HL, Speicher DW, Wingfield PT (1995b) Post-translational modification: Glycosylation. In: Coligan JE et al (eds) Current Protocols In Protein Science.
  16. Collis L et al (1998) Rapid hyaluronan uptake is associated with enhanced motility: implication for an intracellular mode of action. *FEBS Let.* 440 (444):449.
  17. Comtesse N, Maldener E, and Meese E (2001) Identification of a nuclear variant of MGEA5, a cytoplasmic hyaluronidase and a beta-N-acetylglucosaminidase. *Biochem.Biophys.Res.Commun.* 283 (3):634-640.
  18. Csoka AB, Frost GI, and Stern R (2001) The six hyaluronidase-like genes in the human and mouse genomes. *Matrix Biol.* 20 (8):499-508.
  19. Csoka A, Scherer SE, and Stern R (1999) Expression analysis of six paralogous human hyaluronidase genes clustered on chromosomes 3p21 and 7q31. *Genomics* 60:356-361.
  20. Csoka T et al (1997) Purification and microsequencing of hyaluronidase isozymes from human urine. *FEBS Let.* 417:307-310.
  21. Culty M, Nguyen HA, and Underhill CB (1992) The hyaluronan receptor (CD44) participates in the uptake and degradation of hyaluronan. *J.Cell Biol.* 116:1055-1062.
  22. Day, A. J. Understanding hyaluronan-protein interactions. <http://www.glycoforum.gr.jp/science/hyaluronan/HA16/HA16E.html> . 2001. Ref Type: Electronic Citation
  23. de la Motte CA et al (2003) Mononuclear leukocytes bind to specific hyaluronan structures on colon mucosal smooth muscle cells treated with polyinosinic acid:polycytidlic acid:inter-alpha-trypsin inhibitor is crucial to structure and function. *Am.J.Pathol.* 163:121-133.
  24. Delmage JM et al (1986) The selective suppression of immunogenicity by hyaluronic acid. *Ann.Clin.Lab.Sci.* 16:303-310.
  25. Deng X, He Y, and Martin-DeLeon PA (2000) Mouse SPAM1 (PH-20): evidence for its expression in the epididymis and for a new category of spermatogenic-expressed genes. *J.Androl.* 21:822-832.

26. Duksin D and Bornstein P (1977) Impaired conversion of procollagen to collagen by fibroblasts and bone treated with tunicamycin, an inhibitor of protein glycosylation. *J.Biol.Chem* 252 (3):955-962.
27. Evanko, S. P. and Thomas, N. W. Intracellular hyaluronan. <http://www.glycoforum.gr.jp/science/hyaluronan/HA20/HA20E.html> . 7-25-2001. Ref Type: Electronic Citation
28. Evanko SP and Wight TN (1999) Intracellular localization of hyaluronan in proliferating cells. *J.Histochem.Cytochem.* 47 (10):1331-1342.
29. Feinberg RN and Beebe dC (1983) Hyaluronate in vasculogenesis. *Science* 220 (4602):1177-1179.
30. Fieber C et al (2004) Hyaluronan oligosaccharide-induced transcription of metalloproteases. *J.Cell Sci.* 117:359-367.
31. Fiszer-Szafarz B, Litynska A, and Zou L (2000) Human hyaluronidases: electrophoretic multiple forms in somatic tissues and body fluids. Evidence for conserved hyaluronidase potential N- glycosylation sites in different mammalian species. *J.Biochem.Biophys.Methods* 45 (2):103-116.
32. Flannery CR, Little CBHCE, and Caterson B (1998) Expression and activity of articular cartilage hyaluronidases. *Biochem.Biophys.Res.Commun.* 251:824-829.
33. Fraser JRE, Laurent TC, and Laurent UBG (1997) Hyaluronan: its nature, distribution, functions and turnover. *J.Int.Med.* 242:27-33.
34. Fraser JRE and Laurent TC (1989) Turnover and metabolism of hyaluronan. *Ciba Found.Symp.* 143:41-59.
35. Frost GI et al (1997) Purification, cloning, and expression of human plasma hyaluronidase. *Biochem.Biophys.Res.Commun.* 236:10-15.
36. Frost GI et al (2000) HYAL1LUCA-1, a candidate tumor suppressor gene on chromosome 3p21.3, is inactivated in head and neck squamous cell carcinomas by aberrant splicing of pre-mRNA. *Oncogene* 19 (7):870-877.
37. Furukawa K and Terayama H (1977) Isolation and identification of glycosaminoglycans associated with purified nuclei from rat liver. *Biochim.Biophys.Acta* 499:278-289.
38. Furukawa K and Terayama H (1979) Pattern of glycosaminoglycans and glycoproteins associated with nuclei of regenerating liver of rat. *Biochim.Biophys.Acta* 585:575-588.
39. Ginsel LA and Fransen JAM (1991) Mannose 6-phosphate receptor independent targeting of lysosomal enzymes. *Cell Biology International Reports* 15 (12):1167-

1173.

40. Gmachl M et al (1993) The human sperm protein PH-20 has hyaluronidase activity. *FEBS Let.* 336:545-548.
41. Hardingham, T. E. Cartilage: Aggrecan-Link Protein-Hyaluronan aggregates. <http://www.glycoforum.gr.jp/science/hyaluronan/HA05/HA05E.html> . 1998.  
Ref Type: Electronic Citation
42. Hasilik A and Neufeld EF (1980) Biosynthesis of lysosomal enzymes in fibroblasts. *J.Biol.Chem.* 255:4937-4945.
43. Hautmann SH et al (2001) Elevated tissue expression of hyaluronic acid and hyaluronidase validates the HA-HAase urine test for bladder cancer. *J.Urol* 165:2068-2074.
44. Heckel D et al (1998) Novel immunogenic antigen homologous to hyaluronidase in meningioma. *Hum.Molec.Genet.* 7 (12):1859-1872.
45. Hickman S and Neufeld EF (1972) A hypothesis for I-cell disease: defective hydrolases that do not enter lysosomes. *Biochem.Biophys.Res Commun.*
46. Hua Q, Knudson CB, and Knudson W (1993) Internalization of hyaluronan by chondrocytes occurs via receptor-mediated endocytosis. *J Cell Science* 106:365-375.
47. Huey G, Moiin A, and Stern R (1990) Levels of [3H]glucosamine incorporation into hyaluronic acid by fibroblasts is modulated by culture conditions. *Matrix* 10 (2):75-83.
48. Itano N et al (1999a) Relationship between hyaluronan production and metastatic potential of mouse mammary carcinoma cells. *Cancer Res.* 59 (10):2499-2504.
49. Itano N et al (1999b) Three isoforms of mammalian hyaluronan synthases have distinct enzymatic properties. *J.Biol.Chem.* 274 (35):25085-25092.
50. Kaplan A, Adachi M, and Sly WS (1997) Phosphohexosyl components of a lysosomal enzyme are recognized by pinocytosis receptors on human fibroblasts. *Proc.Natl.Acad.Sci.U.S.A* 74:2026-2030.
51. Kjellen L and Lindahl U (1991) Proteoglycans: Structures and Interactions. *Annual Review of Biochemistry* 60 (1):443-475.
52. Knudson CB (1993) Hyaluronan receptor-directed assembly of chondrocyte pericellular matrix. *J.Cell Biol.* 120:825-834.
53. Knudson CB and Knudson W (1993) Hyaluronan-binding proteins in development, tissue homeostasis, and disease. *FASEB J.* 7 (13):1233-1241.

54. Kornfeld S (1986) Trafficking of lysosomal enzymes in normal and disease states. *J.Clin.Invest.* 77:1-6.
55. Kornfeld S (1987) Trafficking of lysosomal enzymes. *FASEB J.* 1:462-468.
56. Kornfeld S (1990) Lysosomal enzyme targeting. *Biochem.Soc.Trans.* 18:367-374.
57. Kornfeld S (1992) Structure and function of the mannose-6-phosphate/insulinlike growth factor II receptors. *Annu.Rev.Biochem.* 61:307-330.
58. Kosaki R, Watanabe K, and Yamaguchi Y (1999) Overproduction of hyaluronan by expression of the hyaluronan synthase Has2 enhances anchorage-independent growth and tumorigenicity. *Cancer Res.* 59 (5):1141-1145.
59. Laemmli UK (1970) Cleavage of structural proteins during the assembly of the head of bacteriophage T4. *Nature* 227:680-685.
60. Laurent TC (1970) Structure of hyaluronic acid. In: Balazs EA (ed) In chemistry and molecular biology of the intercellular biology. Academic: London, pp 703-732.
61. Laurent TC (1998) The Chemistry, Biology and Medical Applications of Hyaluronan and its Derivatives. Portland Press Ltd: London.
62. Laurent TC and Fraser JR (1992) Hyaluronan. *FASEB J.* 6 (7):2397-2404.
63. Laurent TC, Fraser JRE (1986) The properties and turnover of hyaluronan., 86.
64. Laurent TC, Fraser JRE (1991) Catabolism of hyaluronan. In: Henriksen JH (ed) Degradation of Bioactive substances: Physiology and Pathophysiology. CRC Press: Boca Raton, Florida, pp 249-265.
65. Laurent TC, Laurent UB, and Fraser JR (1996) The structure and function of hyaluronan: An overview. *Immunol.Cell Biol.* 74 (2):A1-A7.
66. Laurent UBG and Laurent TC (1981) On the origin of hyaluronate on blood. *Biochem.Int.* 2:195-199.
67. Lepperdinger G, Strobl B, and Kreil G (1998) *HYAL2*, a human gene expressed in many cells, encodes a lysosomal hyaluronidase with a novel type of specificity. *J.Biol.Chem* 273:22466-22470.
68. Lerman MI and Minna JD (2000) The 630-kb lung cancer homozygous deletion region on human chromosome 3p21.3: identification and evaluation of the resident candidate tumor suppressor genes. The International Lung Cancer Chromosome 3p21.3 Tumor Suppressor Gene Consortium. *Cancer Res.* 60 (21):6116-6133.

69. Lodish H, Berk A, Zipursky L, Matsudaira P, Baltimore D, Darnell J (2005) Integrating cells into tissues. *Molecular Cell Biology*.
70. Lokeshwar VB et al (2000) Urinary hyaluronic acid and hyaluronidase: markers for bladder cancer detection and evaluation of grade. *J.Urol* 163:348-356.
71. Lokeshwar VB et al (2001) Stromal and epithelial expression of tumor markers hyaluronic acid and HYAL1 hyaluronidase in prostate cancer. *J.Biol.Chem.* 276 (15):11922-11932.
72. Lokeshwar VB et al (2002) Bladder tumor markers for monitoring recurrence and screening comparison of hyaluronic acid-hyaluronidase and BTA-Stat tests. *Cancer* 95:61-72.
73. Longaker MT et al (1991) Studies in fetal wound healing. V. A prolonged presence of hyaluronic acid characterizes fetal wound fluid. *Ann.Surg.* 213:292-296.
74. Majors AK et al (2003) Endoplasmic reticulum stress induces hyaluronan deposition and leukocyte adhesion. *J Biol.Chem.* 278:4722-4731.
75. Margolis RK et al (1976) Glycosaminoglycans and glycoproteins associated with rat brain nuclei. *Biochim.Biophys.Acta* 451:465-469.
76. McBride WH and Bard JB (1979) Hyaluronidase sensitive halos around adherent cells. Their role in blocking lymphocyte-mediated cytolysis. *J.Exp.Med.* 149:507-515.
77. McDonald J and Hascall VC (2002) Hyaluronan minireview series. *Journal of Biological Chemistry* 277 (7):4575-4579.
78. Meikle, P. J., Hopwood, J. J., Ciague, A. E., and Carey, W. F. Prevalence of lysosomal storage disorders. *J.Am.Med.Assoc* 281, 249-254. 1999.  
Ref Type: Journal (Full)
79. Meyer, K. and Palmer, R. The polysaccharide of the vitreous humor. *J Biol.Chem.* 107, 629-634. 1934.  
Ref Type: Journal (Full)
80. Misumi Y et al (1986) Novel blockade by brefeldin A of intracellular transport of secretory proteins in cultured rat hepatocytes. *J Biol.Chem.* 261 (24):11398-11403.
81. Moore DD, Dowhan D (1991) *Escherichia coli*, Plasmids, and Bacteriophages.
82. Moore DD, Dowhan D (2002) Preparation and Analysis of DNA. *Current protocols in molecular biology*.

83. Natowicz MR et al (1979) Enzymatic identification of mannose 6-phosphate on the recognition marker for receptor-mediated pinocytosis of beta-glucuronidase by human fibroblasts. *Proc.Natl.Acad.Sci.U.S.A* 76 (9):4322-4326.
84. Natowicz MR et al (1996) Clinical and biochemical manifestations of hyaluronidase deficiency. *New Engl.J.Med.* 335:1029-1033.
85. Natowicz MR and Wang Y (1996) Plasma hyaluronidase activity in mucopolidoses II and III: marked differences from other lysosomal enzymes. *Am.J.Med.Genet.* 65:209-212.
86. Neufeld EF, Muenzer J (2001) The Metabolic and Molecular Bases of Inherited Disease. In: Scriver CR et al (eds). McGraw-Hill: New York, pp 3421-3452.
87. Noble PW (2002) Hyaluronan and its catabolic products in tissue injury and repair. *Matrix Biol.* 21:25-29.
88. Novak U et al (1999) Hyaluronidase-2 overexpression accelerates intracerebral but not subcutaneous tumor formation of murine astrocytoma cells. *Cancer Res.* 59 (24):6246-6250.
89. Patel S et al (2002) Hyaluronidase gene profiling and role of HYAL-1 overexpression in an orthotopic model of prostate cancer. *Int.J.Cancer* 97:416-424.
90. Posey JT et al (2003) Evaluation of the prognostic potential of hyaluronic acid and hyaluronidase (HYAL1) for prostate cancer. *Cancer Res.* 63 (10):2638-2644.
91. Rai SK et al (2001) Candidate tumor suppressor HYAL2 is a glycosylphosphatidylinositol (GPI)-anchored cell-surface receptor for jaagsiekte sheep retrovirus, the envelope protein of which mediates oncogenic transformation. *Proc.Natl.Acad.Sci.U.S.A* 98 (8):4443-4448.
92. Reed RK, Lilja K, and Laurent TC (1989) Hyaluronan in the rat with special reference to the skin. *Acta Physiol.Scand.* 134:405-411.
93. Reitman ML and Kornfeld S (1981) lysosomal enzyme targeting. *J.Biol.Chem.* 256:11977-11980.
94. Roden L et al (1989) Enzymic pathways of hyaluronan catabolism. *Ciba Found.Symp.* 143:60-86.
95. Sabeur K et al (1997) The PH-20 protein in human spermatozoa. *J.Androl.* 18:151-158.
96. Sambrook J, Fritsch EF, Maniatis T (1989) Molecular Cloning : a Laboratory Manual.

97. Scott JE et al (1991) Secondary and tertiary structures of hyaluronan in aqueous solution, investigated by rotary shadowing-electron microscopy and computer stimulation. Hyaluronan is very efficient network-forming polymer. *Biochem J* 274:699-705.
98. Scott JE (1989) Secondary structures in hyaluronan solutions: chemical and biological implications. *Ciba Found.Symp.* 143:6-14.
99. Seaton GJ, Hall L, and Jones R (2000) Rat sperm 2B1 glycoprotein (PH20) contains a C-terminal sequence motif for attachment of a glycosyl phosphatidylinositol anchor. Effects of endoproteolytic cleavage on hyaluronidase activity. *Biol.Reprod.* 62 (6):1667-1676.
100. Shuttleworth TL et al (2002) Characterization of the murine hyaluronidase gene region reveals complex organization and cotranscription of Hyal1 with downstream genes, Fus2 and Hyal3. *J.Biol.Chem.* 277 (25):23008-23018.
101. Spicer AP and McDonald JA (1998a) Characterization and molecular evolution of a vertebrate hyaluronan synthase gene family. *J.Biol.Chem* (273):1923-1932.
102. Spicer, A. P. and McDonald, J. A. Eukaryotic Hyaluronan Synthases. 10-15-1998b.  
Ref Type: Report
103. Stern R (2003) Devising a pathway for hyaluronan catabolism: are we there yet? *Glycobiology* 13 (12):105R-115R.
104. Stern R (2004a) Hyaluronan catabolism: a new metabolic pathway. *Eur.J.Cell Biol.* 83:317-325.
105. Stern R (2004b) Hyaluronan catabolism: a new metabolic pathway. *Eur.J.Cell Biol.* 83 (7):317-325.
106. Stern, R. Update on the mammalian Hyaluronidases.  
<http://www.glycoforum.gr.jp/science/hyaluronan/HA15a/HA15aE.html> . 5-18-2004c.  
Ref Type: Electronic Citation
107. Stoker M and Macpherson I (1964) SYRIAN HAMSTER FIBROBLAST CELL LINE BHK21 AND ITS DERIVATIVES. *Nature* 203:1355-1357.
108. Tammi R et al (2001) Hyaluronan enters keratinocytes by a novel endocytic route for catabolism. *J.Biol.Chem.* 276 (37):35111-35122.
109. Tanaka Y et al (1990) Biosynthesis, processing, and intracellular transport of lysosomal acid phosphatase in rat hepatocytes. *J.Biochem.* 108:278-286.
110. Taylor KR et al (2004) Hyaluronan fragments stimulate dermal endothelial

- recognition of injury through TLR4. *J Biol.Chem.* 279:17079-17084.
111. Termeer C et al (2000) Oligosaccharides of hyaluronan are potent activators of dendritic cells. *J.Immunol.* 165:1863-1870.
  112. Termeer C, Sleeman JP, and Simon JC (2003) Hyaluronan-magic glue for the regulation of immune response? *Trends immunology* 24:112-114.
  113. Todd D, Camenisch TD, and McDonald JA (2000) Hyaluronan, Is bigger better? *Am.J.Respir.Cell Mol.Biol.* 23:431-433.
  114. Toole BP (1990) Hyaluronan and its binding proteins,the hyaladherins. *Curr.Opin.Cell Biol.* 2:839-844.
  115. Toole BP (1991) Proteoglycans and hyaluronan in morphogenesis and differentiation. In: Hay ED (ed) *Cell biology of extracellular matrix*. Plenum Press: New York, pp 61-92.
  116. Toole BP (2001) Hyaluronan in morphogenesis. *Semin.Cell Dev.Biol.* 12 (2):79-87.
  117. Toole BP (2002) Hyaluronan promotes the malignant phenotype. *Glycobiology* 12:37-42.
  118. Toole BP and Hascall VC (2002) Hyaluronan and tumor growth. *Am.J.Pathol.* 161 (745):747.
  119. Towbin H, Staechelin T, and Gordon J (1979) Electrophoretic transfer of proteins from polyacrylamide gels to nitrocellulose sheets: procedure and some applications. *Proc.Natl.Acad.Sci.USA* 76:4350-4354.
  120. Triggs-Raine B et al (1999) Mutations in *HYALI*, a member of a tandemly distributed multigene family encoding disparate hyaluronidase activities, cause a newly described lysosomal disorder, mucopolysaccharidosis IX. *PNAS* 96:6296-6300.
  121. Turley EA and Roth S (1980) Interactions between the carbohydrate chains of hyaluronate and chondroitin sulphate. *Nature* 283:268-271.
  122. Wei M et al (1996) Construction of a 600-kilobase cosmid clone contig and generation of a transcriptional map surrounding the lung cancer tumor suppressor gene (TSG) locus on human chromosome 3p21.3: progress toward the isolation of a lung cancer TSG. *Cancer Res.* 56:1487-1492.
  123. Weigel PH, Fuller GM, and LeBoeuf RD (1986) A model for the role of hyaluronic acid and fibrin in the early events during the inflammatory response and wound healing. *j.Theor.Biol.* 119:219-234.

124. Weigel PH, Hascall VC, and Tammi M (1997) Hyaluronan synthases. *J Biol.Chem.* 272:13997-14000.
125. Weissman, B. and Meyer, K. The structure of hyalobiuronic acid and of hyaluronic acid from umbilical cord. *J.Am.Chem.Soc.* 76, 1753-1757. 5-4-1954.  
Ref Type: Journal (Full)
126. West DC et al (1985) Angiogenesis induced by degradation products of hyaluronic acid. *Science* 228:1324-1326.
127. Winchester B, Vellodi A, and Young E (2000) The molecular basis of lysosomal storage diseases and their treatment. *Biochem.Soc.Trans.* 28 (2):150-154.
128. Xu H et al (2002) Effect if hyaluronan oligosaccharides on the expression of heat shock protein. *J Biol.Chem.* 277 (17308):17314.
129. Zhang H and Martin-DeLeon PA (2003) Mouse Spam1 (PH-20) is a multifunctional protein: evidence for its expression in the female reproductive tract. *Biol.Reprod.* 69 (2):446-454.
130. Zhou B et al (2000) Identification of the hyaluronan receptor for endocytosis (HARE). *J.Biol.Chem.* 275 (48):37733-37741.